Journal of Immunology Research

Mycobacterium tuberculosis

Guest Editors: Vishwanath Venketaraman, Deepak Kaushal, and Beatrice Saviola

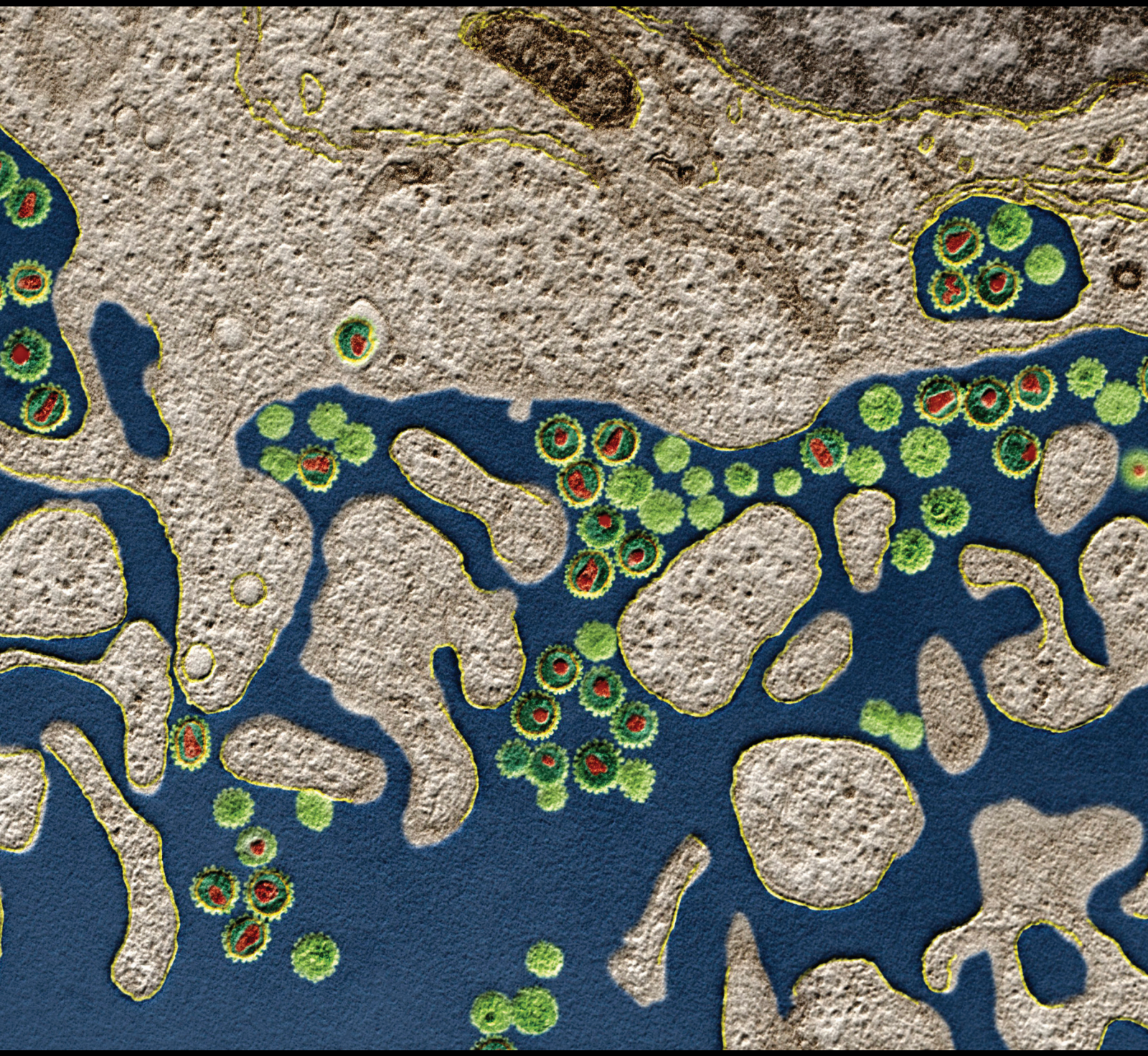

Mycobacterium tuberculosis

Journal of Immunology Research

Mycobacterium tuberculosis

Guest Editors: Vishwanath Venketaraman, Deepak Kaushal, and Beatrice Saviola

Editorial Board

Contents

Hindawi Publishing Corporation
Journal of Immunology Research
Volume 2015, Article ID 857598, 2 pages
http://dx.doi.org/10.1155/2015/857598

Editorial
Mycobacterium tuberculosis

Vishwanath Venketaraman,[1] Deepak Kaushal,[2] and Beatrice Saviola[1]

[1]*Department of Basic Medical Sciences, College of Osteopathic Medicine of the Pacific, Western University of Health Sciences, Pomona, CA 91766-1854, USA*
[2]*Tulane University School of Medicine, Covington, LA 70433, USA*

Correspondence should be addressed to Vishwanath Venketaraman; vvenketaraman@westernu.edu

Received 4 June 2015; Accepted 4 June 2015

Mycobacterium tuberculosis (*M. tuberculosis)*, the causative agent for tuberculosis (TB), is responsible for 1.5 million deaths and 9 million new cases of TB in 2013 [1]. Lack of highly specific and sensitive diagnostic tests, restricted vaccine efficacy, emergence of multidrug and extensively drug-resistant strains of *M. tuberculosis*, and HIV coinfection are the most important factors that result in poor global TB control [1]. It is estimated that, among individuals who are infected with *M. tuberculosis*, around 85–90% are able to control the infection but are unable to completely eradicate the bacillus from their bodies resulting in a latent tuberculosis infection (LTBI) [2]. LTBI is defined by the presence of *M. tuberculosis*-specific immune response with the absence of radiological evidence of clinical disease and clinical signs or symptoms. Approximately one-third of the world's population has LTBI and, among the latently infected population, 5–10% will develop active TB due to reactivation and resuscitation of dormant bacilli [1]. This risk is further increased in immune-compromised individuals and people at the extremes of age. Latently infected individuals are the largest reservoir of potential future source of active TB [2]. In order to reduce the global incidence of TB cases, we urgently need an improved vaccine against *M. tuberculosis* infection. *Mycobacterium bovis* Bacillus Calmette-Guérin (*M. bovis* BCG), currently the only available vaccine against TB, induces variable protection in adults [3]. Immune correlates of protection are lacking, and analyses on cytokine-producing T-cell subsets in protected versus nonprotected cohorts have yielded inconsistent results [3]. This special issue encompasses findings from clinical and translational studies that will further enhance our understanding of the virulence mechanisms of *M. tuberculosis*, impaired host immune responses in individuals with active TB, pathogenesis of the disease, and strategies to enhance the innate and adaptive immune responses against *M. tuberculosis* infection.

Within this special issue are studies that explore the use of BCG vaccines that have been modified in various ways to improve their efficacy. One study uses BCG-Pasteur and BCG-China with DNA vaccine priming and boosting. The vaccine contains coding regions for antigens present within the RD-14 region absent in BCG-Pasteur. In a separate study, BCG was made as a recombinant strain with overexpression of a chimeric protein based on previously studied immunizing antigens. This chimeric antigen is controlled by the iron regulator FurA which regulates gene activity during *in vivo* growth. In another investigation BCG was constructed which overexpresses the cytokine IL-18. When dendritic cells were infected with this recombinant strain, these cells had altered responses and some immune functions were increased, such as improved cytokine production. An alternative approach to vaccination against TB infection is to create mutant *M. tuberculosis* strains that are attenuated but can still stimulate immunity. In this issue a study shows *M. tuberculosis* strain that is mutated in ferritin and is used as a vaccine in a mouse model. While this strategy was comparable to BCG with respect to bacterial burden, pathology of infection seemed to be improved.

Within this issue as well are various studies of immunological tests that can better distinguish between active TB and LTBI. One study shows that LTBI results in a distinctive

CD4+ T-cell cytokine profile. Another study using analysis of antibodies against TB glycolipids was also investigated and compared with those having pulmonary TB, cavitation, and extrapulmonary disease. Also in another study comparing TB infected individuals and healthy subjects, antigen presenting cells seemed to be impaired in TB patients and more severely impaired in PPD-anergic patients.

Vishwanath Venketaraman
Deepak Kaushal
Beatrice Saviola

References

[1] World Health Organization, *Global Tuberculosis Control 2014*, 2014, http://apps.who.int/iris/bitstream/10665/137094/1/9789241564809_eng.pdf.

[2] H. Milburn, "Key issues in the diagnosis and management of tuberculosis," *Journal of the Royal Society of Medicine*, vol. 100, no. 3, pp. 134–141, 2007.

[3] M. C. Boer, C. Prins, K. E. van Meijgaarden, J. T. van Dissel, T. H. Ottenhoff, and S. A. Joosten, "BCG-vaccination induces divergent pro-inflammatory or regulatory T-cell responses in adults," *Clinical and Vaccine Immunology*, 2015.

Hindawi Publishing Corporation
Journal of Immunology Research
Volume 2015, Article ID 385402, 12 pages
http://dx.doi.org/10.1155/2015/385402

Research Article

Vaccination with an Attenuated Ferritin Mutant Protects Mice against Virulent *Mycobacterium tuberculosis*

Selvakumar Subbian,[1] Ruchi Pandey,[2] Patricia Soteropoulos,[2] and G. Marcela Rodriguez[2]

[1]*Laboratory of Mycobacterial Immunity and Pathogenesis, Rutgers, The State University of New Jersey, 225 Warren Street, Newark, NJ 07103, USA*
[2]*Public Health Research Institute at Rutgers Biomedical and Health Sciences, Rutgers, The State University of New Jersey, 225 Warren Street, Newark, NJ 07103, USA*

Correspondence should be addressed to G. Marcela Rodriguez; rodrigg2@njms.rutgers.edu

Received 31 July 2014; Accepted 17 September 2014

Academic Editor: Vishwanath Venketaraman

Mycobacterium tuberculosis the causative agent of tuberculosis affects millions of people worldwide. New tools for treatment and prevention of tuberculosis are urgently needed. We previously showed that a ferritin (*bfrB*) mutant of *M. tuberculosis* has altered iron homeostasis and increased sensitivity to antibiotics and to microbicidal effectors produced by activated macrophages. Most importantly, *M. tuberculosis* lacking BfrB is strongly attenuated in mice, especially, during the chronic phase of infection. In this study, we examined whether immunization with a *bfrB* mutant could confer protection against subsequent infection with virulent *M. tuberculosis* in a mouse model. The results show that the protection elicited by immunization with the *bfrB* mutant is comparable to BCG vaccination with respect to reduction of bacterial burden. However, significant distinctions in the disease pathology and host genome-wide lung transcriptome suggest improved containment of Mtb infection in animals vaccinated with the *bfrB* mutant, compared to BCG. We found that downmodulation of inflammatory response and enhanced fibrosis, compared to BCG vaccination, is associated with the protective response elicited by the *bfrB* mutant.

1. Introduction

Tuberculosis (Tb) continues to be one of the most deadly infectious diseases, causing more than one million deaths in the world per year. The variable efficacy of the BCG vaccine, the synergy between HIV and *M. tuberculosis* (Mtb), and the increase in drug-resistant Mtb strains underscore the urgent need for effective vaccines against Tb.

Iron plays a critical role in the pathogenesis of many organisms including Mtb. It is the preferred redox cofactor in several basic cellular processes, but due to its insolubility and potential toxicity under physiological conditions, iron is a limiting nutrient in the host environment. Therefore, successful pathogens must possess high affinity iron acquisition systems and exert strict control over intracellular free iron to establish a productive infection. In addition to its ability to induce iron acquisition systems, iron limitation encountered in the host is a signal for pathogen's induction of virulence determinants and reprogramming of many cellular processes including central metabolism, secretion, surface remodeling, stress responses, and membrane vesicle generation [1, 2]. Thus, due to its impact on the pathogen's physiology, iron homeostasis can influence many host-pathogen interactions.

Previously, we demonstrated that Mtb requires the iron storage protein ferritin (BfrB), for its adaptation to changes in iron availability [3]. When available, iron is safely stored in ferritin and released as needed to overcome iron limitation. Lack of storage results in free iron mediated toxicity and increased vulnerability to oxidative and nitrosative stress. In mice lungs, Mtb lacking *bfrB* (Δ*bfrB*) proliferates initially, in the first 4 weeks, but it succumbs to the effects of the adaptive immune response failing to establish a chronic infection [3]. Additionally, though Δ*bfrB* disseminates to the spleen, it fails to colonize the liver [3]. Thus, although unable to establish a

successful infection Δ*bfrB* persists long enough to stimulate host immunity suggesting that this strain could serve as a potential vaccine candidate.

In this study, we tested whether subcutaneous vaccination with Δ*bfrB* could protect mice against a subsequent aerosol challenge with virulent Mtb. The results show that immunization with the Δ*bfrB* stimulates protective immunity associated with reduced disease pathology and better containment of the infection compared to vaccination with BCG. Genome-wide transcriptome analysis showed a distinct expression pattern of significantly differentially expressed genes (SDEG) between the Δ*bfrB* and BCG-vaccinated, Mtb-infected mice lungs. Our network/pathway analysis of SDEG revealed significant downregulation of inflammatory response and activation of fibrosis network genes in the Δ*bfrB*, compared to BCG vaccinated, Mtb-infected mice lungs, which is potentially associated with the improved protection by the former vaccine strain. The results provide a framework for the identification of new immunological correlates and mechanisms of protection, relevant for the design of better Tb prevention strategies.

2. Materials and Methods

2.1. Animal Ethics Statement. All animal procedures mentioned in this study were approved by the Rutgers Institutional Animal Care and Use Committee (IACUC) and all possible steps were taken to avoid animal suffering at each stage of the experiments.

2.2. Bacterial Strains and Chemicals. The wild type and Δ*bfrB* strains of Mtb H37Rv were grown in Middlebrook 7H9 media (Difco BD, Sparks, MD) as described previously [3]. Stock cultures were prepared at mid-log growth phase and stored at −80°C until they were ready to use. All chemicals were purchased from Sigma (Sigma-Aldrich, St. Louis, MO), unless specified otherwise. BCG-Pasteur strain was obtained from ATCC.

2.3. Mouse Vaccination and Infection. Female C57BL/6 mice ($n = 15$) were vaccinated subcutaneously with 1×10^6 CFU of Δ*bfrB* or BCG suspended in 0.1 mL PBS containing 0.05% Tween 80 (PBST). A control group of mice was mock-vaccinated with PBST. At 4 or 8 weeks postvaccination, groups of 5 mice ($n = 5$) were aerosol infected with Mtb H37Rv as described earlier [3]. Briefly, Mtb aerosols were generated by a Lovelace nebulizer (In-tox Products, Albuquerque, NM) with a 10 mL bacterial suspension of about 1×10^6 bacilli/mL in saline containing 0.04% Tween 80 and the mice were exposed to the aerosol for 30 minutes which results in approximately 100 colonizing CFUs per lung. A separate group of vaccinated but uninfected mice were included as controls. Infected mice were sacrificed 4 weeks postinfection and lungs and spleen were removed. Portions of the tissue were homogenized in PBST and serial dilutions of the homogenates were plated onto Middlebrook 7H10 agar (Difco BD, Sparks, MD) to determine the number of bacterial CFUs. Portions of mice lungs were also stored immediately at −80°C for total lung RNA isolation or fixed in 10% formalin for histological analysis.

2.4. Histopathology. The formalin-fixed lung portions from vaccinated and vaccinated-Mtb-infected mice ($n = 5$ per group) were paraffin embedded, cut into 5 μM slices, and used for histopathological analysis. Lung sections were stained either with haematoxylin and eosin (H&E), Mason's trichrome, or Ziehl-Neelsen staining method for assessing the pathology, tissue remodeling and fibrosis, and the presence of acid-fast bacilli (AFB), respectively. Stained lung sections were analyzed and photographed in a Nikon Microphot-FX microscope (Nikon Instruments, Melville, NY). Morphometric analysis was performed on the H&E stained histologic sections to determine the area of granulomas in the lungs of Mtb-infected mice using Sigmascan Pro software, following the instructions supplied by the manufacturer (Systat Software, Inc., San Jose, CA).

2.5. Total RNA Isolation. Total lung RNA from vaccinated and vaccinated plus Mtb-infected mice ($n = 5$ per group) was extracted and purified to remove contaminating DNA, using the RNeasy Midi kit (Qiagen Inc., Valencia, CA) following the manufacturer instructions. The quality and quantity of purified RNA was estimated using a Nanodrop instrument (Nanodrop, Wilmington, DE).

2.6. Microarray Gene Expression Procedure and Data Analysis. Total RNA extracted from each of the BCG or Δ*bfrB* vaccinated and Mtb-infected mouse lungs ($n = 3$ per group) was processed separately for microarray analysis as reported earlier [4]. Gene expression profiling was performed using the Mouse Gene 2.0 ST Array slides and the GeneChip whole transcript (WT) protocol following the manufacturer's protocol (Affymetrix, Santa Clara, CA). Briefly, total RNA (250 ng) was used for cDNA synthesis. The cDNA was fragmented and end-labeled with biotin. The biotin labeled cDNA was hybridized to the array for 16 hours at 45°C using the GeneChip Hybridization Oven 640. Washing and staining with streptavidin-phycoerythrin was performed using the GeneChip Fluidics Station 450. Images were acquired using the Affymetrix Scanner 3000 7G Plus and the Affymetrix Command Console Software (Affymetrix, Santa Clara, CA). The arrays were normalized using robust multiarray (RMA) method. Gene expression data from three independent samples per group was cumulated, averaged, annotated, and processed at group level (i.e., BCG vaccinated and Mtb-infected versus Δ*bfrB* vaccinated and Mtb-infected) using Partek Genomics Suite (Partek Inc., St. Louis, MO). We applied one-way ANOVA with equal variance between comparator groups. Significantly differentially expressed genes (SDEG) were derived using 5% false discovery rate (FDR). The list of SDEG was analyzed for gene ontology and pathway/network derivation using ingenuity pathway analysis (IPA; Ingenuity Systems, Redwood City, CA). A z-score based gene ontology algorithm was used from IPA to categorize the biological functions affected by SDEG. This algorithm identifies biological functions expected to be increased (activated) or decreased (suppressed), in

the user datasets, based on the nonrandom expression pattern of genes in the dataset, relative to the knowledgebase from published results. Thus, a z-score of ≥ 2 indicates activation of a biological function, while a z-score of ≤ 2 shows suppression of a biological function. The microarray gene expression data was submitted to Gene Expression Omnibus (GEO).

2.7. Quantitative Real-Time PCR (qPCR). The mouse lung total RNA utilized for microarrays was also used for qPCR experiments. For reverse transcription, a ThermoScript RT-PCR system with random hexamer primers was used according to the manufacturer instructions (Life Technologies, Grand Island, NY). Briefly, 200 ng of total lung RNA from each mouse was used for cDNA synthesis. Control reactions without reverse transcriptase were also performed to exclude significant DNA contamination. The amplified cDNA samples were diluted 50-fold and used for qPCR with a SYBR green qPCR super Mix Universal (Life Technologies, Grand Island, NY) in a Stratagene Mx3005p system (Agilent Technologies, Santa Clara, CA). The 10 μL PCR mixture contained 1.5 μL (5 ng) of cDNA template, 5 μL of SYBR Green Master Mix, 2 μL of primers (10 pM), and 1.5 μL nuclease-free water. The PCR conditions were one cycle of 10 min at 94°C followed by 40 cycles of amplification, each with 95°C for 30 s, 55°C for 30 s, and 72°C for 30 s. The oligonucleotide primers used for qPCR are listed in Supplementary Table 1 in Supplementary Material available online at http://dx.doi.org/10.1155/2015/385402. Threshold cycle (Ct) values of test and control (*Gapdh*) genes were measured and used to calculate the fold change in expression using Mx4000 software (Agilent Technologies, Santa Clara, CA).

3. Results

*3.1. Growth of Mtb in Δ*bfrB* or BCG Vaccinated Mice.* We have shown previously that, after aerosol exposure, Δ*bfrB* replicates in the mice lungs during the first 4 weeks of infection but is unable to persist and establish a chronic infection. We postulated that the inability of Δ*bfrB* to persist in the infected mice lungs was due to the effects of the adaptive immune response and hypothesized that the transient replication of Δ*bfrB* might stimulate an immune response that could protect against subsequent infection with a fully virulent Mtb. To test this, groups of mice ($n = 5$) were vaccinated with a single dose of Δ*bfrB* or the standard BCG vaccine and at four or eight weeks postvaccination a group of mice were sacrificed to determine CFUs of each vaccine strain in the lungs whereas a second group of mice were challenged via aerosol infection with virulent wild type H37Rv (Figure 1(a)). Enumeration of lung CFUs from vaccinated, uninfected mice lungs show that at the high dose used for subcutaneous administration the attenuation of Δ*bfrB* and BCG was comparable (Supplementary Figure 1). Among the Mtb-infected mice, those vaccinated with Δ*bfrB* or BCG had significantly less number of bacilli in their lungs and spleen, compared to the sham (PBS-)vaccinated controls (Figure 1(b) and Supplementary Figure 2). A further reduction in bacillary load was observed in Δ*bfrB* compared to the BCG in the 8 weeks vaccinated, Mtb-infected mice lungs, though this difference was not statistically significant ($P = 0.63$). Thus, we conclude that Δ*bfrB* vaccinated mice controlled bacterial multiplication in the lungs to a similar extent as the BGC vaccinated mice. Since there was no significant difference in the level of protection between animals vaccinated for 4 or 8 weeks prior to challenge, we decided to focus on the longer lasting response of animals vaccinated for 8 weeks before infection, for subsequent analyses.

*3.2. Histopathology of Δ*bfrB* or BCG Vaccinated Mtb-Infected Mice Lungs.* To examine the gross pathology of the Δ*bfrB* or BCG vaccinated and Mtb-infected mice, we examined the H&E stained lung sections from the respective animals (Figures 1(c)–1(f)). No obvious granulomas were found in the Δ*bfrB* or BCG vaccinated, uninfected mice lungs, while well-formed granulomas were noted in the vaccinated-Mtb-infected mice lungs. The lung granulomas appeared bigger and more cellular in the BCG vaccinated, compared to the Δ*bfrB* vaccinated mice, where multiple, smaller granulomas were found. Thus, suggesting that vaccination with these two strains differentially influenced the host immune response and granuloma development.

Analysis of the lung sections at higher magnifications revealed a mostly clear and functional parenchyma without inflammation or pneumonia in the Δ*bfrB* or BCG vaccinated, uninfected animals, though very few, small, localized perivascular cellular aggregates were found in the former group (Figures 2(a)–2(d)). These cellular aggregates were comprised of foamy histiocytes and lymphocytes (Figures 2(c) and 2(d)). This indicates that a distinct lung-immune response and cell recruitment was elicited by the two vaccines. Among the Mtb-infected mice, the lungs of BCG vaccinated animals had well-organized peribronchial and perivascular granulomas that occasionally coalesce to form bigger lesions (Figure 2(e)). These highly cellular and diffused granulomas contained densely arranged foamy and nonfoamy histiocytes that appear to be macrophages and polymorphonuclear cells (PMN) at the center, surrounded by a cuff of lymphocytes at the periphery (Figure 2(f)). In contrast, the granulomatous lesions in the Δ*bfrB* vaccinated, Mtb-infected mice lungs appeared smaller, diffused, and contained more lymphocytes at the periphery of the lesions (Figures 2(g) and 2(h)). Relatively more fibrosis was also noted in these well-confined granulomas (see below). Although no necrosis was found in any of these granulomas, elevated immune cell accumulation, specifically foamy macrophages, reminiscent of lipid-pneumonia was noted in both Δ*bfrB* or BCG vaccinated, Mtb-infected mice lungs (Figures 2(e)–2(h)). Morphometric analysis of lung granulomas in the Mtb-infected mice revealed about two-fold higher lesion volume, corresponding to more lung involvement, in the BCG vaccinated, compared to the Δ*bfrB* vaccinated animals; however, the difference was not statistically significant (Supplementary Figure 3).

*3.3. Genome-Wide Transcriptional Analysis of Δ*bfrB* or BCG Vaccinated Mtb-Infected Mice Lungs.* To determine the correlates of immune response elicited in the Δ*bfrB* vaccinated Mtb-infected mice, we performed a genome-wide lung gene

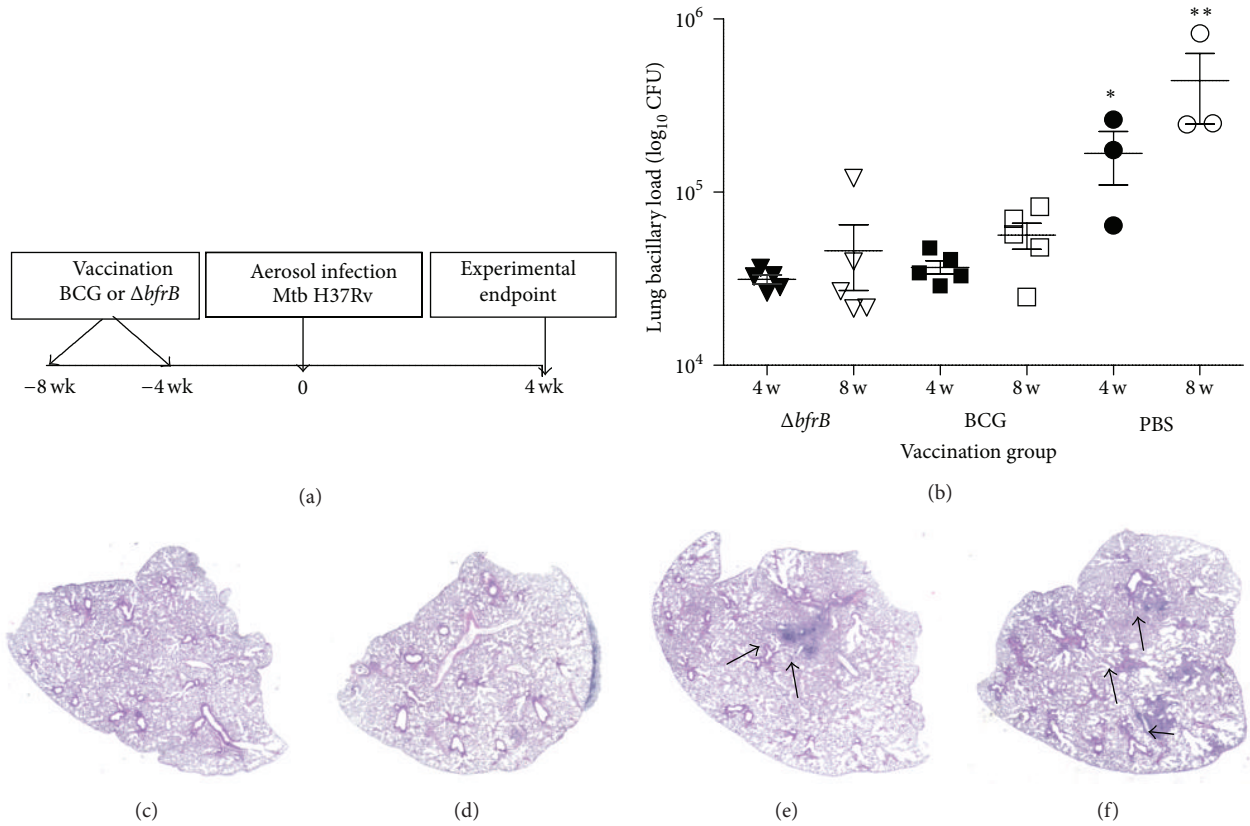

Figure 1: Experimental design, lung bacillary burden, and gross pathology of vaccinated and uninfected or Mtb-infected mice. (a) Schema of the mice vaccination schedule and Mtb infection experiment. (b) Lung bacillary load in mice infected with virulent Mtb H37Rv after vaccination with PBS (sham) or BCG or Δ*bfrB* for 4 ($^{*}P = 0.033$) or 8 weeks ($^{**}P = 0.035$). Gross lung pathology of vaccinated and uninfected or Mtb-infected-mice. (c) H&E stained lung section of BCG vaccinated (for 8 weeks) and uninfected mice. (d) H&E stained lung section of Δ*bfrB* vaccinated (for 8 weeks) and uninfected mice. (e) H&E stained lung section of BCG vaccinated (for 8 weeks) and Mtb-infected (for 4 weeks) mice. The arrows in (e) show a multifocal, coalescent granuloma. (f) H&E stained lung section of Δ*bfrB* vaccinated (for 8 weeks) and Mtb-infected (for 4 weeks) mice. The arrows in (f) show multiple, small granulomas.

expression profile in these mice and compared the results with the transcriptional profile of BCG vaccinated Mtb-infected mice lungs.

The principal component analysis (PCA) mapping showed clustering of dataset from multiple samples within each group that was distinct from each other (Figure 3(a)). The reproducibility of variance in the x-axis, y-axis, and z-axis as shown by PC#1, 2, and 3 were 45.6%, 20.7%, and 14.7%, respectively. Of the 35,556 probes present in the mouse microarray, 21,760 were annotated. After normalization, data from the two vaccinated groups (Δ*bfrB* versus BCG) were analyzed by one-way ANOVA and compared groupwise (Figure 3(b)). Using 5% false discovery rate (FDR) (Q value < 0.05) as significance cut-off, we identified 1,545 significantly differentially expressed genes (SDEG). Of these SDEG, about 61% were upregulated in the Δ*bfrB* vaccinated, relative to the BCG vaccinated, Mtb-infected mouse lungs (Figures 3(b) and 3(c)). The microarray gene expression data was validated with qPCR on a randomly selected list of genes (Supplementary Table 2). The pattern and directionality of expression of selected genes was consistent between microarray and qPCR, though the absolute expression levels for some genes were different, due to inherent differences in these two methodologies.

The z-score based functional prediction analysis of enriched set of SDEG using IPA suggested dampening of host biological functions associated with inflammation, cellular movement, and cell death and survival, while other functions such as regulation of cell morphology, lipid metabolism, lymphoid tissue structure and development, and small molecule transport were activated in the Δ*bfrB* vaccinated, relative to the BCG vaccinated, Mtb-infected mouse lungs (Table 1).

3.4. Gene Networks Affected in the ΔbfrB or BCG Vaccinated Mtb-Infected Mice Lungs. Among various biological functions impacted by the enriched set of SDEG, we selected the most statistically significant and potentially relevant to Tb pathogenesis for more detailed network/pathway analysis. The selected networks are inflammatory response, the STAT-1 regulon, phosphatidylcholine (PC) metabolism, and PPAR-γ regulon (Figure 4).

3.4.1. Inflammatory Response Network. There were 70 SDEG associated with the inflammatory response that contributes

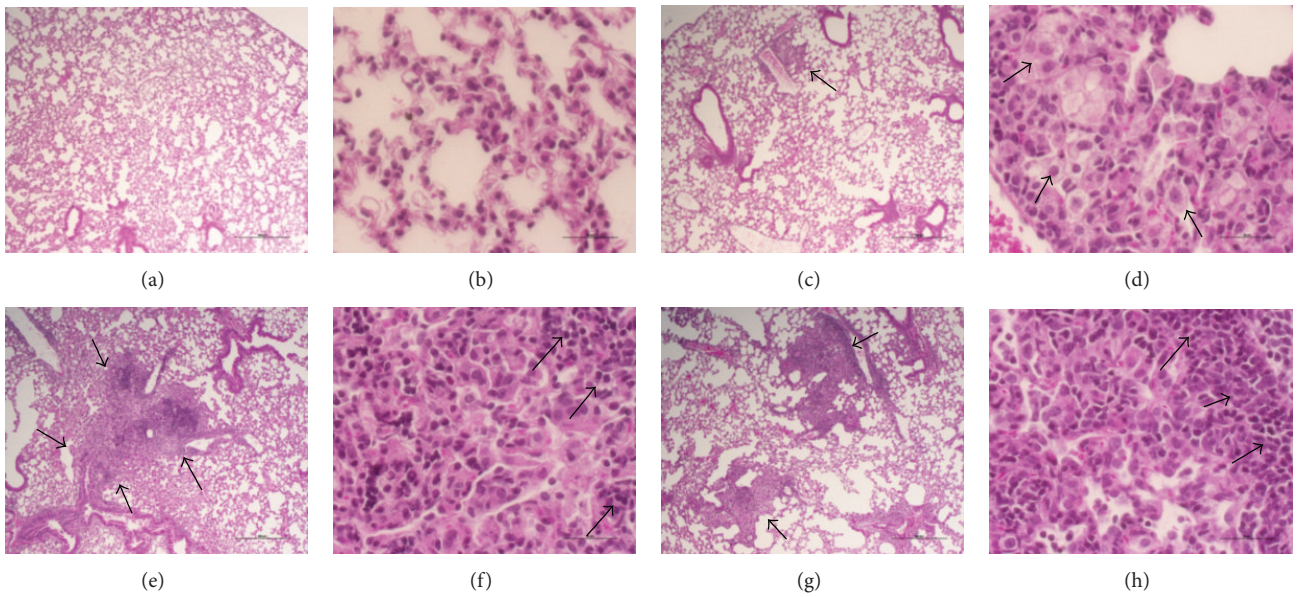

Figure 2: Histopathology of vaccinated and uninfected or Mtb-infected mice lungs. ((a)-(b)) H&E stained lung section of BCG vaccinated (for 8 weeks) and uninfected mice. ((c)-(d)) H&E stained lung section of Δ*bfrB* vaccinated (for 8 weeks) and uninfected mice. The arrow in (c) shows cellular aggregation. The arrows in (d) show foamy histiocytes. ((e)-(f)) H&E stained lung section of BCG vaccinated (for 8 weeks) and Mtb-infected (for 4 weeks) mice. The arrows in (e) show a multifocal, coalescent granuloma. The arrows in (f) show lymphocyte cuff at the periphery of a granuloma. ((g)-(h)) H&E stained lung section of Δ*bfrB* vaccinated (for 8 weeks) and Mtb-infected (for 4 weeks) mice. The arrows in (g) show multiple, smaller granulomas (compared to (e)). The arrows in (h) show lymphocyte cuff at the periphery of a granuloma. Magnification: 4x ((a), (c), (e), and (g)) or 40x ((b), (d), (f), and (h)).

to exacerbated disease pathology during Mtb infection. These genes code for cytokines, enzymes, G-protein coupled receptors, ion channels, transcriptional regulators, transmembrane receptors, and transporters. Of these, 19 were upregulated and 51 were downregulated in the Δ*bfrB* vaccinated, relative to the BCG vaccinated, Mtb-infected mouse lungs (Figure 4(a) and Supplementary Table 3). The expression pattern of SDEG in this network showed a negative z-score (−4.0) in the functional prediction analysis, which suggests significant downmodulation of the inflammatory response, including reduced chemotaxis and activation of leukocytes, and the acute phase response. This result is associated with and supported by our histopathology analysis that revealed smaller granulomas and reduced immunopathology in the lungs of Δ*bfrB* vaccinated, relative to the BCG vaccinated, Mtb-infected mouse lungs.

3.4.2. STAT-1 Regulon Network. The signal transducer and activator of transcription-1 (STAT-1) is one of the key regulators of T-cell activation that has been shown to impact the host protective immunity during Mtb infection in humans and animal models [5–8]. We analyzed the expression pattern of SDEG that are the members of the STAT-1 regulon network, where the genes are controlling or controlled by STAT-1. Fifty-five SDEG in our dataset were involved in STAT-1 regulon network (Figure 4(b) and Supplementary Table 3). Of these, more than 87% (48 genes) were downregulated, while 7 genes were upregulated in the lungs of Δ*bfrB* vaccinated, relative to the BCG vaccinated, Mtb-infected mice. The pattern of expression of SDEG suggests inhibition of this network in the Δ*bfrB* vaccinated, Mtb-infected mice. The deactivation of STAT-1 regulon network is also associated with the downmodulation of inflammatory response in these animal lungs.

3.4.3. Phosphatidylcholine Metabolism Network. Our functional prediction analysis of SDEG revealed that host lipid metabolism, specifically phosphatidylcholine (PC) biosynthesis and metabolism, was one of the top biological functions that were significantly activated (z-score +2.2) in the Δ*bfrB* vaccinated, relative to the BCG vaccinated, Mtb-infected mice lungs. A subset of 42 SDEG involved in the PC metabolism network were differentially regulated between Δ*bfrB* and BCG vaccinated, Mtb-infected mice lungs (Figure 4(c) and Supplementary Table 3). Of the 42 SDEG, 30 genes, including 19 (out of 20 genes) that code for enzymes, were upregulated only in the Δ*bfrB* vaccinated animals.

3.4.4. PPAR-γ Regulon Network. One of the transcriptional regulators associated with host lipid metabolism during disease pathology is the peroxisome-proliferator-activated receptor-gamma (PPAR-γ) [9, 10]. Expression of *Pparγ* was upregulated in the Δ*bfrB* vaccinated, relative to the BCG vaccinated, Mtb-infected mice lungs. In addition, 15 of the PC metabolism network genes that were upregulated in the Δ*bfrB* vaccinated and Mtb-infected mice lungs were also regulated

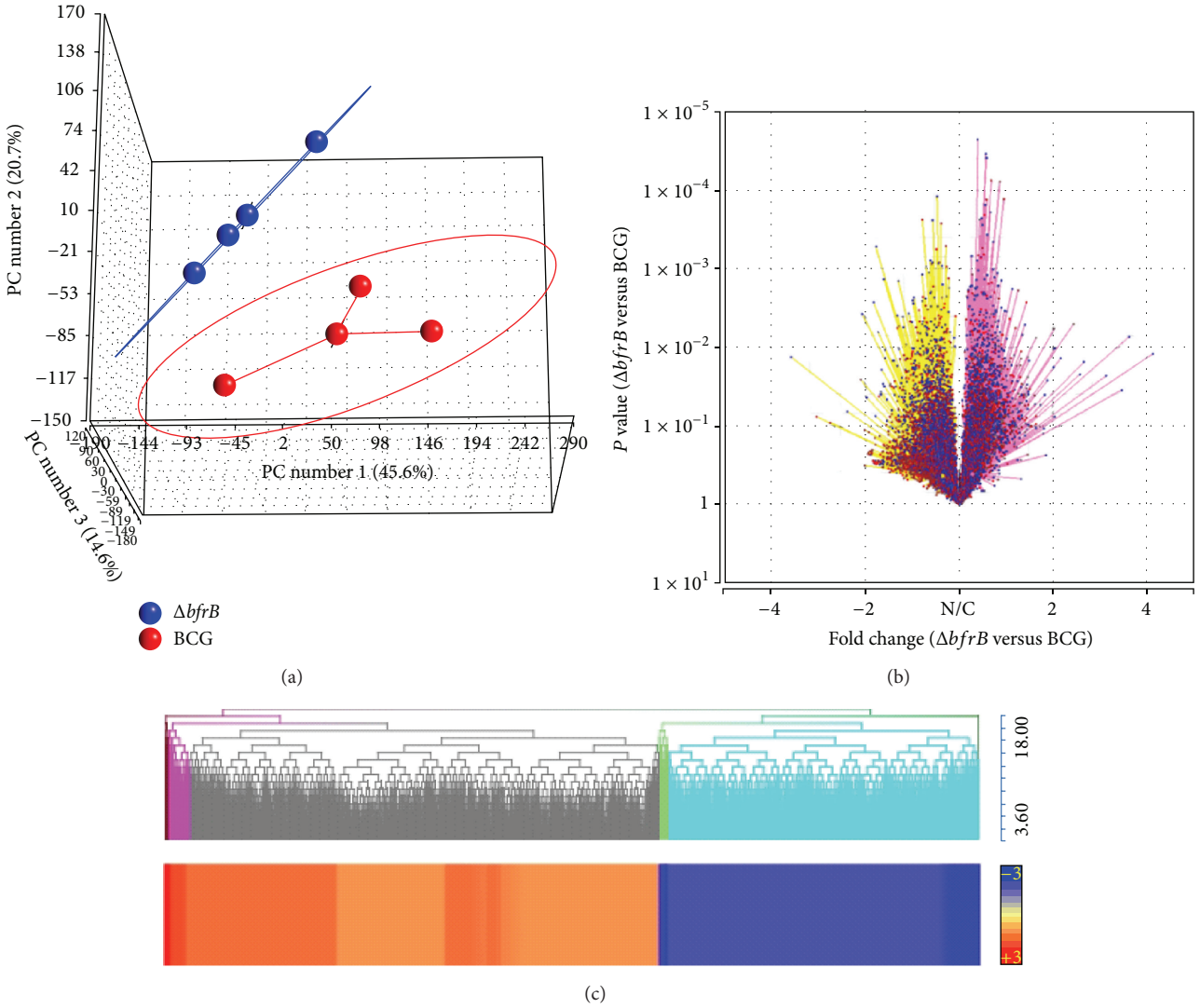

Figure 3: Genome-wide gene expression profiling of vaccinated and Mtb-infected mice lungs. (a) Principal component analysis of lung transcriptome data from Δ*bfrB* (blue) or BCG (red) vaccinated, Mtb-infected mice. The eclipse around each group denotes the standard deviation of the datasets. (b) Volcano plot of lung global gene expression showing the *P* value significance (*y*-axis; log scale) and fold change (*x*-axis). Upregulated genes are shaded in purple and downregulated genes are in yellow. N/C denotes no change. Each spot (blue) in the plot corresponds to a gene. (c) Intensity plot and dendrogram of significantly differentially expressed genes in the Δ*bfrB* vaccinated, compared to BCG vaccinated, Mtb-infected mice lungs. Upregulated genes are in red and downregulated genes are in blue. The color scale bar ranges from +3 (red) to −3 (blue).

by PPAR-γ. Therefore, we investigated the expression pattern of PPAR-γ regulon network genes. These genes are either regulating or regulated by *Pparγ*. Of all the SDEG, 42 were associated with the PPAR-γ regulon network. Similar to the expression pattern observed for the PC metabolism network genes, more than 73% (31 genes) of the PPAR-γ regulon network genes were upregulated only in the Δ*bfrB* vaccinated, Mtb-infected mice lungs (Figure 4(d) and Supplementary Table 3).

Taken together, the comparative lung transcription profiling, between Δ*bfrB* and BCG vaccinated, Mtb-infected mice lungs, is strongly associated with significant down-modulation of the host inflammatory response, perhaps by deactivation of STAT-1 network and activation of host PC metabolism probably through induction of the PPAR-γ regulon network in the Δ*bfrB* vaccinated animals.

3.5. Differential Fibrosis in the Lung Granulomas of ΔbfrB or BCG Vaccinated Mtb-Infected Mice. Fibrosis is a cellular process important in the evolution of granulomas in Mtb-infected tissues. Resorbing and healing granulomas are reported to be encapsulated by a thick fibrotic layer, compared to an actively progressing cavitary granuloma [11]. Our histopathologic analysis of lung sections from Δ*bfrB* or BCG vaccinated, Mtb-infected mice revealed distinct cellular distribution and structural differences in the architecture of granulomas and suggested more fibrosis in the Δ*bfrB*

Table 1: z-score based functional prediction of SDEG.

Category	Functions annotation	P value	z-score	Number of molecules
Downregulated				
Inflammatory Response	Activation of leukocytes	$3.35E-12$	−4	103
	Activation of myeloid cells	$7.94E-06$	−4	39
	Activation of phagocytes	$4.51E-06$	−3.7	45
	Activation of antigen presenting cells	$2.02E-06$	−3.3	38
	Inflammatory response	$1.24E-10$	−3.1	107
	Chemotaxis of granulocytes	$6.58E-06$	−3.1	31
	Activation of mononuclear leukocytes	$2.75E-10$	−3	77
	Chemotaxis of neutrophils	$1.92E-05$	−3	27
	Chemotaxis of myeloid cells	$5.25E-07$	−2.9	45
	Activation of macrophages	$1.03E-04$	−2.9	25
	Activation of lymphocytes	$2.01E-10$	−2.8	75
	Phagocytosis	$1.91E-06$	−2.5	45
	Chemotaxis of leukocytes	$9.02E-10$	−2.2	60
	Acute phase reaction	$3.65E-04$	−2.2	7
Cellular movement	Cell movement of leukocytes	$3.00E-13$	−2.7	122
	Lymphocyte migration	$2.17E-08$	−2.7	55
Cell death and survival	Cell death	$6.41E-14$	−2.6	400
Upregulated				
Cell morphology	Morphology of mononuclear leukocytes	$1.63E-10$	2.9	45
	Morphology of lymphocytes	$1.26E-09$	2.9	42
	Morphology of leukocytes	$2.64E-09$	2.8	63
	Morphology of blood cells	$1.67E-07$	2.8	68
	Morphology of T lymphocytes	$1.85E-06$	2.2	26
	Morphology of B lymphocytes	$3.15E-05$	2.1	17
Lipid metabolism	Synthesis of phosphatidylcholine	$1.77E-05$	2.2	9
	Metabolism of phosphatidylcholine	$1.16E-04$	2.2	10
Lymphoid tissue structure and development	Morphology of lymph follicle	$2.57E-10$	3.4	28
	Morphology of germinal center	$6.05E-10$	3.2	21
	Development of lymphatic system component	$1.96E-08$	2.3	61
	Development of lymph node	$2.36E-08$	2.9	23
	Lack of germinal center	$4.84E-07$	3.2	11
Molecular transport	Transport of molecule	$1.03E-05$	2.8	176

vaccinated, compared to BCG vaccinated, Mtb-infected mice. To determine the extent of differential fibrosis between these two groups of mice, we analyzed the lung sections for collagen deposition after staining with Mason's trichrome staining method.

The lungs of Δ*bfrB* or BCG vaccinated, uninfected mice had similar levels of background fibrosis (Figures 5(a) and 5(c)). Among the Mtb-infected mice, those vaccinated with Δ*bfrB* had more abundant fibrosis than the BCG vaccinated animals (Figures 5(b) and 5(d)). These collagen fibers were predominantly present at the periphery of the granulomas and appeared in distinct clusters in the Δ*bfrB* vaccinated mice, compared to a more diffused pattern seen in the BCG vaccinated mice. We also interrogated the SDEG to determine the expression pattern of genes associated with fibrosis in these vaccinated and Mtb-infected mice lungs. The IPA analysis of SDEG identified a subset of 39 genes enriched for fibrosis and tissue remodeling network (Figure 5(e) and Supplementary Table 3). Of these, 27 were upregulated and 12 were downregulated in the Δ*bfrB* vaccinated, relative to the BCG vaccinated, Mtb-infected mice lungs. The expression pattern of genes predicted activation of fibrosis network in the Δ*bfrB* vaccinated Mtb-infected mice. In fact, the products of several of the upregulated genes, including *Col4a5*, *Col14a1,* and *Timp2,* are reported to be directly involved in the regulation of collagen synthesis/metabolism [12–14].

Taken together, these results suggest that the reduction in granuloma size and alleviation of lung pathology in the Δ*bfrB*

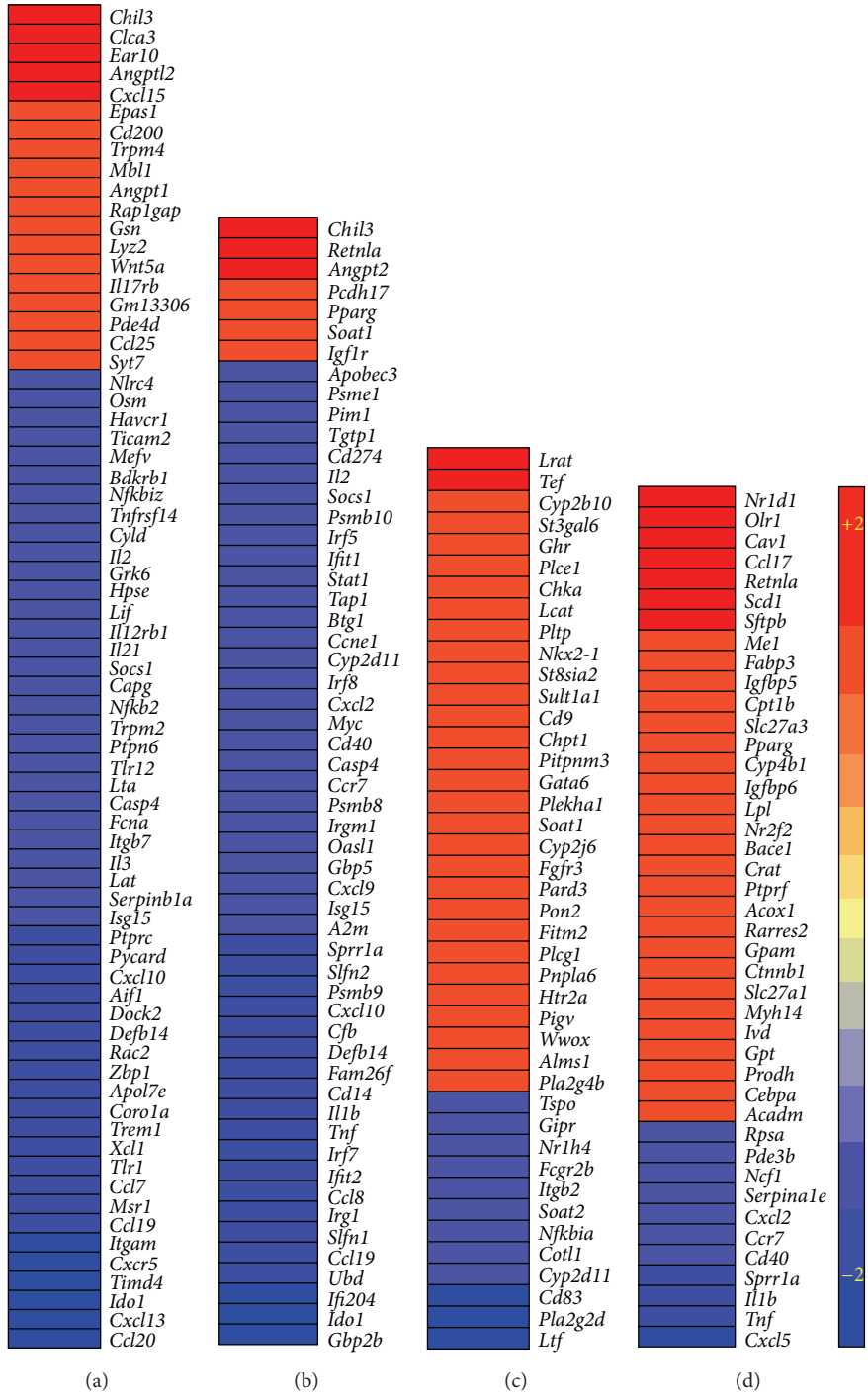

Figure 4: Intensity plot of network genes differentially expressed in the vaccinated and Mtb-infected mice lungs. (a) Intensity plot of significantly differentially expressed genes involved in the inflammatory response network. (b) Intensity plot of significantly differentially expressed genes involved in the STAT-1 regulon network. (c) Intensity plot of significantly differentially expressed genes involved in the PC metabolism network. (d) Intensity plot of significantly differentially expressed genes involved in the PPAR-γ regulon network. The values plotted in (a)–(d) are different in fold change in the Δ*bfrB* vaccinated, compared to BCG vaccinated, Mtb-infected mice lungs. Upregulated genes are in red and downregulated genes are in blue. The color scale bar ranges from +2 (red) to −2 (blue).

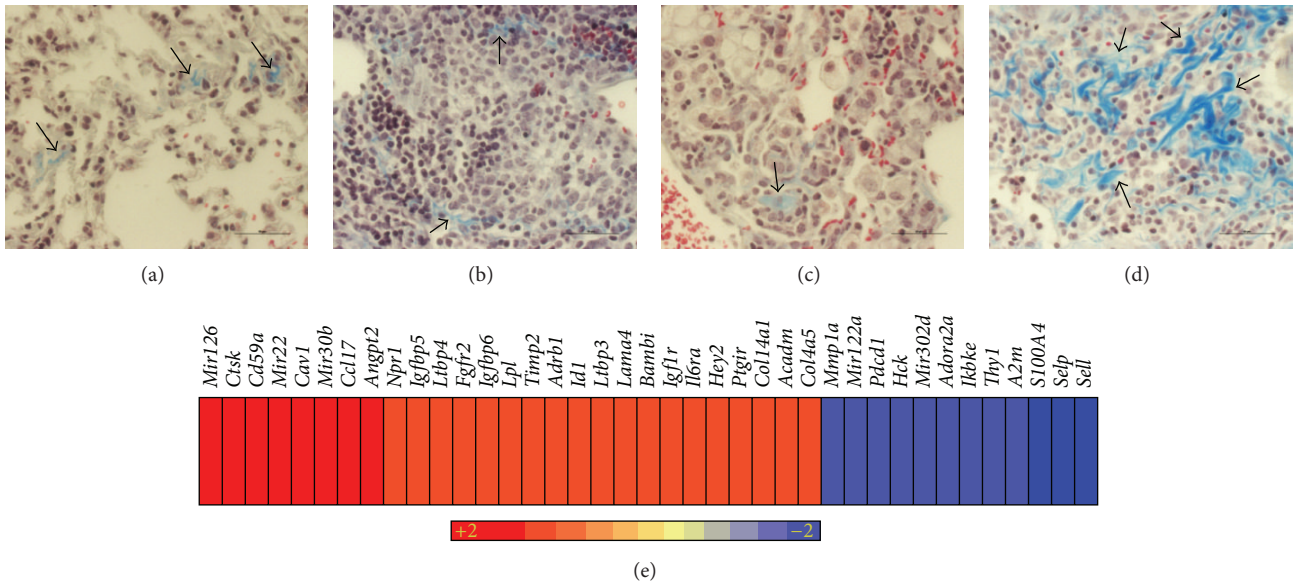

Figure 5: Fibrosis in the lungs of vaccinated and uninfected or Mtb-infected mice. ((a)-(b)) Masson's trichrome stained lung section of BCG vaccinated (for 8 weeks) and uninfected (a) or Mtb-infected (b) mice. ((c)-(d)) Masson's trichrome stained lung section of Δ*bfrB* vaccinated (for 8 weeks) and uninfected (c) or Mtb-infected (d) mice. The arrows in (a) and (c) show basal level of fibrosis (blue color). The arrows in (b) show minimal fibrosis in the BCG vaccinated and Mtb-infected mice. The arrows in (d) show extensive fibrosis in the Δ*bfrB* vaccinated and Mtb-infected mice. Magnification: 4x ((a) and (c)) or 40x ((b) and (d)). (e) Intensity plot of significantly differentially expressed genes involved in the fibrosis network. The values plotted are the difference in fold change in the Δ*bfrB* vaccinated, compared to BCG vaccinated, Mtb-infected mice lungs. Upregulated genes are in red and downregulated genes are in blue. The color scale bar ranges from +2 (red) to −2 (blue).

vaccinated, relative to the BCG vaccinated, Mtb-infected mice lungs, is associated with increased fibrosis and wound healing processes.

3.6. Expression of Selected Host Immunity Related Genes in Vaccinated Animals. To gain insight on the distinctive features of the immune response induced by Δ*bfrB* and BCG vaccination, we determined the level and pattern of expression of a selected panel of 20 genes encoding various components of the immune response in the lungs of vaccinated animals (Table 2). These genes encode for proteins associated with the Th1, Th2, or Th17 type immune response, which are key components of the host response during pulmonary Mtb infection [15, 16]. The qPCR results showed similar level and directionality of expression for the majority of the tested genes, including *Il1a*, *Il1b*, *Il10*, *Il13*, *Il12a*, *Il12b*, *Il18ra*, *Tgfb*, *Timp1*, *Il1r2,* and *Nos2* in the Δ*bfrB* or BCG vaccinated mice lungs. However, expression of chemokine genes *Ccl2*, *Ccl7*, *Ccl12*, *Cxcl1*, *Cxcl3*, *Cxcl5,* and *Cxcl11* were elevated in the Δ*bfrB*, compared to BCG, vaccinated mice lungs, though the differences were not statistically significant for any of these genes ($P > 0.05$). Taken together, vaccination with Δ*bfrB* appear to elicit a similar host immune response as BCG, though elevated chemokine expression associated with cell recruitment could contribute to increased cellularity in the lungs of Δ*bfrB* vaccinated animals.

4. Discussion

Primary immunity to Mtb infection in mice and humans is thought to be dependent on the type-1 T helper (Th1) cell-responses that produce interferon gamma (IFN-γ) and tumor necrosis factor alpha (TNFα) which activate macrophages within the granuloma and contribute to the control of intracellular Mtb growth [17]. However, vaccine strategies that target increased Th1 response and IFN-γ generation did not lead to enhanced protection against Mtb infection [18]. These findings have highlighted the need to identify new correlates of protection and additional protective immune mechanisms that can be targeted to improve the efficacy of Mtb vaccines [19, 20]. In this study, we investigated the potential of the attenuated Mtb Δ*bfrB* strain to confer protection against aerosol challenge with virulent Mtb in a mouse model. Due to the effects of the *bfrB* mutation on Mtb's iron homeostasis [3], expression of genes regulated directly or indirectly by iron is altered in the Δ*bfrB* (Rodriguez G.M, unpublished). We hypothesized that the protective immune response stimulated in mice upon infection by Δ*bfrB* strain could be due to the host cell exposure to specific antigens, which might not be normally expressed by the wild type strain. Importantly, Δ*bfrB* administered subcutaneously to mice was attenuated, like BCG, supporting the safety of vaccination with this strain. The level of protection conferred by Δ*bfrB*, measured as reduction in lung bacillary load,

Table 2: Expression of selected immunity related genes in vaccinated animals.

Genes	BCG		Δ*bfrB*		Immunity type
	Mean*	SE	Mean*	SE	
Il1a	1.28	0.59	1.23	0.57	Th1
Il1b	−1.09	0.10	−1.05	0.19	Th1
Il10	1.20	0.21	1.04	0.18	Th2, Th17
Il13	1.11	0.14	1.16	0.15	Th2, Th17
Il12a	−5.86	0.10	−2.21	0.28	Th1
Il12b	1.18	0.38	1.17	0.51	Th1, Th17
Il18ra	−1.04	0.18	−1.19	0.26	Th1
Ccl2	−1.09	0.11	1.13	0.07	Th17
Ccl7	−8.65	0.10	1.22	0.64	Th2, Th17
Ccl8	−4.12	0.17	5.34	4.82	Th2
Ccl12	1.81	1.04	4.78	3.64	Th17
Cxcl1	−1.72	0.38	7.13	6.25	Th17
Cxcl3	−1.27	0.37	4.92	3.40	Th2
Cxcl5	2.53	1.13	5.11	4.55	Th17
Cxcl11	−1.03	0.12	1.01	0.08	Th1
Tnfa	1.13	0.59	−2.51	0.29	Th1, Th17
Tgfb	−1.35	0.36	−1.27	0.41	Th2
Timp1	1.35	0.46	1.43	0.18	Th1, Th17
Il1r2	−1.48	0.22	−1.26	0.21	Th2
Nos2	−2.36	0.13	−1.03	0.39	Th1

*values shown are average from eight data points (duplicates of 4 animals per group).

was comparable to the standard BCG vaccination both at 4 and 8 weeks postvaccination. In addition, no significant difference was detected in the expression of a selected group of immunity related genes in the mice lungs, after vaccination with BCG or Δ*bfrB*. However, the lung histopathology and gene expression analysis, determined in animals challenged at 8 weeks postvaccination, suggested sings of an improved control of infection in Δ*bfrB* vaccinated mice, including reduced inflammation, smaller lung granulomas, and extensive fibrosis. Fibrosis is a part of tissue remodeling after injury, in which dead cells and debris accumulated during an inflammatory response are replaced. The repair process involves a regenerative phase in which injured cells are replaced by cells of the same type and a fibrosis phase in which connective tissue replaces normal tissue. In human pulmonary Tb, resorbing and healing granulomas are characterized by a fibrotic capsule that contains the infection and prevents dissemination [11]. Mature fibrotic granulomas are also associated with infection containment and resolution in some animals models of Tb [21, 22]. Though fibrosis is not commonly observed in Mtb-infected mice lungs, a differential fibrotic response was reported between resistant and susceptible strains of mice [23] and improved control of Mtb infection in the lungs of IL-10 deficient CBA/J mice was reported to be associated with fibrosis [24]. In our studies, increased fibrosis in the Δ*bfrB* vaccinated mice lungs was associated with the upregulation of fibrosis and tissue remodeling network genes, compared to BCG vaccinated animals. One of the mechanisms underlying the increased fibrosis may be linked to the upregulation of profibrotic Th2-cell responses [25] in the Δ*bfrB*, compared to BCG vaccinated, Mtb-infected mice. This is suggested by the enhanced expression of *Chil3/Ym1* encoding chitinase-3 like 1 protein, which was the most highly upregulated gene in the Δ*bfrB*-vaccinated, Mtb-infected mice and it is also upregulated by Th2 cytokines [26, 27]. In addition, Ym1 produced by dendritic cell and macrophages has Th2-inducing properties [28] and plays a critical role in inflammation, tissue remodeling, and injury. It inhibits oxidant-induced lung injury, regulates apoptosis, stimulates alternative macrophage activation, and contributes to fibrosis and wound healing. Taken together, the induction of Ym1 and its known roles in host immunity, it is possible that Ym1 and augmentation of Th2 responses may underlie the increased fibrosis and restricted disease pathology in Δ*bfrB* vaccinated, Mtb-infected mice. Future experiments will investigate that possibility.

The gene expression analyses also suggested downmodulation of inflammatory response in the Δ*bfrB* vaccinated, relative to the BCG vaccinated, Mtb-infected mice lungs. In association with this, the expression pattern of many STAT-1 mediated proinflammatory pathway genes, including *Cxcl10* (*IP-10*) and *Ccl20* that are considered biomarkers of active Tb disease, were also downregulated in the Δ*bfrB* vaccinated mice lungs [29, 30]. In contrast, expression of PC metabolism genes was upregulated in the lungs of Δ*bfrB* vaccinated mice. PC has been shown to have anti-inflammatory effects; it inhibits TNF-α induced proinflammatory responses, including actin filament assembly, activation of NF-κB, and synthesis of proinflammatory cytokines [31].

Taken together, the modulation of disease pathology and associated gene expression profile observed in the lungs of Δ*bfrB* vaccinated, compared to BCG vaccinated Mtb-infected mice, suggests that the immune response induced by the antigenic repertoire expressed by Δ*bfrB* is distinct to that induced by BCG and it may be more effective in controlling the immunopathology during Mtb infection, thus, contributing to a better control of the disease. Further studies to determine the innate and adaptive immune response as well as cytokines and chemokines induced by Δ*bfrB* compared to BCG, will help to define specific mechanisms underlying the protection elicited by Δ*bfrB*.

5. Conclusions

The attenuated ferritin mutant of Mtb (Δ*bfrB*) is able to confer protection against aerosol infection with a virulent strain of Mtb. The results shown in this study suggest that, compared to BCG vaccination, reduced inflammation, limited immunopathology, and enhanced resolution of inflammation manifested as increased fibrosis are associated with the protection provided by Δ*bfrB* vaccination.

Conflict of Interests

The authors declare that there is no conflict of interests regarding the publication of this paper.

Authors' Contribution

Selvakumar Subbian and Ruchi Pandey contributed equally to this paper.

Acknowledgments

The authors would like to thank Saleena Ghanny for her technical assistance with the microarray experiments. This work was supported by NIH Grant AI044856 (GMR).

References

[1] G. M. Rodriguez, "Control of iron metabolism in *Mycobacterium tuberculosis*," *Trends in Microbiology*, vol. 14, no. 7, pp. 320–327, 2006.

[2] R. Prados-Rosales, B. C. Weinrick, D. G. Piqué, W. R. Jacobs Jr., A. Casadevall, and G. M. Rodriguez, "Role for *Mycobacterium tuberculosis* membrane vesicles in iron acquisition," *Journal of Bacteriology*, vol. 196, no. 6, pp. 1250–1256, 2014.

[3] R. Pandey and G. M. Rodriguez, "A ferritin mutant of Mycobacterium tuberculosis is highly susceptible to killing by antibiotics and is unable to establish a chronic infection in mice," *Infection and Immunity*, vol. 80, no. 10, pp. 3650–3659, 2012.

[4] M.-S. Koo, S. Subbian, and G. Kaplan, "Strain specific transcriptional response in *Mycobacterium tuberculosis* infected macrophages," *Cell Communication and Signaling*, vol. 10, article 2, 2012.

[5] D. Averbuch, A. Chapgier, S. Boisson-Dupuis, J.-L. Casanova, and D. Engelhard, "The clinical spectrum of patients with deficiency of signal transducer and activator of transcription-1," *Pediatric Infectious Disease Journal*, vol. 30, no. 4, pp. 352–355, 2011.

[6] R. Condos, B. Raju, A. Canova et al., "Recombinant gamma interferon stimulates signal transduction and gene expression in alveolar macrophages in vitro and in tuberculosis patients," *Infection and Immunity*, vol. 71, no. 4, pp. 2058–2064, 2003.

[7] G. S. Tomlinson, T. J. Cashmore, P. T. G. Elkington et al., "Transcriptional profiling of innate and adaptive human immune responses to mycobacteria in the tuberculin skin test," *European Journal of Immunology*, vol. 41, no. 11, pp. 3253–3260, 2011.

[8] S. Subbian, N. Bandyopadhyay, L. Tsenova et al., "Early innate immunity determines outcome of Mycobacterium tuberculosis pulmonary infection in rabbits," *Cell Communication and Signaling*, vol. 11, no. 1, article 60, 2013.

[9] M. Kiss, Z. Czimmerer, and L. Nagy, "The role of lipid-activated nuclear receptors in shaping macrophage and dendritic cell function: from physiology to pathology," *Journal of Allergy and Clinical Immunology*, vol. 132, no. 2, pp. 264–286, 2013.

[10] S. Mahajan, H. K. Dkhar, V. Chandra et al., "*Mycobacterium tuberculosis* modulates macrophage lipid-sensing nuclear receptors PPARγ and TR4 for survival," *Journal of Immunology*, vol. 188, no. 11, pp. 5593–5603, 2012.

[11] R. L. Hunter, "Pathology of post primary tuberculosis of the lung: an illustrated critical review," *Tuberculosis*, vol. 91, no. 6, pp. 497–509, 2011.

[12] J. M. Sand, L. Larsen, C. Hogaboam et al., "MMP mediated degradation of type IV collagen alpha 1 and alpha 3 chains reflects basement membrane remodeling in experimental and clinical fibrosis—validation of two novel biomarker assays," *PLoS ONE*, vol. 8, no. 12, Article ID e84934, 2013.

[13] D. Fan, A. Takawale, R. Basu et al., "Differential role of TIMP2 and TIMP3 in cardiac hypertrophy, fibrosis, and diastolic dysfunction," *Cardiovascular Research*, vol. 103, no. 2, pp. 268–280, 2014.

[14] K. E. Nakken, S. Nygård, T. Haaland et al., "Multiple inflammatory-, tissue remodelling- and fibrosis genes are differentially transcribed in the livers of Abcb4 (-/-) mice harbouring chronic cholangitis," *Scandinavian Journal of Gastroenterology*, vol. 42, no. 10, pp. 1245–1255, 2007.

[15] K. Chen and J. K. Kolls, "T cell-mediated host immune defenses in the lung," *Annual Review of Immunology*, vol. 31, pp. 605–633, 2013.

[16] A. M. Cooper, "Cell-mediated immune responses in tuberculosis," *Annual Review of Immunology*, vol. 27, pp. 393–422, 2009.

[17] A. M. Cooper and S. A. Khader, "The role of cytokines in the initiation, expansion, and control of cellular immunity to tuberculosis," *Immunological Reviews*, vol. 226, no. 1, pp. 191–204, 2008.

[18] I. S. Leal, B. Smedegård, P. Andersen, and R. Appelberg, "Failure to induce enhanced protection against tuberculosis by increasing T-cell-dependent interferon-γ generation," *Immunology*, vol. 104, no. 2, pp. 157–161, 2001.

[19] S. C. Cowley and K. L. Elkins, "$CD4^+$ T cells mediate IFN-γ-independent control of *Mycobacterium tuberculosis* infection both in vitro and in vivo," *The Journal of Immunology*, vol. 171, no. 9, pp. 4689–4699, 2003.

[20] A. M. Gallegos, J. W. J. van Heijst, M. Samstein, X. Su, E. G. Pamer, and M. S. Glickman, "A gamma interferon independent mechanism of CD4 T cell mediated control of *M. tuberculosis* infection in vivo," *PLoS Pathogens*, vol. 7, no. 5, Article ID e1002052, 2011.

[21] O. Gil, I. Díaz, C. Vilaplana et al., "Granuloma encapsulation is a key factor for containing tuberculosis infection in minipigs," *PLoS ONE*, vol. 5, no. 4, Article ID e10030, 2010.

[22] D. J. Ordway, C. A. Shanley, M. L. Caraway et al., "Evaluation of standard chemotherapy in the guinea pig model of tuberculosis," *Antimicrobial Agents and Chemotherapy*, vol. 54, no. 5, pp. 1820–1833, 2010.

[23] J.-F. Marquis, A. Nantel, R. LaCourse, L. Ryan, R. J. North, and P. Gros, "Fibrotic response as a distinguishing feature of resistance and susceptibility to pulmonary infection with *Mycobacterium tuberculosis* in mice," *Infection and Immunity*, vol. 76, no. 1, pp. 78–88, 2008.

[24] J. C. Cyktor, B. Carruthers, R. A. Kominsky, G. L. Beamer, P. Stromberg, and J. Turner, "IL-10 inhibits mature fibrotic granuloma formation during mycobacterium tuberculosis infection," *Journal of Immunology*, vol. 190, no. 6, pp. 2778–2790, 2013.

[25] T. A. Wynn, "Fibrotic disease and the TH1/TH2 paradigm," *Nature Reviews Immunology*, vol. 4, no. 8, pp. 538–594, 2004.

[26] M. G. Nair, I. J. Gallagher, M. D. Taylor et al., "Chitinase and Fizz family members are a generalized feature of nematode infection with selective upregulation of Ym1 and Fizz1 by antigen-presenting cells," *Infection and Immunity*, vol. 73, no. 1, pp. 385–394, 2005.

[27] J. S. Welch, L. Escoubet-Lozach, D. B. Sykes, K. Liddiard, D. R. Greaves, and C. K. Glass, "T_H2 cytokines and allergic challenge induce Ym1 expression in macrophages by a STAT6-dependent mechanism," *The Journal of Biological Chemistry*, vol. 277, no. 45, pp. 42821–42829, 2002.

[28] M. Arora, L. Chen, M. Paglia et al., "Simvastatin promotes Th2-type responses through the induction of the chitinase family member Ym1 in dendritic cells," *Proceedings of the National Academy of Sciences of the United States of America*, vol. 103, no. 20, pp. 7777–7782, 2006.

[29] M. Liu, S. Guo, J. M. Hibbert et al., "CXCL10/IP-10 in infectious diseases pathogenesis and potential therapeutic implications," *Cytokine & Growth Factor Reviews*, vol. 22, no. 3, pp. 121–130, 2011.

[30] J.-S. Lee, J.-Y. Lee, J. W. Son et al., "Expression and regulation of the CC-chemokine ligand 20 during human tuberculosis," *Scandinavian Journal of Immunology*, vol. 67, no. 1, pp. 77–85, 2008.

[31] I. Treede, A. Braun, R. Sparla et al., "Anti-inflammatory effects of phosphatidylcholine," *The Journal of Biological Chemistry*, vol. 282, no. 37, pp. 27155–27164, 2007.

Hindawi Publishing Corporation
Journal of Immunology Research
Volume 2015, Article ID 793292, 14 pages
http://dx.doi.org/10.1155/2015/793292

Research Article

Impairments of Antigen-Presenting Cells in Pulmonary Tuberculosis

Ludmila V. Sakhno,[1] Ekaterina Ya. Shevela,[1] Marina A. Tikhonova,[1] Sergey D. Nikonov,[2] Alexandr A. Ostanin,[1] and Elena R. Chernykh[1]

[1]*Research Institute of Clinical Immunology, Russian Academy of Medical Sciences (RAMS), Siberian Branch (SB), Yadrintsevskaya Street 14, Novosibirsk 630099, Russia*
[2]*Novosibirsk Tuberculosis Clinical Hospital No. 1, Vavilova Street 14, Novosibirsk 630082, Russia*

Correspondence should be addressed to Ludmila V. Sakhno; lsahno53@mail.ru

Received 19 September 2014; Revised 16 December 2014; Accepted 16 December 2014

Academic Editor: Vishwanath Venketaraman

The phenotype and functional properties of antigen-presenting cells (APC), that is, circulating monocytes and generated *in vitro* macrophages and dendritic cells, were investigated in the patients with pulmonary tuberculosis (TB) differing in lymphocyte reactivity to *M. tuberculosis* antigens (PPD-reactive versus PPD-anergic patients). We revealed the distinct impairments in patient APC functions. For example, the monocyte dysfunctions were displayed by low CD86 and HLA-DR expression, 2-fold increase in $CD14^+CD16^+$ expression, the high numbers of IL-10-producing cells, and enhanced IL-10 and IL-6 production upon LPS-stimulation. The macrophages which were *in vitro* generated from peripheral blood monocytes under GM-CSF were characterized by Th1/Th2-balance shifting (downproduction of IFN-γ coupled with upproduction of IL-10) and by reducing of allostimulatory activity in mixed lymphocyte culture. The dendritic cells (generated *in vitro* from peripheral blood monocytes upon GM-CSF + IFN-α) were characterized by impaired maturation/activation, a lower level of IFN-γ production in conjunction with an enhanced capacity to produce IL-10 and IL-6, and a profound reduction of allostimulatory activity. The APC dysfunctions were found to be most prominent in PPD-anergic patients. The possible role of APC impairments in reducing the antigen-specific T-cell response to *M. tuberculosis* was discussed.

1. Introduction

The immune response against *M. tuberculosis* (*Mtb*) is a complex process which involves many components of immune system. Professional antigen-presenting cells (APCs), including monocytes/macrophages and dendritic cells (DCs), play a major role in generating a protective immune response against *Mtb* by presenting antigens to T cells, recruiting immune cells at the site of infection, and directing T-cell response [1–3]. Therefore, functional impairments of APCs are considered to be an important mechanism of immune escape leading to *Mtb* persistence. Defective functions of APCs can be caused by a direct effect of *Mtb* on expression of surface molecules and production of cytokines by infected macrophages and DCs [4, 5]. *Mtb* impairs DC maturation, reduces their ability to present mycobacterial antigens and to stimulate specific $CD4^+$ T cells, inhibits secretion of IL-12 by DCs, and increases production of IL-10 which is able to suppress T-cell response and migration of DCs to draining lymph nodes [6–10]. Interaction of macrophages with pathogen causes pronounced alterations of phagosome function and suppresses their antigen-presenting function through the inhibition of synthesis and expression of MHC class II molecules [11–14].

Importantly, blood monocytes represent an important source of APCs capable of migrating to the infected site and differentiating into macrophages and DCs. Despite the absence of direct infection of circulating monocytes with *Mtb* many studies reported an altered phenotype and functions of monocytes in pulmonary tuberculosis [15–17]. Given an important role of monocytes as precursors of

DCs and macrophages, their dysfunctions can result in pronounced impairments of monocyte-derived DCs (MDDC) and monocyte-derived macrophages (MDM).

In the present study we investigated whether blood monocytes, MDM and MDDC obtained from TB patients and healthy donors, differed in any significant way. Besides we attempted to clarify whether impairments of antigen-presenting function and cytokine secretion are similar in different APC types and how they are related to the defect of the antigen specific T-cell response in pulmonary tuberculosis. As T-cell impairments in pulmonary TB patients are manifested *in vitro* by downregulation of proliferative activity and/or production of IFN-γ in response to tuberculin purified protein derivative (PPD) [6, 18], the comparative analysis of APCs was conducted not only between TB patients and healthy subjects, but also between PPD-anergic and PPD-reactive patients.

2. Materials and Methods

2.1. Patients. The patients with active pulmonary tuberculosis (TB) were recruited from Novosibirsk Tuberculosis Clinical Hospital No. 1. The study involved 192 patients with pulmonary TB (125 males and 67 females aged from 20 to 64 years) including 68 with fibrocavernous, 100 with infiltrative, and 24 with disseminated TB. Positive for *M. tuberculosis* sputum specimens were revealed in 123 patients. Multidrug resistance (MDR) was registered in 69 patients. The TB patients underwent the standard antimicrobial treatment, including first-line drugs (combination of tubazid, rifampicin, streptomycin, ethambutol, and pyrazinamide) and in patients with MDR the second-line drugs (the combination of fluoroquinolones with amikacin or kanamycin, capriomycin, and cycloserine). The control group included 90 sex- and age-matched healthy subjects. The signed informed consent was obtained before the examination from all the patients.

2.2. Isolation of Cells and Evaluation of Proliferative Response. Mononuclear cells (MNCs) were isolated from heparinized venous blood by Ficoll-Verographin density gradient centrifugation and cultivated in 96-well plates (0.1×10^6 per well) in RPMI-1640 (Sigma-Aldrich, USA) medium, completed with 0.3 mg/mL L-glutamine, 5 mM HEPES buffer, 100 μg/mL gentamycin, and 10% inactivated human AB serum. In order to stimulate cell proliferative response, tuberculin-purified protein derivative (PPD) was used in a dose of 50 μg/mL. Proliferation intensity was evaluated on the 6th day based on ^{3}H-thymidine incorporation (1 μCi per well), adding 18 hours before the end of cultivation. Depending on proliferative response level, patients were divided into 2 subgroups: those with retained (>12,500 cpm; PPD-reactive TB patients) and those with reduced (<12,500 cpm; PPD-anergic TB patients) response to PPD.

2.3. Isolation of Monocytes and Generation of Monocyte-Derived Macrophages and Monocyte-Derived Dendritic Cells. Monocytes (Mo) were isolated in 6-well plates (Nuclon, Denmark) by adhesion of MNCs (3×10^6 cells/mL) to the plastic in the presence of 5% human AB serum. Monocyte-derived macrophages (MDM) were generated by culturing adherent fraction of MNCs during 7 days in RPMI-1640 medium completed with 5% autoplasma, 2% fetal calf serum (FCS, Biolot, Russia), 2-mercaptoethanol (5×10^{-5} M, Serva, Germany), pyruvate Na (2×10^{-3} M, Sigma-Aldrich, USA), and 1% nonessential amino acid solution in the presence of GM-CSF (50 ng/mL, Sigma-Aldrich, USA). In 7 days macrophages were harvested using 0.25% trypsin/EDTA solution. Monocyte-derived dendritic cells (MDDC) were generated by culturing adherent fraction of MNCs during 4 days in RPMI-1640 medium with 5% FCS in the presence of GM-CSF (40 ng/mL) and IFN-α (1,000 U/mL, Roferon-A, Roche, Switzerland), followed by maturation over 24 hours in the presence of 10 μg/mL lipopolysaccharide (LPS *E. coli* 0111:B4, Sigma-Aldrich, USA).

2.4. Phenotypic Analysis of Mo, MDM, and MDDC. Evaluation of surface markers expression on antigen-presenting cells was conducted with phycoerythrin- (PE-) labeled monoclonal anti-CD14 antibodies and FITC-labeled anti-CD16, CD25, CD83, CD86, and HLA-DR (PharMingen, USA) using flow cytofluorometry (FASC Calibur, Becton Dickinson, USA). To evaluate $CD14^+CD16^+$ cells, Mo were incubated with FITC-labeled anti-CD16 and PE-labeled anti-CD14 antibodies and then two-color cytometry analysis was conducted.

2.5. Intracellular Cytokine Assay. The estimation of intracellular expression of TNF-α and IL-10 in $CD14^+$ Mo was performed by flow cytometry assays using permeabilization of cells. The number of cells with intracellular expression of TNF-α or IL-10 was estimated in monocytic gate using PerCP-labeled anti-CD14, FITC-labeled anti-TNF-α, and PE-labeled anti-IL-10 antibodies (Becton Dickinson).

2.6. The Estimation of Cytokine-Secreting Activity of Mo, MDM, and MDDC. The cytokines were assessed in 7-day MDM culture supernatants and in 5-day MDDC culture supernatants which were collected and stored at −80°C until measurement. The concentrations of TNF-α, IFN-γ, IL-6, IL-10, and IL-18 were evaluated by commercial ELISA kits (Vector-Best, Russia). The production of IL-6 and IL-10 was measured in Mo cultures which were harvested, washed, and then cultivated for additional 48 h with or without LPS (10 μg/mL).

2.7. Evaluation of Allostimulatory Activity of MDM and MDDC. Allostimulatory activity of MDM and MDDC was evaluated in mixed lymphocyte culture (MLC) after cultivation of donor MNCs (0.1×10^6/well) in round-bottom 96-well plates in the presence of allogeneic antigen-presenting cells from donors or TB patients in the ratio 10 : 1. Proliferation intensity was evaluated using radiometry on the 5th day based on ^{3}H-thymidine incorporation.

2.8. Statistical Analysis. Statistical analysis was carried out using software package "Statistica 6.0." To reveal

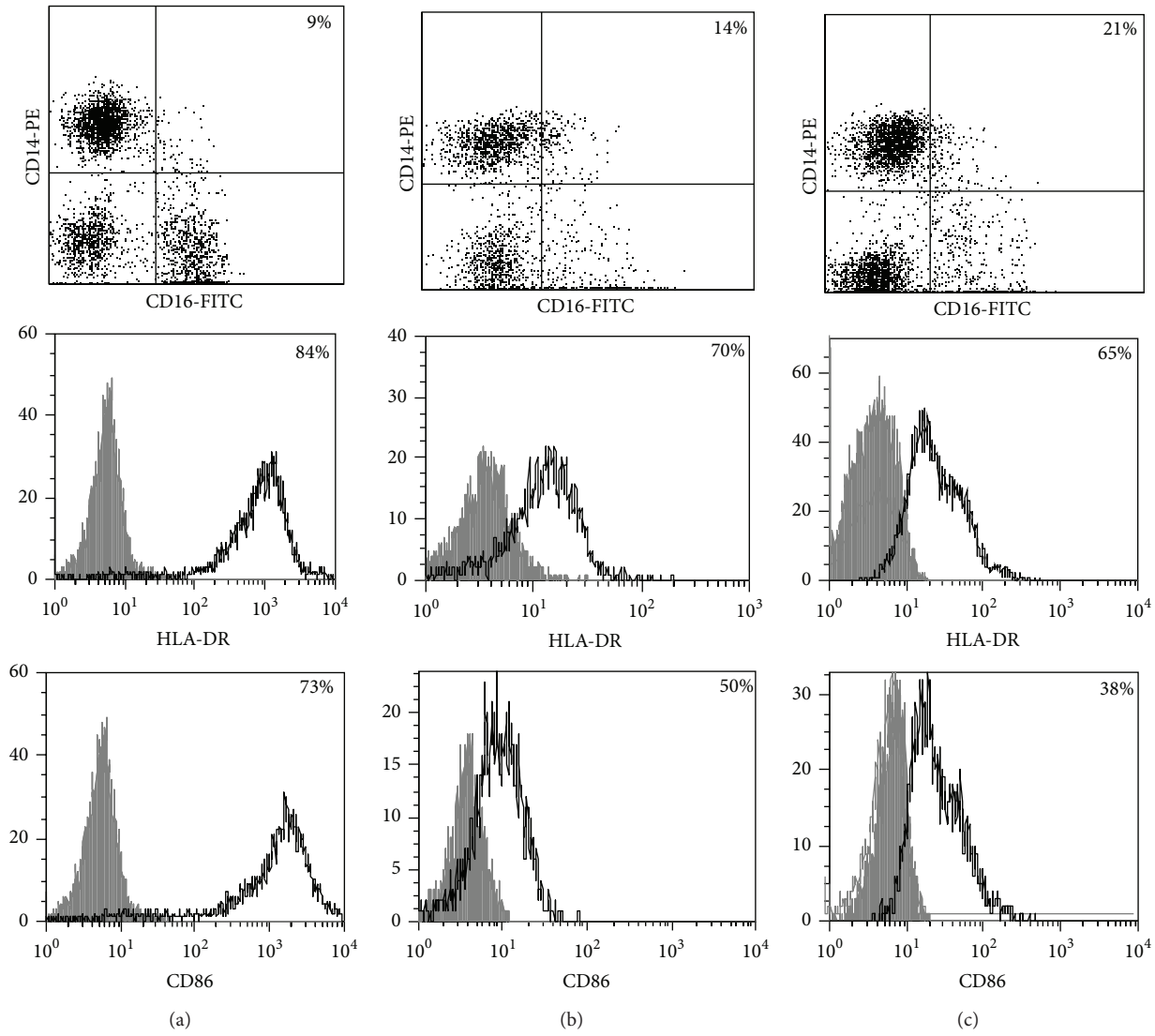

Figure 1: Surface antigen expression on circulating monocytes obtained from peripheral blood of TB patients (a), PPD-reactive (b) and PPD-anergic (c) TB patients. Open histogram represents stained cells (patient Mo) and the filled histogram represents isotype specific control.

significant difference of values compared, nonparametric Mann-Whitney U test was employed. The level of $P < 0.05$ was considered significant. Spearman rank correlation was used to investigate relationships between characteristics.

3. Results

Phenotypic analysis of freshly isolated monocytes (Table 1, Figure 1) revealed that monocytes from TB patients had a lower number of HLA-DR$^+$ and CD86$^+$ cells. Monocytes obtained from both PPD-reactive and PPD-anergic patients showed a decrease in HLA-DR and CD86 expression. Besides, TB patients demonstrated a significant increase in CD14$^+$CD16$^+$ monocytes, the level of which on average twice exceeded that of healthy subjects. The most pronounced increase in CD14$^+$CD16$^+$ monocytes was revealed in the PPD-anergic patients. The elevated rate (>17%) of CD14$^+$CD16$^+$ cells in this group (62%, 16/26) was observed twice oftener than among patients with the undiminished proliferative MNC response to PPD (26%, 10/39, $P_{\text{TM}\Phi} = 0.04$).

An evaluation of intracellular cytokine expression showed that monocytes from TB patients were characterized by a 3-fold decrease of TNF-α-secreting cells and a 6-fold increase of IL-10 secreting cells as compared to monocytes from healthy subjects (Figure 2). What is more, there appeared to exist an inverse correlation ($r_S = -0.62$, $P_S < 0.01$; $n = 19$) between the numbers of CD14$^+$CD16$^+$ cells and TNF-α^+ monocytes.

To ascertain whether an increase in IL-10$^+$ monocytes was accompanied by an increased production of immunosuppressive/anti-inflammatory cytokines we additionally evaluated the production of IL-10 and IL-6 in 48-hour monocyte cultures. Concentrations of IL-6 and IL-10

Table 1: The phenotypic characteristics of monocytes obtained from peripheral blood of healthy donors and TB patients.

Markers (%)	Healthy donors	TB patients		
		All patients	PPD-reactive patients	PPD-anergic patients
$CD14^+CD16^+$	8.9 ± 1.2 (15)	18.0 ± 1.2 (65)*	15.4 ± 1.0 (39)*	21.4 ± 2.4 (26)*#
$HLA\text{-}DR^+$	84.1 ± 1.5 (10)	69.7 ± 1.8 (72)*	69.8 ± 2.2 (50)*	69.1 ± 3.7 (22)*
$CD86^+$	66.1 ± 4.5 (9)	48.3 ± 4.9 (18)*	48.6 ± 5.4 (12)*	40.5 ± 4.6 (6)*

The relative numbers of Mo (M ± S.E.) expressing different markers were presented in healthy donors and TB patients (the whole group), including PPD-reactive and PPD-anergic TB patients. The number of cases is indicated in parentheses. *$P_U < 0.05$ (Mann-Whitney U-criterion) with healthy donors; #$P_U < 0.05$ between PPD-reactive and PPD-anergic TB patients.

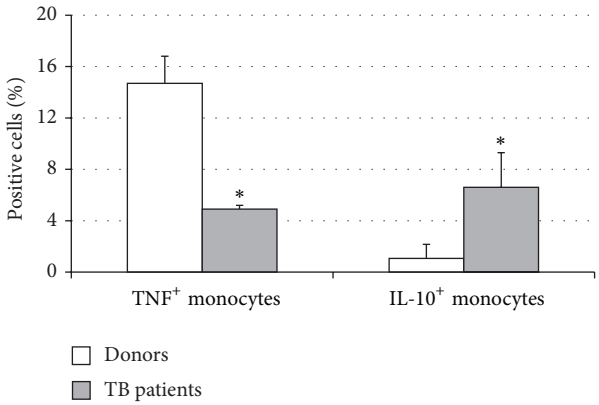

Figure 2: The spontaneous intracellular expression of TNF-α and IL-10 in donor ($n = 8$) and TB patient ($n = 8$) circulating $CD14^+$ monocytes. The data are presented as M ± S.E. *$P_U < 0.05$ (Mann-Whitney U-criterion) between healthy donors and TB patients.

in LPS-stimulated supernatants from patient monocyte cultures (Table 2) were significantly higher than in donor cultures. Notably, the most pronounced increase of LPS-induced production of IL-6 and IL-10 was registered in PPD-anergic patients. The obtained data showed TB infection is associated with a decrease in proinflammatory and an increase in anti-inflammatory/immunosuppressive activity which resulted in suppressing of PPD-response.

Considering the monocyte dysfunctions in TB patients, we further investigated the monocyte-derived macrophages (MDM). MDM viability on 7th day was no lower than 90% in all experiments. MDM yield was found to be similar in donors and TB patients (29,000 ± 4,000 and 31,000 ± 5,000/10^6 MNC, resp.). Phenotypic analysis (Table 3) showed that both donor and patient MDM were highly positive (about 80%) for CD 14. MDM from TB patients with PPD-anergy displayed a significant decrease of $HLA\text{-}DR^+$ and $CD86^+$ cells, whereas the expression of these molecules on MDM from PPD-reactive patients did not differ from that of donors. In contrast to monocytes, an increased number of MDM expressing CD16 (about 50%) was found in patients with the intact response to PPD that was significantly higher than in donors and patients with lowered PPD-induced proliferative response. These data mean the regulatory functions of $CD16^+$ monocytes and $CD16^+$MDM could differ. Thus, MDM from patients with an adequate antigen-specific response do not differ in expression of antigen-presenting and costimulatory molecules from donor MDM while MDM from PPD-anergic patients show a lowered expression of molecules necessary for an effective antigen presentation and T-lymphocyte costimulation.

An important function of MDM during immune response is cytokine production. An analysis of cytokine concentration in 7-day patient MDM cultures did not reveal a significant difference in the TNF-α, IL-6, and IL-18 levels as compared to healthy individuals. At the same time MDM from PPD-reactive and PPD-anergic patients displayed a 10-fold decrease of IFN-γ production. However, concentration of IL-10 in MDM cultures from PPD-anergic patients was 3 times higher than in MDM cultures from healthy subjects and PPD-reactive patients. These results testified to a higher MDM immunosuppressing potential in patients with decreased PPD response.

An evaluation of MDM allostimulatory activity in a mixed lymphocyte culture revealed that macrophages from PPD-reactive patients, similar to donor MDM, effectively stimulated the proliferation of allogeneic MNC (Table 4).

At the same time a proliferative response of alloantigen-stimulated T-lymphocytes induced by MDM from PPD-anergic patients was almost 6 times lower as compared to donors ($P_U < 0.05$). Thus, the lowered expression of antigen-presenting and costimulatory molecules and the increased level of IL-10 production by MDM obtained from PPD-anergic patients were associated with a decreased macrophage ability to stimulate T-cell proliferation in a mixed lymphocyte culture.

Thereafter, we compared phenotypic and functional properties of monocyte-derived dendritic cells (MDDC) in TB patients and healthy individuals. Donor and patient MDDC yield did not differ and comprised accordingly 27,000 ± 7,000 and 35,000 ± 6,000/10^6 MNC. In addition, donor and patient MDDC did not vary in the number of $HLA\text{-}DR^+$ and $CD83^+$ cells (Table 5). Nevertheless, patient MDDC were characterized by an increased level of $CD14^+$ cells more pronounced in PPD-anergic patients and a decreased level of $CD25^+$ cells registered in patients with both a lowered and an intact proliferative response of MNC to PPD.

Evaluation of cytokine levels in 5-day DC cultures showed that patient MDDC were characterized by an increased production of IL-6 and Il-10 and highly decreased level of IFN-γ (Table 4). It is typical that IL-10 production in MDDC cultures from PPD-anergic patients was significantly higher than in MDDC cultures from PPD-reactive patients. When investigating MDDC allostimulatory activity, we discovered that patient MDDC possessed an impaired ability to stimulate

Table 2: The production of cytokines by Mo obtained from peripheral blood of healthy donors and TB patients.

Cytokine (pg/mL)	Stimulator	Healthy donors ($n = 8$)	TB patients		
			All patients ($n = 17$)	PPD-reactive patients ($n = 8$)	PPD-anergic patients ($n = 9$)
IL-6	0	1,509 ± 781	2,995 ± 390	2,748 ± 756	3,206 ± 374
	LPS	1,902 ± 720	4,015 ± 315*	3,596 ± 708	4,329 ± 146*
IL-10	0	27 ± 17	59 ± 12.8	59 ± 19.4	58 ± 18.1
	LPS	70 ± 30.9	201 ± 44.7*	166 ± 65.5	233 ± 62.8*

The average values (M ± S.E.) of spontaneous (0) and LPS-stimulated (LPS) cytokine production in 48-hour cultures of monocytes (10^5/per well) obtained from peripheral blood of healthy individuals and TB patients were presented. * $P_U < 0.05$ (Mann-Whitney U-criterion) with healthy donors.

T-cell proliferative response in mixed lymphocyte cultures (Table 4). The most pronounced defect of MDDC allostimulatory activity was found in PPD-anergic patients.

4. Discussion

Our data conclusively show that in TB patients phenotypic and functional disorders are typical both for circulating monocytes and for MDM and MDDC. Our results displaying a decrease in HLA-DR$^+$ and CD86$^+$ monocytes and an increase in CD14$^+$CD16$^+$ cells in pulmonary tuberculosis confirm the results of other investigators [19, 20]. Balboa et al. showed that CD14$^+$CD16$^+$ cell functions could significantly differ depending on their localization [17]. For example, CD16$^+$ monocytes in pleural effusion represent effective APCs since these monocytes express receptors for *Mtb* recognition and antigen presentation (DC-SIGN, MR, CD11b, and CD1b). At the same time increase in peripheral blood CD16$^+$ monocytes is associated with the severity of pulmonary TB. In this respect our data showing a more pronounced augmentation of CD14$^+$CD16$^+$ monocytes in PPD-anergic patients which differ by higher severity [18] is still another argument of an unfavorable prognostic role of CD16$^+$ monocytes in pulmonary tuberculosis. We should note that CD14$^+$CD16$^+$ monocytes are characterized by an increased proinflammatory activity [21] and according to Balboa the number of these cells in circulation correlates with TNF-α level in blood plasma [17]. Nevertheless, we found an inverse correlation ($r_S = -0.62$, $P < 0.01$) between the number of CD14$^+$CD16$^+$ cells and a percentage of monocytes with an intracellular TNF-α expression. Earlier we showed that the number of IL-10$^+$ cells within CD16$^+$ population is significantly higher in TB patients than in healthy subjects [15]. These data together with our present results showing that the most pronounced increase of CD14$^+$CD16$^+$ cells in PPD-anergic patients was associated with the highest increase of IL-10 can testify to a high monocyte suppressive activity and its crucial role in suppressing an antigen specific response.

We should note that monocyte alterations were found in TB patients regardless of the level of antigen specific response though some parameters (i.e., the number of CD14$^+$CD16$^+$ cells, IL-6 and IL-10 production) were more pronounced in PPD-anergic patients. At the same time an impaired macrophage function (i.e., a decreased number of CD86$^+$ and HLA-DR$^+$ cells, an increased IL-10 production, and a decreased ability to stimulate allogeneic T-cell proliferation) was only typical for MDM from PPD-anergic patients.

The main approach to study macrophages during TB in humans is an analysis of how *Mtb* interferes with these cells. MDM generated in the presence of *Mtb* were previously observed to have decreased MHC class II, CD68, CD86, and CD36 expression [16]. Additionally, *Mtb*-infected monocyte-derived macrophages were found to produce the immunosuppressive cytokine IL-10 which inhibited IL-12 secretion [2]. Nagabhushanam et al. showed that IL-6 secreted by *Mtb*-infected macrophages inhibits the responses to IFN-γ [12], thus limiting the ability of IFN-γ to stimulate macrophages to kill *Mtb*. In the present study we were the first to describe the properties of monocyte-derived macrophages from active TB patients and to show that an impairment of monocyte-derived macrophages is similar to the impairment observed upon infecting macrophages with *Mtb*.

In contrast to MDM, MDDC dysfunction was found in both PPD-anergic and PPD-reactive patients, but it was more pronounced in patients with a decreased PPD response. Earlier Rajashree et al. showed that TB patient MDDC generated with GM-CSF and IL-4 are characterized by downregulation of CD1a, MHC class II, CD80, and CD83 expression and impaired allostimulatory activity [22]. In turn, Balboa et al. showed that the impairment of DC maturation in GM-CSF and IL-4 cultures was caused by a high content of CD16$^+$ monocytes [23] which differentiated into a CD1a$^-$DC-SIGN^{low} population characterized by a poor mycobacterial Ag-presenting capacity. In our study we generated MDDC with GM-CSF and IFN-α. This type of DCs has a number of phenotypic and functional differences from IL-4-derived DCs [24–26]. At the same time, a typical feature of MDDC in our study was a decreased ability to stimulate allogeneic T-cell proliferation. Thus, DC impairments were revealed not only in IL-4-derived DCs but also in IFN-derived cells.

A common MDM/MMDC functional defect is an impairment of their secretory activity (IFN-γ production deficit in couple with an increased IL-10 secreting activity) and a decreased ability to stimulate allogeneic T-cell proliferation. The cell-mediated immune response is known to be critical in the host defense against *Mtb*. Activated T helper 1 (Th1) lymphocytes play an important role in granuloma formation and through production of IFN-γ stimulate the antimicrobial activity of infected macrophages, allowing intracellular bacterial killing. In contrast, IL-10 inhibits antimicrobial effector

Table 3: Surface antigen expression on monocyte-derived macrophages from TB patients (A), PPD-reactive (B) and PPD-anergic (C) TB patients. (I) Open histogram represents stained cells and the filled histogram represents isotype specific control. (II) The number of $CD14^+$, $CD16^+$, $HLA\text{-}DR^+$, and $CD86^+$ MDM is presented as M ± S.E. $^*P_U < 0.05$ (Mann-Whitney U-criterion) with healthy donors; $^\#P_U < 0.05$ between PPD-reactive and PPD-anergic TB patients.

MDM	(A)	(B)	(C)
(I)			
CD14	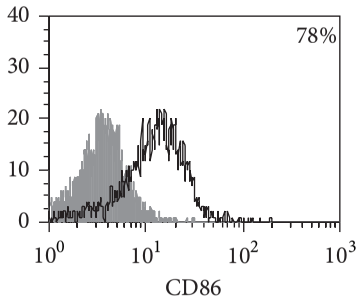	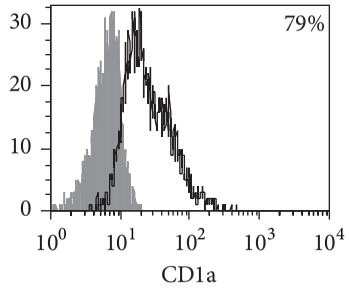	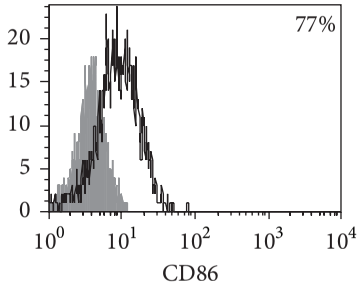
CD16	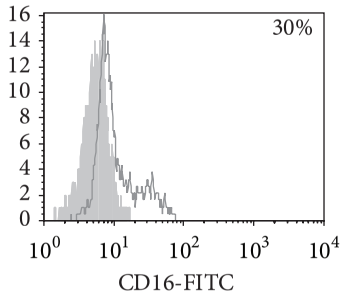	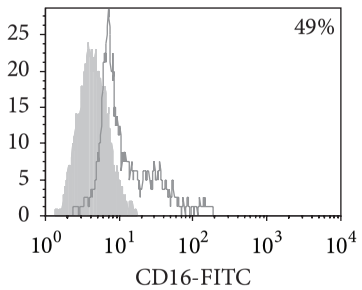	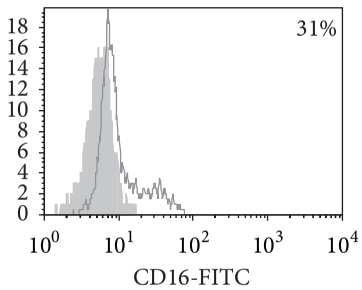
HLA-DR	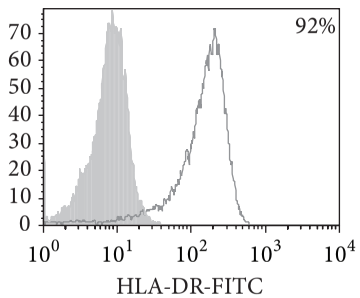	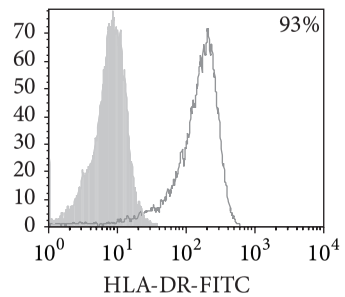	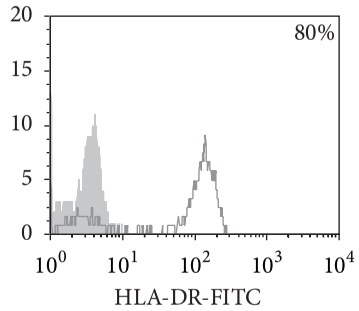

Table 3: Continued.

MDM	(A)	(B)	(C)
CD86	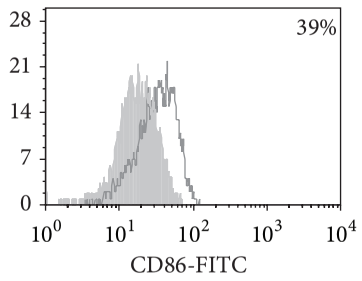	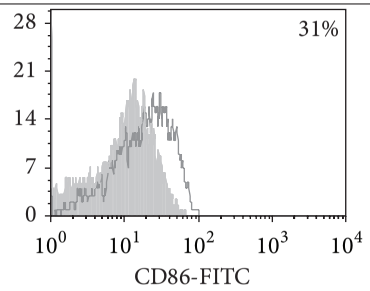	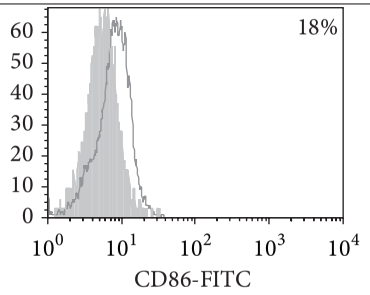
(II)	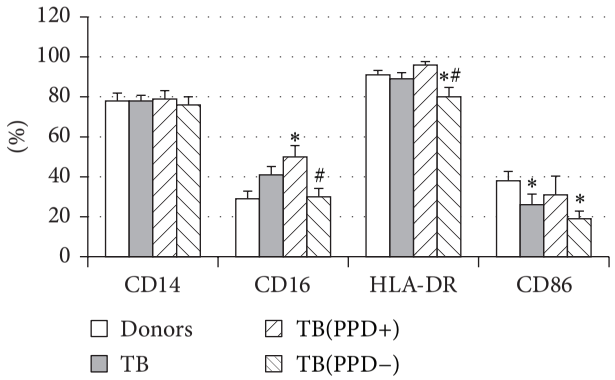		

Table 4: Secretory and allostimulatory activities of MDM and MDDC. The data are presented as M ± S.E. $^{*}P_U < 0.05$ (Mann-Whitney U-criterion) with healthy subjects; $^{\#}P_U < 0.05$ between PPD-reactive and PPD-anergic TB patients.

MDM	MDDC
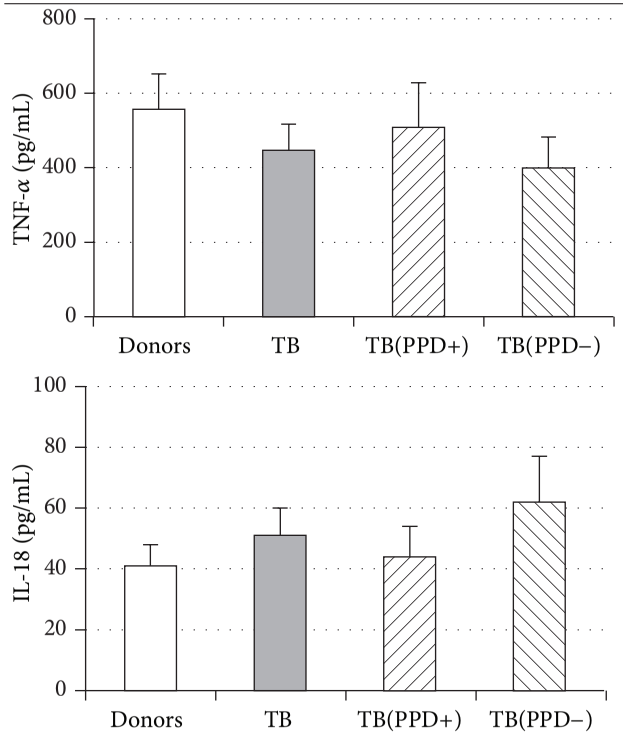	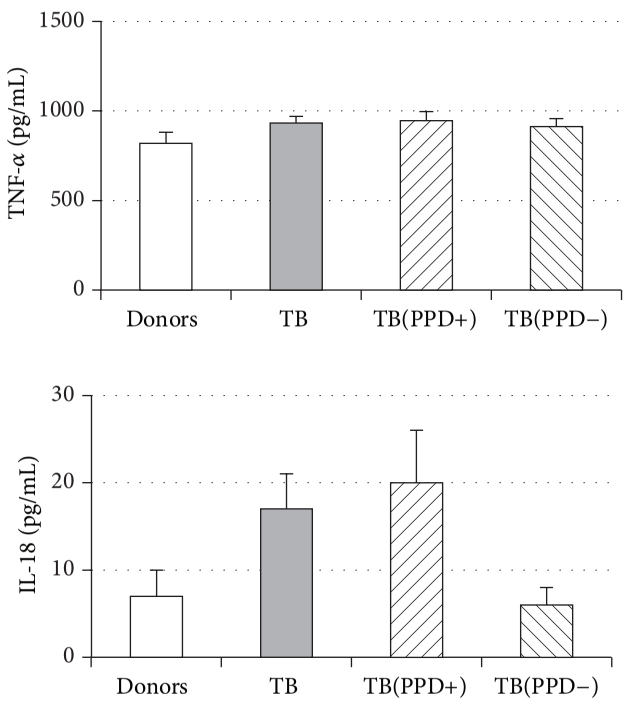

Table 4: Continued.

MDM	MDDC
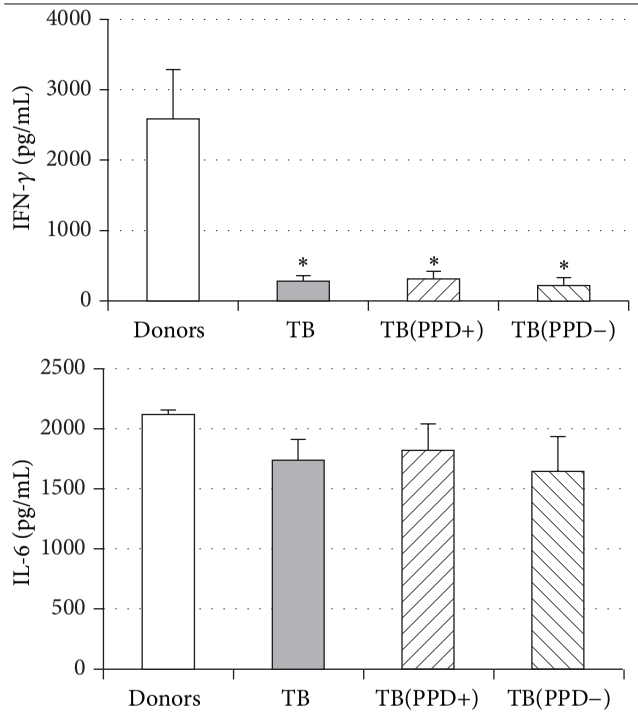	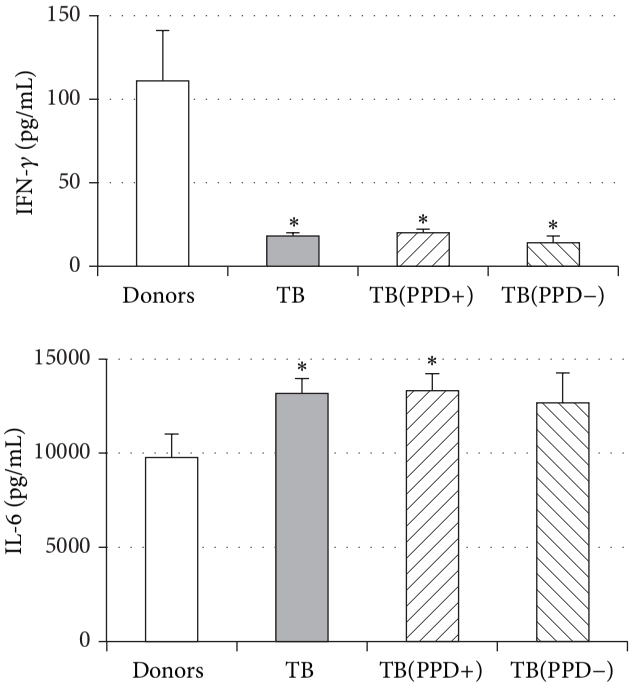

Table 4: Continued.

MDM	MDDC
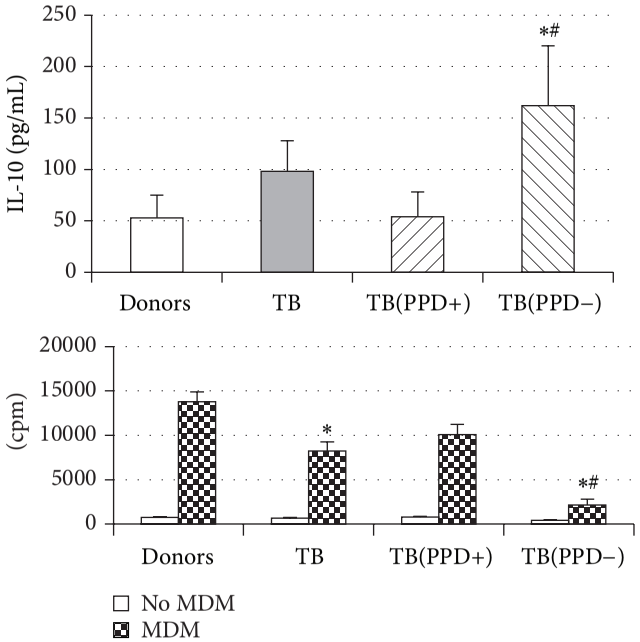	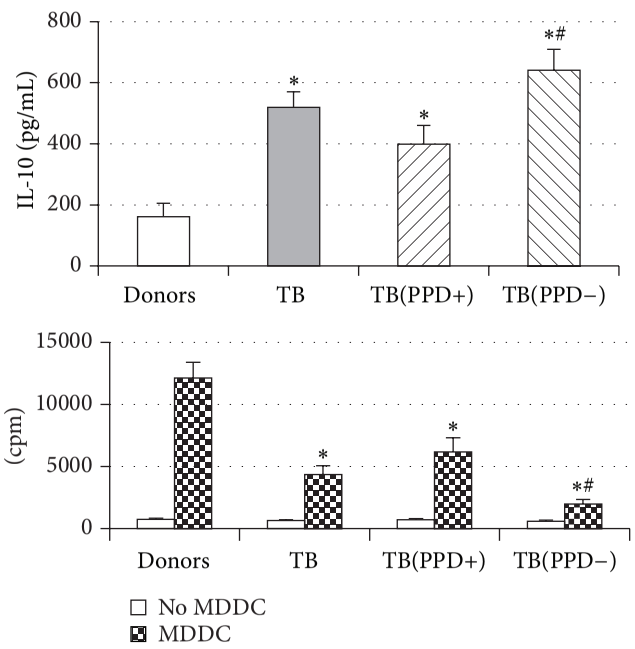

Table 5: Surface antigen expression on monocyte-derived DCs from TB patients (A), PPD-reactive (B) and PPD-anergic (C) TB patients. (I) Open histogram represents stained cells and the filled histogram represents isotype specific control. (II) The number of $CD14^+$, $CD25^+$, $HLA\text{-}DR^+$, and $CD83^+$ MDDC is presented as M ± S.E. $^*P_U < 0.05$ (Mann-Whitney U-criterion) with healthy subjects; $^\#P_U < 0.05$ between PPD-reactive and PPD-anergic TB patients.

MDDC	A	B	C
CD14	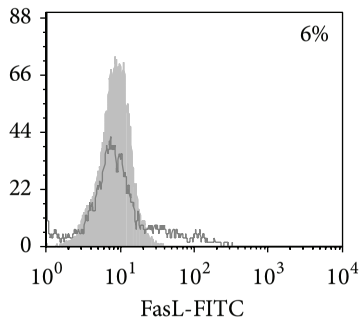	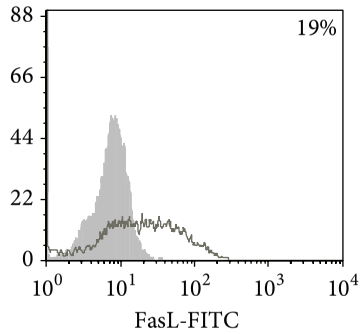	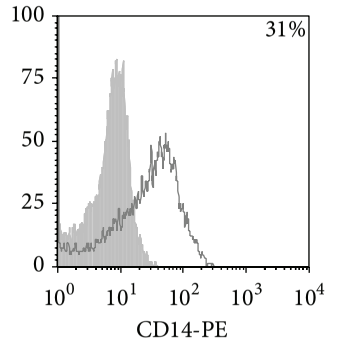
CD25	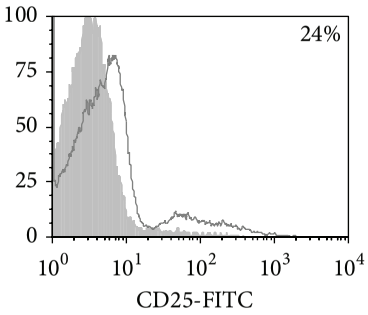	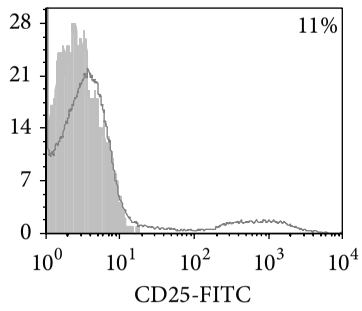	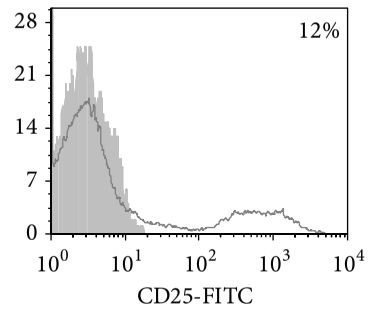
HLA-DR	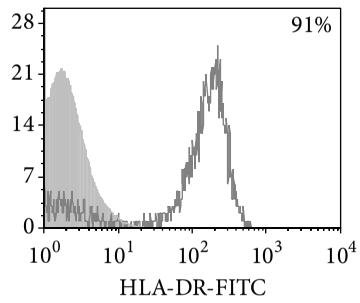	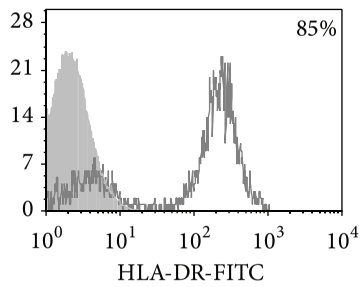	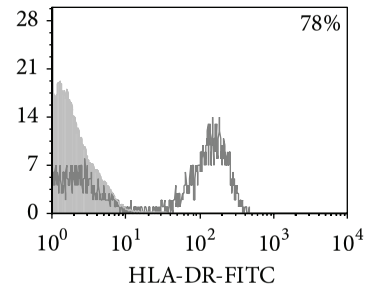

Table 5: Continued.

MDDC	A	B	C
CD83	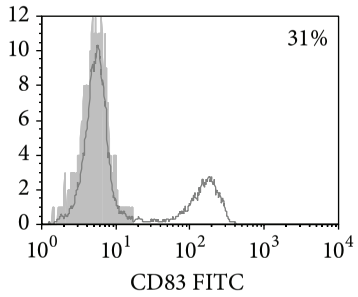	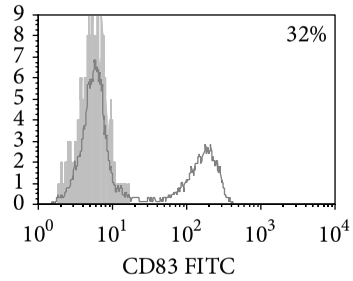	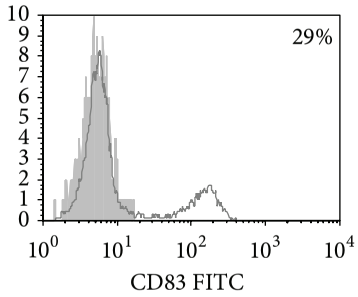

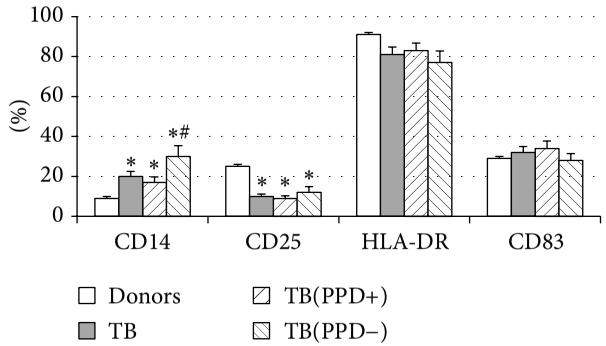

mechanisms, the expression of costimulatory molecules, and the production of proinflammatory cytokines by APCs [27]. It is well known that IL-6 can induce naïve $CD4^+$ T-lymphocyte polarization toward the Th2, and IL-10 is an inhibitor of Th1 cells [2, 27]. In this respect the imbalance of IFN-γ/IL-10, IL-6 production typical for APCs in TB patients is apparently a cause of low antigen-specific response in PPD-anergic patients. As an additional mechanism of PPD-anergy in TB, we can consider a decreased expression of antigen-presenting and costimulatory molecules in APCs which causes an impairment of their antigen-presenting function. Indeed, we found the most expressed inhibition of macrophage and DC allostimulatory activity in PPD-anergic patients.

5. Conclusions

The phenotype and functional properties of antigen-presenting cells, that is, circulating monocytes and *in vitro* generated macrophages and dendritic cells, are altered in TB patients. These impairments are most pronounced in PPD-anergic patients and may be the cause of low antigen-specific T-cell response.

Conflict of Interests

The authors declare that there is no conflict of interests regarding the publication of this paper.

Acknowledgment

The authors are grateful to Larisa A. Sviridova for her contribution to this paper.

References

[1] J. L. Flynn and J. Chan, "Immunology of tuberculosis," *Annual Review of Immunology*, vol. 19, pp. 93–129, 2001.

[2] E. Giacomini, E. Iona, L. Ferroni et al., "Infection of human macrophages and dendritic cells with *Mycobacterium tuberculosis* induces a differential cytokine gene expression that modulates T-cell response," *Journal of Immunology*, vol. 166, no. 12, pp. 7033–7041, 2001.

[3] A. Mihret, "The role of dendritic cells in *Mycobacterium tuberculosis* infection," *Virulence*, vol. 3, no. 7, pp. 654–659, 2012.

[4] C. V. Harding and W. H. Boom, "Regulation of antigen presentation by *Mycobacterium tuberculosis*: a role for Toll-like receptors," *Nature Reviews Microbiology*, vol. 8, no. 4, pp. 296–307, 2010.

[5] C. R. Shaler, C. Horvath, R. Lai, and Z. Xing, "Understanding delayed T-cell priming, lung recruitment, and airway luminal T-cell responses in host defense against pulmonary tuberculosis," *Clinical and Developmental Immunology*, vol. 2012, Article ID 628293, 13 pages, 2012.

[6] W. A. Hanekom, M. Mendillo, C. Manca et al., "*Mycobacterium tuberculosis* inhibits maturation of human monocyte-derived dendritic cells in vitro," *Journal of Infectious Diseases*, vol. 188, no. 2, pp. 257–266, 2003.

[7] N. Dulphy, J.-L. Herrmann, J. Nigou et al., "Intermediate maturation of *Mycobacterium tuberculosis* LAM-activated human dendritic cells," *Cellular Microbiology*, vol. 9, no. 6, pp. 1412–1425, 2007.

[8] A. Motta, C. Schmitz, L. Rodrigues et al., "*Mycobacterium tuberculosis* heat-shock protein 70 impairs maturation of dendritic cells from bone marrow precursors, induces interleukin-10 production and inhibits T-cell proliferation in vitro," *Immunology*, vol. 121, no. 4, pp. 462–472, 2007.

[9] A. J. Wolf, B. Linas, G. J. Trevejo-Nuñez et al., "*Mycobacterium tuberculosis* infects dendritic cells with high frequency and impairs their function in vivo," *The Journal of Immunology*, vol. 179, no. 4, pp. 2509–2519, 2007.

[10] C. Demangel, T. Garnier, I. Rosenkrands, and S. T. Cole, "Differential effects of prior exposure to environmental mycobacteria on vaccination with *Mycobacterium bovis* BCG or a recombinant BCG strain expressing RD1 antigens," *Infection and Immunity*, vol. 73, no. 4, pp. 2190–2196, 2005.

[11] M. Podinovskaia, W. Lee, S. Caldwell, and D. G. Russell, "Infection of macrophages with *Mycobacterium tuberculosis* induces global modifications to phagosomal function," *Cellular Microbiology*, vol. 15, no. 6, pp. 843–859, 2013.

[12] V. Nagabhushanam, A. Solache, L.-M. Ting, C. J. Escaron, J. Y. Zhang, and J. D. Ernst, "Innate inhibition of adaptive immunity: *Mycobacterium tuberculosis*-induced IL-6 inhibits macrophage responses to IFN-γ," *Journal of Immunology*, vol. 171, no. 9, pp. 4750–4757, 2003.

[13] R. K. Pai, M. Convery, T. A. Hamilton, W. H. Boom, and C. V. Harding, "Inhibition of IFN-γ-induced class II transactivator expression by a 19-kDa lipoprotein from *Mycobacterium tuberculosis*: a potential mechanism for immune evasion," *The Journal of Immunology*, vol. 171, no. 1, pp. 175–184, 2003.

[14] E. H. Noss, R. K. Pai, T. J. Sellati et al., "Toll-like receptor 2-dependent inhibition of macrophage class II MHC expression and antigen processing by 19-kDa lipoprotein of *Mycobacterium tuberculosis*," *The Journal of Immunology*, vol. 167, no. 2, pp. 910–918, 2001.

[15] L. V. Sakhno, M. A. Tikhonova, V. S. Kozhevnikov et al., "The phenotypic and functional characteristic of monocytes in pulmonary tuberculosis," *Medical Immunolology*, vol. 7, pp. 49–56, 2005 (Russian).

[16] D. Castaño, L. F. García, and M. Rojas, "Increased frequency and cell death of $CD16^+$ monocytes with *Mycobacterium tuberculosis* infection," *Tuberculosis*, vol. 91, no. 5, pp. 348–360, 2011.

[17] L. Balboa, M. M. Romero, J. I. Basile et al., "Paradoxical role of $CD16^+CCR2^+CCR5^+$ monocytes in tuberculosis: efficient APC in pleural effusion but also mark disease severity in blood," *Journal of Leukocyte Biology*, vol. 90, no. 1, pp. 69–75, 2011.

[18] L. V. Sakhno, M. A. Tikhonova, A. A. Ostanin, S. D. Nikonov, O. A. Zhdanov, and E. R. Chernykh, "Interleukin-2 in the correction of T-cell anergy in patients with pulmonary tuberculosis," *Problemy Tuberkuleza i Bolezneĭ Legkikh*, no. 1, pp. 48–52, 2006 (Russian).

[19] G. Vanham, K. Edmonds, L. Qing et al., "Generalized immune activation in pulmonary tuberculosis: co-activation with HIV infection," *Clinical and Experimental Immunology*, vol. 103, no. 1, pp. 30–34, 1996.

[20] G. Vanham, Z. Toossi, C. S. Hirsch et al., "Examining a paradox in the pathogenesis of human pulmonary tuberculosis: immune activation and suppression/anergy," *Tubercle and Lung Disease*, vol. 78, no. 3-4, pp. 145–158, 1997.

[21] J. E. Scherberich and W. A. Nockher, "$CD14^{++}$ monocytes, $CD14^+/CD16^+$ subset and soluble CD14 as biological markers

of inflammatory system diseases and monitoring immunosuppressive therapy," *Scandinavian Journal of Immunology*, vol. 55, pp. 629–638, 2002.

[22] P. Rajashree, G. Krishnan, and S. D. Das, "Impaired phenotype and function of monocyte derived dendritic cells in pulmonary tuberculosis," *Tuberculosis*, vol. 89, no. 1, pp. 77–83, 2009.

[23] L. Balboa, M. M. Romero, E. Laborde et al., "Impaired dendritic cell differentiation of CD16-positive monocytes in tuberculosis: role of p38 MAPK," *European Journal of Immunology*, vol. 43, no. 2, pp. 335–347, 2013.

[24] S. D. Bella, S. Nicola, A. Riva, M. Biasin, M. Clerici, and M. L. Villa, "Functional repertoire of dendritic cells generated in granulocyte macrophage-colony stimulating factor and interferon-α," *Journal of Leukocyte Biology*, vol. 75, no. 1, pp. 106–116, 2004.

[25] S. M. Santini, T. Di Pucchio, C. Lapenta, S. Parlato, M. Logozzi, and F. Belardelli, "A new type I IFN-mediated pathway for the rapid differentiation of monocytes into highly active dendritic cells," *Stem Cells*, vol. 21, no. 3, pp. 357–362, 2003.

[26] O. Y. Leplina, M. A. Tikhonova, T. V. Tyrinova et al., "Comparative characteristic of phenotype and cytokine-secretory activity of human dendritic cells generated in vitro with IFN-alpha and IL-4," *Immunology*, no. 2, pp. 60–65, 2012.

[27] P. J. Murray, "Understanding and exploiting the endogenous interleukin-10/STAT3-mediated anti-inflammatory response," *Current Opinion in Pharmacology*, vol. 6, no. 4, pp. 379–386, 2006.

Hindawi Publishing Corporation
Journal of Immunology Research
Volume 2015, Article ID 359153, 13 pages
http://dx.doi.org/10.1155/2015/359153

Research Article

Dendritic Cell Activity Driven by Recombinant *Mycobacterium bovis* BCG Producing Human IL-18, in Healthy BCG Vaccinated Adults

Piotr Szpakowski,[1] Franck Biet,[2] Camille Locht,[3,4,5,6] Małgorzata Paszkiewicz,[1] Wiesława Rudnicka,[1] Magdalena Druszczyńska,[1] Fabrice Allain,[6,7] Marek Fol,[1] Joël Pestel,[6,7] and Magdalena Kowalewicz-Kulbat[1]

[1] *Department of Immunology and Infectious Biology, Institute of Microbiology, Biotechnology and Immunology, University of Lodz, Banacha Street 12/19, 90-237 Lodz, Poland*
[2] *UMR1282, Infectiologie et Santé Publique (ISP-311), INRA-Centre Val de Loire, 37380 Nouzilly, France*
[3] *Center for Infection and Immunity of Lille, Institut Pasteur de Lille, 59019 Lille, France*
[4] *Inserm U1019, 59019 Lille, France*
[5] *CNRS UMR 8204, 59019 Lille, France*
[6] *Université Lille Nord de France, 59019 Lille, France*
[7] *CNRS-UMR 8576, Unité de Glycobiologie Structurale et Fonctionnelle, IFR 147, Université Lille Nord de France, Université de Lille 1, 59655 Villeneuve d'Ascq, France*

Correspondence should be addressed to Magdalena Kowalewicz-Kulbat; mkow@biol.uni.lodz.pl

Received 8 July 2014; Revised 24 September 2014; Accepted 25 September 2014

Academic Editor: Vishwanath Venketaraman

Tuberculosis remains an enormous global burden, despite wide vaccination coverage with the Bacillus Calmette-Guérin (BCG), the only vaccine available against this disease, indicating that BCG-driven immunity is insufficient to protect the human population against tuberculosis. In this study we constructed recombinant BCG producing human IL-18 (rBCGhIL-18) and investigated whether human IL-18 produced by rBCGhIL-18 modulates DC functions and enhances Th1 responses to mycobacterial antigens in humans. We found that the costimulatory CD86 and CD80 molecules were significantly upregulated on rBCGhIL-18-infected DCs, whereas the stimulation of DCs with nonrecombinant BCG was less effective. In contrast, both BCG strains decreased the DC-SIGN expression on human DCs. The rBCGhIL-18 increased IL-23, IL-10, and IP-10 production by DCs to a greater extent than nonrecombinant BCG. In a coculture system of $CD4^+$ T cells and loaded DCs, rBCGhIL-18 favoured strong IFN-γ but also IL-10 production by naive T cells but not by memory T cells. This was much less the case for nonrecombinant BCG. Thus the expression of IL-18 by recombinant BCG increases IL-23, IP-10, and IL-10 expression by human DCs and enhances their ability to induce IFN-γ and IL-10 expression by naive T cells, without affecting the maturation phenotype of the DCs.

1. Introduction

The global burden of mycobacterial infections is still one of the major public health concerns, despite the widespread use of the Bacillus Calmette-Guérin (BCG) vaccine, which confers good protection against disseminated childhood tuberculosis (TB), but provides variable protection against pulmonary disease in adults.

There is good evidence that the protection obtained by BCG vaccination declines with age. Thus, improved vaccines are desperately needed, but their development is hampered by the insufficient knowledge of the immune protection mechanisms. One approach to develop a new TB vaccine is improving BCG by the expression of immune modulators for superior targeting of immune pathways, which are essential in protective immunity [1]. The Th-1 responses have

long been recognized as essential mechanisms of protection against mycobacterial diseases, including tuberculosis [2, 3]. Interleukin 18, first described in 1989 as "IFN-γ-inducing factor," initially isolated from the serum of *M. bovis* BCG-infected mice challenged with LPS [4], is considered to play a significant role in promoting Th1 responses. It is produced by activated macrophages and dendritic cells (DCs) but also by T and B cells and many other cell types [5–7]. IL-18 can be a potent therapeutic tool against severe bacterial infections [8]. Moreover, it has been shown that systematic administration of IL-18 enhances the regression of well-established primary tumors by a mechanism that depends on CD8+ T cell, Fas/FasL, and endogenous IFN-γ, particularly in combination with other cytokines [9–11]. However, recent studies have shown that exogenous IL-18 given to mice induced an exaggerated inflammatory reaction, which led to adverse effects including neutrophil-mediated lung and/or intestinal injuries [12]. It may limit the potential use of IL-18 as a therapeutic agent in humans. To overcome this difficulty, we hypothesized that a bacterial construct producing a small amount of IL-18 could directly modulate the antigen presentation by DCs for the upregulation of Th1 responses, yet avoiding the potential harmful effects of exogenous IL-18. BCG bacilli, which are strong Th1 inducers, seem to be a useful platform for IL-18 expression. IL-18 has been shown to enhance the host defense against mycobacterial infections [13–15]. Mice deficient for IL-18, but not for the IL-18 receptor, are highly susceptible to *M. tuberculosis* infection [16]. In mice, BCG can synergize with IL-18 for IFN-γ production, potentially leading to enhanced protective immunity against mycobacteria [17]. The synergistic effect of IL-18 on IFN-γ production depends on the IL-18 receptors expressed on Th1 but not on Th2 cells [18]. It was observed that infection of mice with recombinant BCG strain producing murine IL-18 (rBCGmIL-18) strongly enhanced the ability of BCG to polarize the immune response towards a Th1 type [19]. In a mouse model of MBT-2 superficial bladder cancer, recombinant BCG secreting IL-18 also enhanced macrophage cytotoxicity against cancer cells in an IFN-γ dependent manner [20]. In a murine experimental allergic asthma model rBCGmIL18 was shown to be more efficient in suppressing allergen-driven pulmonary Th2 responses and eosinophilia than nonrecombinant BCG [21]. IL-18 also augments IFN-γ in human macrophages infected with *M. tuberculosis* [22]. However, still little is known about the combined effect of mycobacteria and IL-18 on human DCs.

In this study, we constructed a recombinant BCG strain producing human IL-18 (rBCGhIL-18) and examined its effects on human monocyte-derived DCs (MoDCs), obtained from healthy young subjects who had been immunized with BCG at birth and school age. In this human model we compared the effects of BCG and rBCGhIL-18 on MoDC taking into account: (a) the expression of cell-surface signaling receptors, which are engaged in the direct interaction between DCs and T cells, (b) the production of cytokines, which provide the differentiation of responding T cells, and (c) the efficient induction of antigen-specific effector functions of $CD4^+$ T cells.

2. Materials and Methods

2.1. Construction of the Human IL-18 Expression Vector. The *M. bovis* BCG vaccine strain 1173P2 (World Health Organization, Stockholm, Sweden) was genetically modified to produce mature human IL-18 (hIL-18) by transformation with pENhIL-18 (Figure 1), a pRR3 derivative [23] containing the mature hIL-18-encoding gene under the control of the BCG *hsp60* promoter and modified by replacing the original signal peptide cleavage sequence with the mycobacterial signal peptide coding sequence from the BCG α-antigen. The 512 bp DNA fragment encoding hIL-18 was obtained by reverse transcription-PCR on total RNA from U-937 cells activated for 6 h with LPS (1 μg/mL). Total RNA was extracted using RNAzol (Applied Oncor) according to the manufacturer's recommendation. Reverse transcription-PCR was carried out as described previously [17] with the gene-specific primers with the following sequences: 5′-TATAGGATCCTACTT-TGGCAAGCTTGAA-3′ and 5′-TATAGGTACCGGCAT-GAAATTTTAATAGC-3′ (Eurogentec, Liège, Belgium). The 126-bp DNA fragment encoding the α-antigen signal sequence was amplified by PCR using chromosomal BCG DNA extracted as described previously [24] with the primers 5′-GGCACAGGTCATGACAGACGTGAGCCGAAAGAT-TCGA-3′ and 5′-GCCGGGATCCCGCGCCCGCGGTTG-CCGCTCCGCC-3′ (Eurogentec). The PCR fragment encoding hIL-18 restricted by *Bgl*II and *Asp*718 and the PCR fragment encoding the α-antigen signal sequence restricted by *Bsp*HI and *Bam*HI were inserted into pUC::*hsp60* [24] restricted by *Nco*I and *Asp*718, thereby generating pUC::hIL-18. The 1.32 kb *Pvu*II fragment from pUC::hIL-18 spanning the BCG *hsp60* promoter, the ribosomal binding site, the α-antigen signal peptide coding sequence, and the mature hIL-18 coding sequence, was inserted into pRR3, previously digested with *Sca*I. The resulting shuttle vector, pENhIL-18, was used to transform BCG, and the transformants were selected by their resistance to Kanamycin. Kanamycin-resistant BCG colonies were analyzed for their plasmid content by using electroduction [25]. The recombinant strain was named rBCGhIL-18.

2.2. Detection of HIL-18 in Recombinant Mycobacteria. Mycobacterial cell extracts were prepared as described previously [19] from 10 mL cultures harvested at mid-log phase. The proteins in the lysates, corresponding to ca. 5×10^6 bacteria, were separated by SDS-PAGE on a 15% polyacrylamide gel [26]. Total proteins were then transferred onto a Hybond-C extra membrane (Amersham France). The membrane was saturated with 1% bovine serum albumin in phosphate-buffered saline (PBS)—0.1% Tween 20 (PBST) and then incubated with rabbit anti-IL-18 antiserum diluted 1/2,000. Goat anti-rabbit alkaline phosphatase-conjugated antibodies (Promega, Madison, Wis. USA) diluted 1/7.000 in PBST were then used to develop the immunoblots.

2.3. Bacterial Strains and Growth Conditions. M. bovis BCG (Pasteur strain 117P2; WHO Stockholm, Sweden) and rBCGhIL-18 were grown to the mid-log phase in stationary flasks, at 37°C in 7H9 Middlebrook liquid medium (Becton

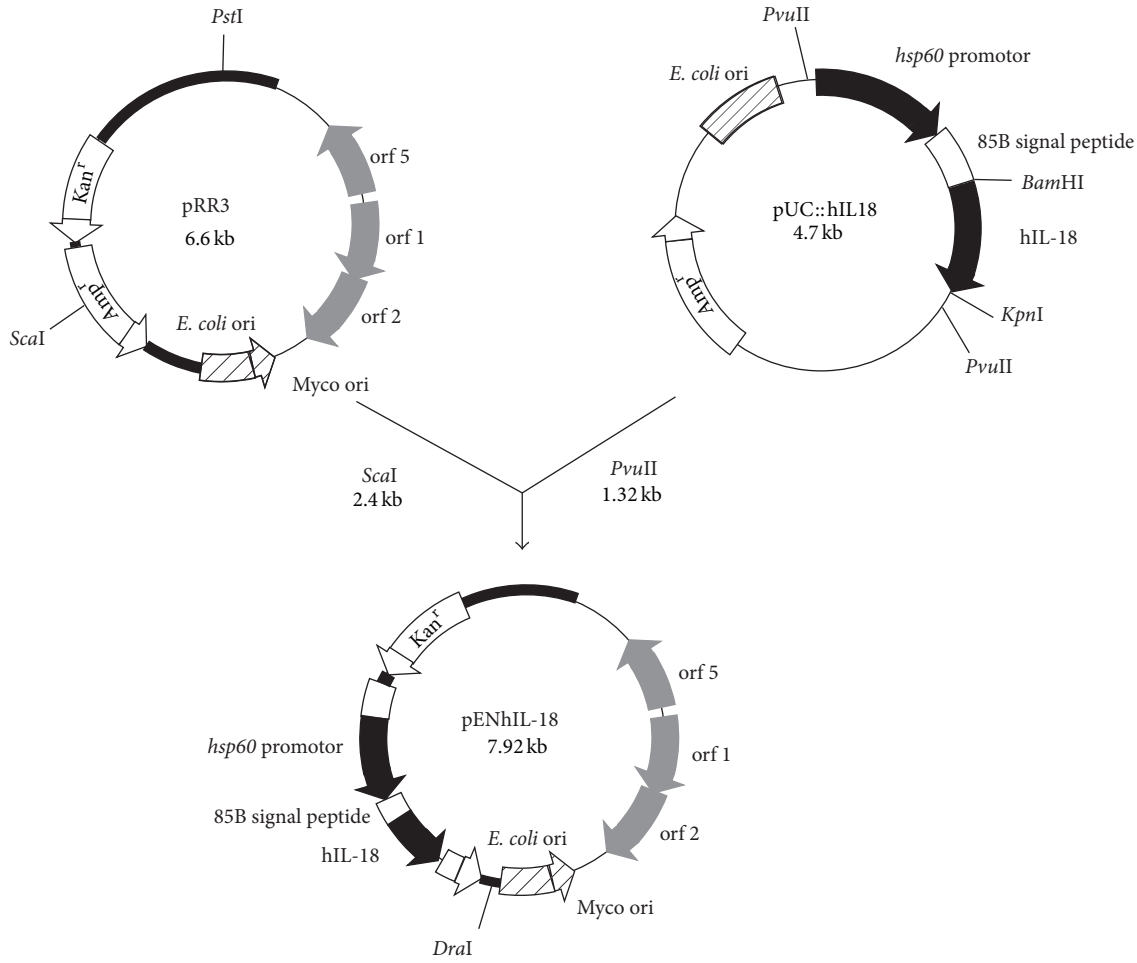

Figure 1: Construction of pENhIL-18 used to produce and secrete hIL-18 by rBCGhIL-18. White arrows Kan^R and Amp^R represent the kanamycin and ampicillin resistance genes, respectively. ColE1 represents the origin of replication from *E.coli* (hatched boxes), and oriM represents the mycobacterial origin of replication (hatched arrows). The expression cassette contains the BCG *hsp60* promoter, the ribosome-binding site, and the *hsp60* initiating codon represented by the black box. The *M. tuberculosis* alpha-antigen signal peptide coding sequence is represented by the white box, whereas the IL-18 coding sequence is shown in black. The grey boxes indicate open reading frames of the mycobacterial plasmid, necessary for replication in BCG.

Dickinson) supplemented with: 10% oleic acid-albumin-dextrose catalase (OADC) (Difco, BD Biosciences) and 0.05% Tween 80, and frozen until use.

For the colony forming units (CFU) counts, bacteria were serially diluted in PBS containing 0.05% Tween 80 and plated on Middlebrook 7H11 agar supplemented with 10% OADC enrichment. Bacteria were grown for 3-4 weeks at 37°C for CFU enumeration.

2.4. Blood Donors. Blood was collected from 60 young healthy volunteers aged 25–35, vaccinated with BCG in childhood, according to state policy. All studies were approved by the local Ethic Commitee. Healthy volunteers signed the consent for the participation in the study before blood collection.

2.5. Monocyte-Derived DC Preparation. Peripheral blood was obtained using vacutainer tubes with spray-coated heparin (Becton Dickinson). Monocytes were separated from PBMC by immunomagnetic positive separation using $CD14^+$ Microbeads (Miltenyi Biotech, Germany) [27]. $CD14^+$ cell purity was determined to be 96% to 99% on the basis of forward and side scatter gating in conjunction with CD14 staining using standard flow cytometry (data not shown).

Monocytes were suspended in RPMI-1640 (Sigma-Aldrich, Germany) supplemented with 100 U/mL penicillin, 0.1 mg/mL streptomycin and L-glutamine (Polfa Tarchomin, Poland) and enriched with 10% (v/v) fetal calf serum (FCS, heat inactivated; Cambrex, Belgium). The density was adjusted to 1×10^6/mL, and the monocytes were placed into 6-well flat-bottomed culture plates and allowed to differentiate into DCs by incubation for 6 days in RPMI-1640 supplemented with 1% antibiotics and 10% FCS in the presence of 25 ng/mL human GM-CSF and 10 ng/mL human recombinant IL-4 (R&D Systems, USA). After 6 days of culture, the cells were harvested, pooled, and counted.

2.6. Stimulation of DC with BCG, rBCGhIL-18 or Purified Protein Derivative (PPD). Immature DCs were placed into

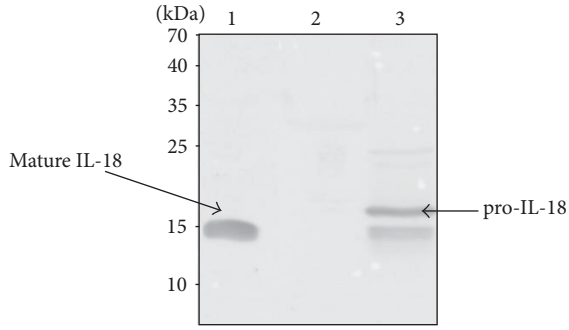

Figure 2: Immunoblot analysis of rBCGhIL-18. Lane 1 contains 100 ng of mature IL-18. Whole-cell extracts of nonrecombinant BCG (lane 2) or rBCGhIL-18 (lane 3), each corresponding to an optical density at 600 nm of 0.2 were subjected to SDS-PAGE and analyzed by immunoblotting using rabbit anti-IL-18 antibodies. The sizes of the molecular weight markers are indicated in the left margin, and the presence of mature IL-18 and pro-IL-18 is indicated by arrows.

6-well plates at a density of 1×10^6 cells/mL and incubated for 24 h (37°C, 5% CO_2) with live BCG, rBCGhIL-18 at a multiplicity of infection (MOI) of 1:1 or with 10 μg/mL PPD (Statens Serum Institut, Copenhagen, Denmark). Lipopolysaccharide (LPS) from *Escherichia coli* O55:B5 (1 μg/mL) (Sigma) was used as positive control of DC activity and DC in medium alone (unpulsed DC) represented the negative control. To assess whether neutralizing anti-human IL-18 antibodies reduce the effect of rBCGhIL-18 on activating cells, mouse monoclonal anti-human IL-18 antibody (MBL) (1 μg/mL) was added to the culture of unstimulated and stimulated DC.

2.7. DCs Preparation for Flow Cytometry. The antigen-stimulated and unstimulated DCs were collected from the 6-well plate by using PBS/2 mM EDTA. After washing in PBS the DC were incubated for 30 min at 4°C with the following mAb: fluorescein isothiocyanate (FITC)-conjugated anti-CD86, anti-CD40, anti-HLA-DR, anti-DC-SIGN; phycoerythrin (PE)-conjugated anti-CD80, or an irrelevant isotype-matched mAb used as control. All mAbs were purchased from Becton Dickinson (BD). Data were acquired and analyzed using the FACS LSRII (BD) and FlowJo software, a minimum 10,000 events were collected. The calculated mean fluorescence intensity represents the molecule density on the cell surface and the percentage of positive DC for each marker.

2.8. Cytokine and Chemokine Concentration. Supernatants of 1×10^6 purified DCs, pulsed or not with BCG, rBCGhIL-18, PPD, or LPS, were harvested 24 h following stimulation, centrifuged (400 ×g for 10 min), and stored at −20°C until further used. Supernatants were then tested by the ELISA, (Elipair Diaclone test) for the presence of IL-10, IL-12p70, and IL-23 (detection sensitivity: 5 pg/mL for IL-10 and IL-12p70; 20 pg/mL for IL-23), human IL-18 (RayBiotech: detection sensitivity 0.5 pg/mL) and for the presence of IP-10 (CXCL10) by using specific ELISA (R&D systems: detection sensitivity: 5 pg/mL). The cytokines were quantified by reference to a standard curve obtained for individual cytokine standards provided by the manufacturers.

2.9. T Cell Preparation. Autologous naive $CD45RA^+CD4^+$ and memory $CD45RO^+CD4^+$ cells were isolated from the eluted $CD14^-$ cell fraction by using a naive $CD4^+$ T-cell isolation kit, as previously described [28], or the memory $CD4^+$ T-cell isolation kit (Miltenyi), according to the manufacturer's protocol. Both isolated cell fractions (purity > 95%) were frozen until use.

2.10. DC-T Cell Coculture. The preserved naive and memory T lymphocytes 1×10^7 cells/mL were thawed and cocultured with BCG-, rBCGhIL-18-,or PPD- (10 μg/mL) primed DC at a ratio of 10 T cells per one infected DC, for 5 days at 37°C with 5% CO_2. Collected supernatants were tested for IFN-γ and IL-10 production by ELISA using commercially available kits (Diaclone). The limit of detection was 5 pg/mL for both IFN-γ and IL-10.

2.11. Statistical Analysis. All data were analyzed using the STATISTICA 8.0 PL software. Differences between antigens were evaluated for each parameter using nonparametric Kruskal-Wallis test. When statistical significance was observed, differences were analyzed by Mann-Whitney U test (for impaired data) to verify the hypothesis that two analyzed samples came from two statistically different populations. P values < 0.05 were considered significant.

3. Results

3.1. Production and Secretion of hIL-18 by rBCGhIL-18. To construct rBCGhIL-18, the hIL-18-encoding cDNA was prepared as described previously [19] and modified by substituting the original IL-18 signal peptide coding sequence with the mycobacterial secretion signal sequence from the BCG α-antigen [29]. The modified hIL-18 cDNA was inserted into the expression vector pRR3 [23] (Figure 1) and then introduced into BCG. The recombinant BCG construction, named rBCGhIL-18, was found to produce human IL-18, as shown by immunoblot analyses using an anti-human IL-18 rabbit antiserum. Immunoreactive proteins were detected in the lysate of rBCG producing hIL-18, but not in the lysate of the nonrecombinant control strain (Figure 2). The rBCGhIL-18 extract contained an immune-reactive protein with a size expected for noncleaved pro-IL-18, as well as bands whose M_r are similar to that of mature IL-18, indicating that the pro-hIL-18 in rBCGhIL-18 is partially processed into the mature form, similarly to our previous study describing the expression and immunological activity of murine IL-18 produced by recombinant BCG [19]. The IL-18 expression by recombinant BCG was checked during the entire study period, always with the same results. The concentration of hIL-18 was quantified by ELISA in cell culture supernatants of BCG- or rBCGhIL-18-stimulated DC. For the three healthy individuals-tested, cultures contained 5–10 pg/mL and 18–22 pg/mL hIL-18, after 24 h stimulation with BCG or rBCGhIL-18, respectively. Unstimulated cultures contained only 3–7 pg/mL hIL-18.

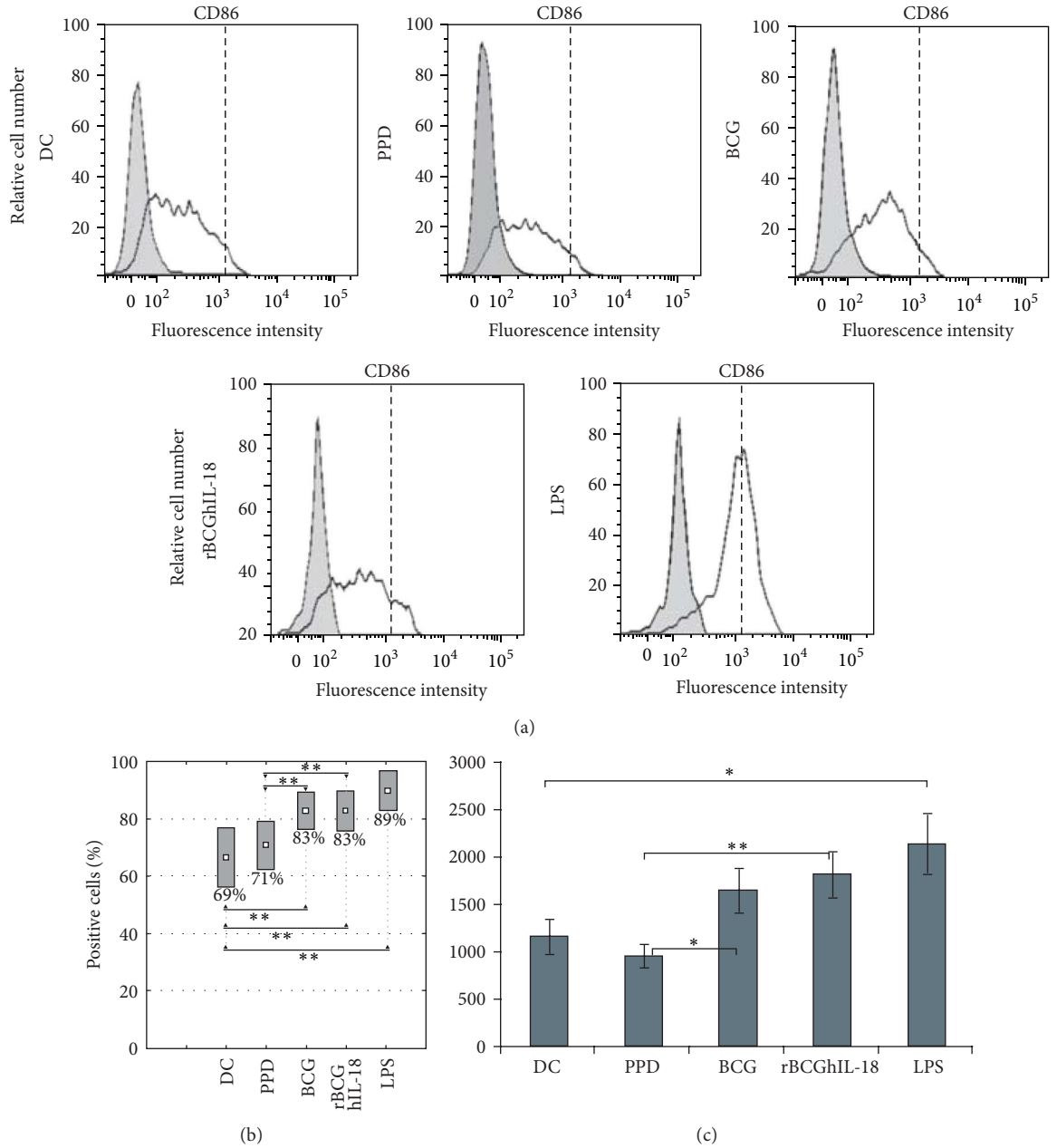

Figure 3: CD86 surface expression of MoDCs. Human MoDCs were pulsed either with PPD (10 μg/mL), BCG (1 : 1), rBCGhIL-18 (1 : 1), or LPS (1 μg/mL) for 24 h or were left unstimulated (DC). (a) One representative experiment out of 20 independent ones is shown. Grey histograms represent the cell reactivity to fluorochrome-matched isotype control antibodies. The white histograms represent the reactivity with the anti-CD86 antibody. The vertical broken lines represent the upregulation obtained by LPS stimulation; (b) percentage of positive cells with the CD86 expression; (c) median fluorescence intensity (MFI) values (median ± SEM of 20 independent donors). Fluorescence intensity was calculated by the MFI of the receptor expression from which the MFI obtained with a nonrelevant, isotype-matched antibody was substracted. Statistical analyses were performed using the Kruskal-Wallis test. $^{*}P < 0.05$; $^{**}P < 0.01$.

3.2. Maturation Marker Expression by Mycobacteria-Pulsed DCs. To investigate the effect of rBCGIL-18 on human monocyte-derived DC maturation, the DCs were pulsed with rBCGhIL-18, BCG, or PPD and compared to control conditions (i.e., unstimulated DCs as a negative control, and LPS-pulsed DCs as a positive control). Various T cell costimulation surface markers (CD86, CD80, and CD40), as well as HLA-DR expression, were assessed by flow cytometry. LPS induced the upregulation of CD86 (Figure 3(a)) and CD80 (Figure 4(a)) as well as CD40 and HLA-DR (data not shown), and the downregulation of DC-SIGN. DC incubation with PPD did not modify the expression of CD86, CD80, CD40, and HLA-DR, but downregulated the expression of DC-SIGN. In contrast, the incubation with either of the two BCG

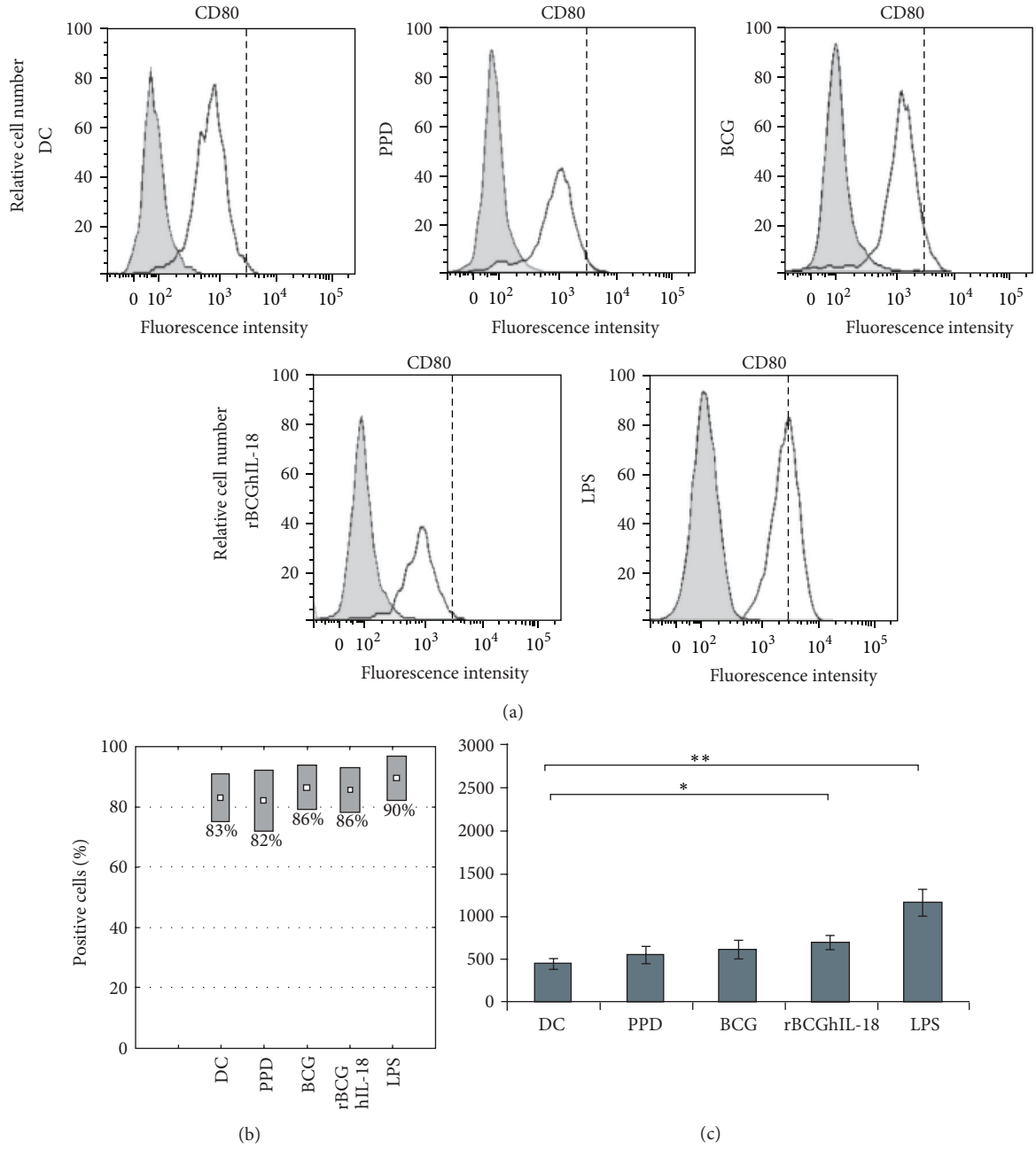

Figure 4: CD80 surface expression of MoDCs. Human MoDCs were pulsed either with PPD (10 μg/mL), BCG (1:1), rBCGhIL-18 (1:1), or LPS (1 μg/mL) for 24 h or were left unstimulated (DC). (a) One representative experiment out of 20 independent ones is shown. Grey histograms represent the cell reactivity to fluorochrome-matched isotype control antibodies. The white histograms represent the reactivity with the anti-CD80 antibody. The vertical broken lines represent the upregulation obtained by LPS stimulation; (b) percentage of positive cells with the CD80 expression; (c) median fluorescence intensity (MFI) values (median ± SEM of 20 independent donors). Fluorescence intensity was calculated by the MFI of the receptor expression from which the MFI obtained with a nonrelevant, isotype-matched antibody was substracted. Statistical analyses were performed using the Kruskal-Wallis test. $^{*}P < 0.05$; $^{**}P < 0.01$.

strains at an MOI of 1:1 induced the upregulation of some of these surface markers and again the downregulation of DC-SIGN. Moreover, we could detect a higher proportion of BCG- and rBCGhIL-18-stimulated MoDCs with CD86 expression, as compared to unstimulated DC, and those incubated with PPD (Figure 3(b)). This difference was not observed in the case of CD80 (Figure 4(b)), HLA-DR, CD40 markers (data not shown) and DC-SIGN (Figure 5(a)). When the median of 20 different donors was analyzed, a significant increase in CD86 expression was observed upon incubation with BCG or with rBCGhIL-18 compared with untreated DC and those incubated with PPD (Figure 3(c)). In parallel, a

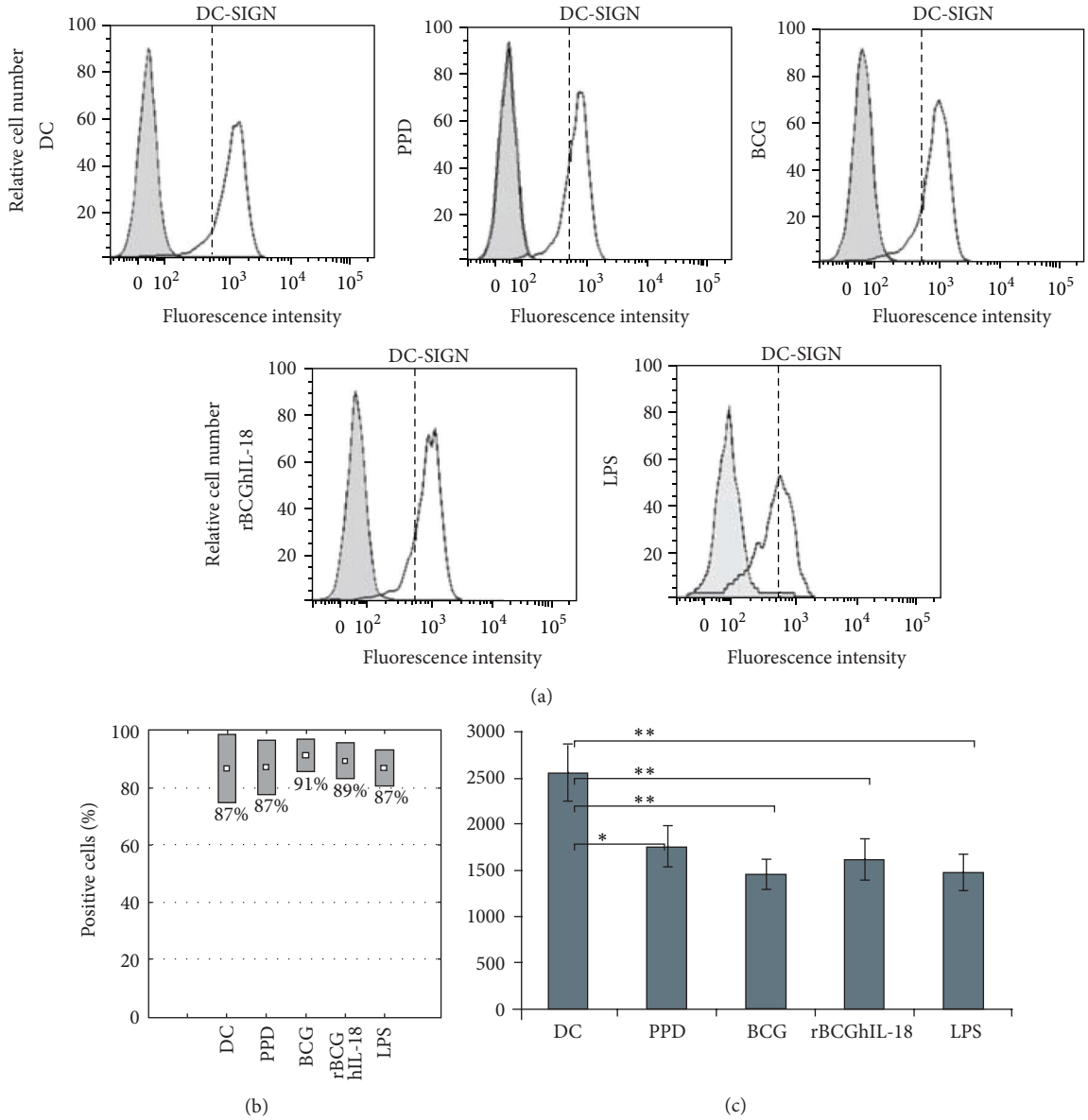

Figure 5: DC-SIGN surface expression of MoDCs. Human MoDCs were pulsed either with PPD (10 μg/mL), BCG (1 : 1), rBCGhIL-18 (1 : 1), or LPS (1 μg/mL) for 24 h or were left unstimulated (DC). (a) One representative experiment out of 20 independent ones is shown. Grey histograms represent the cell reactivity to fluorochrome-matched isotype control antibodies. The white histograms represent the reactivity with the anti-DC-SIGN antibody. The vertical broken lines represent the upregulation obtained by LPS stimulation; (b) percentage of positive cells with the DC-SIGN expression; (c) median fluorescence intensity (MFI) values (median ± SEM of 20 independent donors). Fluorescence intensity was calculated by the MFI of the receptor expression from which the MFI obtained with a nonrelevant, isotype-matched antibody was substracted. Statistical analyses were performed using the Kruskal-Wallis test. $^{*}P < 0.05$; $^{**}P < 0.01$.

significant decrease in DC-SIGN expression was observed upon incubation with BCG, rBCGhIL-18, PPD or LPS, consistent with a DC maturation phenotype. However, there was no significant difference between BCG and rBCGhIL-18. (Figure 5(c)).

3.3. Effect of BCG and rBCGhIL-18 on Cytokine and Chemokine Production by Human DCs. Next we analyzed the cytokine profile of the mycobacterial-pulsed DC that might affect the T-cell polarization. In particular, we analyzed IL-12, IL-23, and IL-10 in the supernatants of the DCs incubated with PPD, BCG, or rBCGhIL-18. In all blood donors, LPS-primed MoDCs produced significant levels of IL-12p70. In contrast, DCs infected with BCG and rBCGhIL-18 or stimulated with PPD, failed to secrete IL-12p70 in 6-hour cultures (data not shown) as well as in 24 hour cultures (Figure 6). Since bioactive IL-12 consists of p35 and p40 subunits, and the p40 subunit is also present in other IL-12 family members, such as IL-23, we determined the amount of secreted IL-23 in the supernatants of mycobacterial-stimulated DC cultures. Among the mycobacterial products, only rBCGhIL-18 induced significant IL-23 production compare to unpulsed

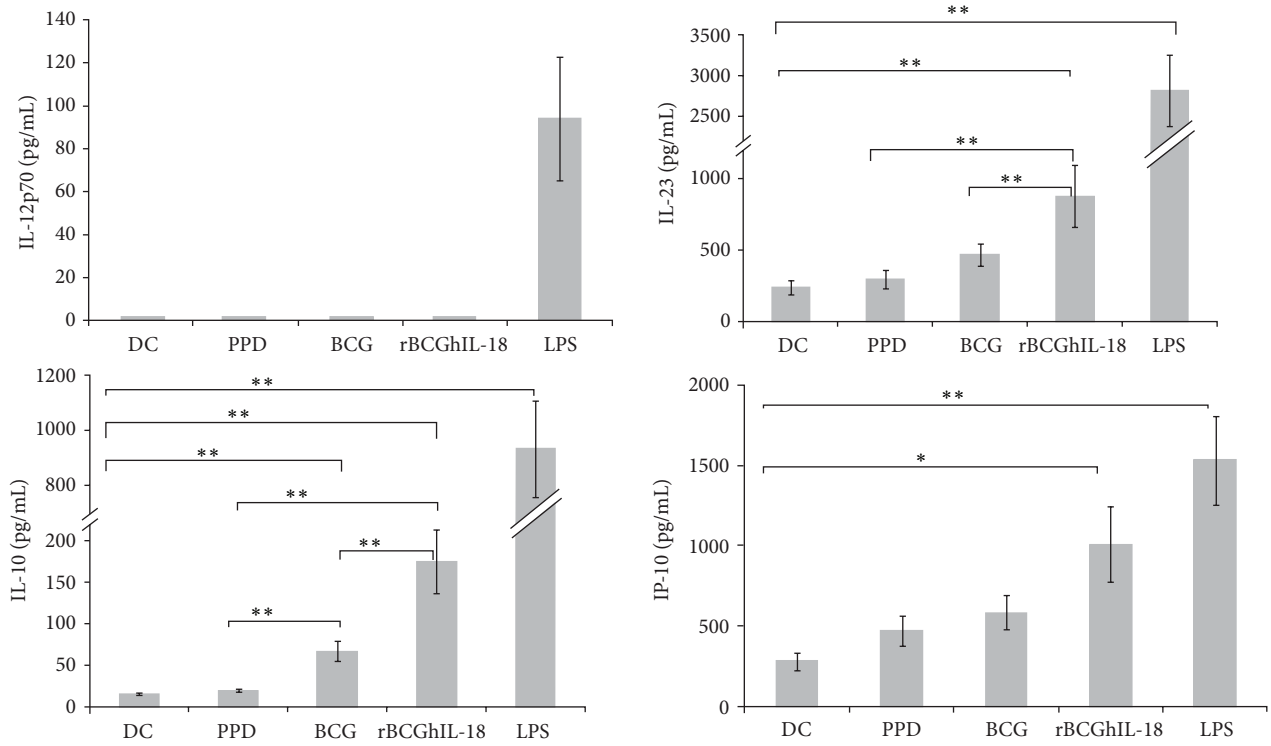

Figure 6: IL-12p70, IL-10, IL-23, and IP-10 production by stimulated MoDCs. Human MoDCs were stimulated with PPD (10 μg/mL), BCG (1 : 1), rBCGIL-18 (1 : 1), or LPS (1 μg/mL) for 24 h or were left untreated (DC). The cytokine and chemokine levels in the culture were measured by ELISA. Data shown are the mean ± SEM of 40 independent donors. Statistical analyses were performed using the Kruskal-Wallis test. $^{*}P < 0.05$; $^{**}P < 0.01$.

DCs ($P = 0.001$), albeit much less than LPS (roughly 1/3 less). A trend was also seen for nonrecombinant BCG, but did not reach statistical significance, leading therefore to statistical significance between BCG and rBCGhIL-18 (Figure 6). In addition to IL-23, rBCGhIL-18 also induced the production of IL-10 by the DCs, although significant amounts of IL-10 were also produced upon stimulation with BCG, but not with PPD. However, rBCGhIL-18 induced significantly more IL-10 than BCG ($P = 0.001$), albeit again much less than LPS. Finally, rBCGhIL-18 also induced significant levels of IP-10 (CXCL10), known to be involved in Th1 cell recruitment, whereas this was not the case for PPD or nonrecombinant BCG, suggesting that rBCGhIL-18 might favor T cell towards a Th1 profile.

3.4. rBCGhIL-18 Induces IFN-γ and IL-10 Production by Naive T Cells rather than by Memory T Cells. In order to investigate whether rBCGhIL-18-pulsed DC can polarize T cells towards the Th1 profile, we analyzed the cytokine responses of the autologous naive and memory $CD4^{+}$ T cells upon incubation with DCs stimulated with PPD, BCG, or rBCGhIL-18. As shown in Figure 7(a), naive T cells produced significantly more IFN-γ in response to rBCGhIL-18-stimulated DC coincubation, as compared to T cells incubation with DCs stimulated with PPD or BCG, both after 24 h and after 96 h of culture. PPD- or BCG-stimulated DCs induced only low levels of IFN-γ by the naive T cells. Similarly, rBCGhIL-18-pulsed DC also stimulated the secretion of IL-10 by naive T cells, whereas this was much less the case for PPD- or BCG-pulsed DCs (Figure 7(b)) In contrast to the naive T cells, memory T cells produced IFN-γ upon coculture with BCG-, rBCGhIL-18-, or PPD-pulsed DC at comparable levels. Similar results were obtained for the production of IL-10 by the T cells. Interestingly, both IFN-γ and IL-10 were produced at higher levels by naive T cells upon incubation with rBCGhIL-18-pulsed DC, compared to memory T, whereas the reverse was seen for IFN-γ upon coculture with PPD- or BCG-pulsed DCs. There were no differences in the IL-10 production by naive and memory T cells in response to PPD-pulsed MoDCs.

The IL-18 specificity of rBCGhIL-18-driven enhancement of IFN-γ production in DC-naive T cell cocultures was demonstrated in the anti-IL-18 neutralizing experiments conducted for three individuals (Figure 8). As shown in Figure 8, in the presence of the human anti-IL-18 antibody, the production of IFN-γ by naive T cells was reduced in response to rBCGhIL-18-stimulated DC coincubation, both after 24 and 96 h of culture; this was much less the case for rBCGhIL-18-stimulated DC-memory T cell cultures.

4. Discussion

Previous studies in mice have shown that, in response to BCG, IL-18 might favor the Th1 cytokine production. The synergistic effects between IL-18 and BCG in IFN-γ-dependent anti-mycobacterial protective immunity have been reported.

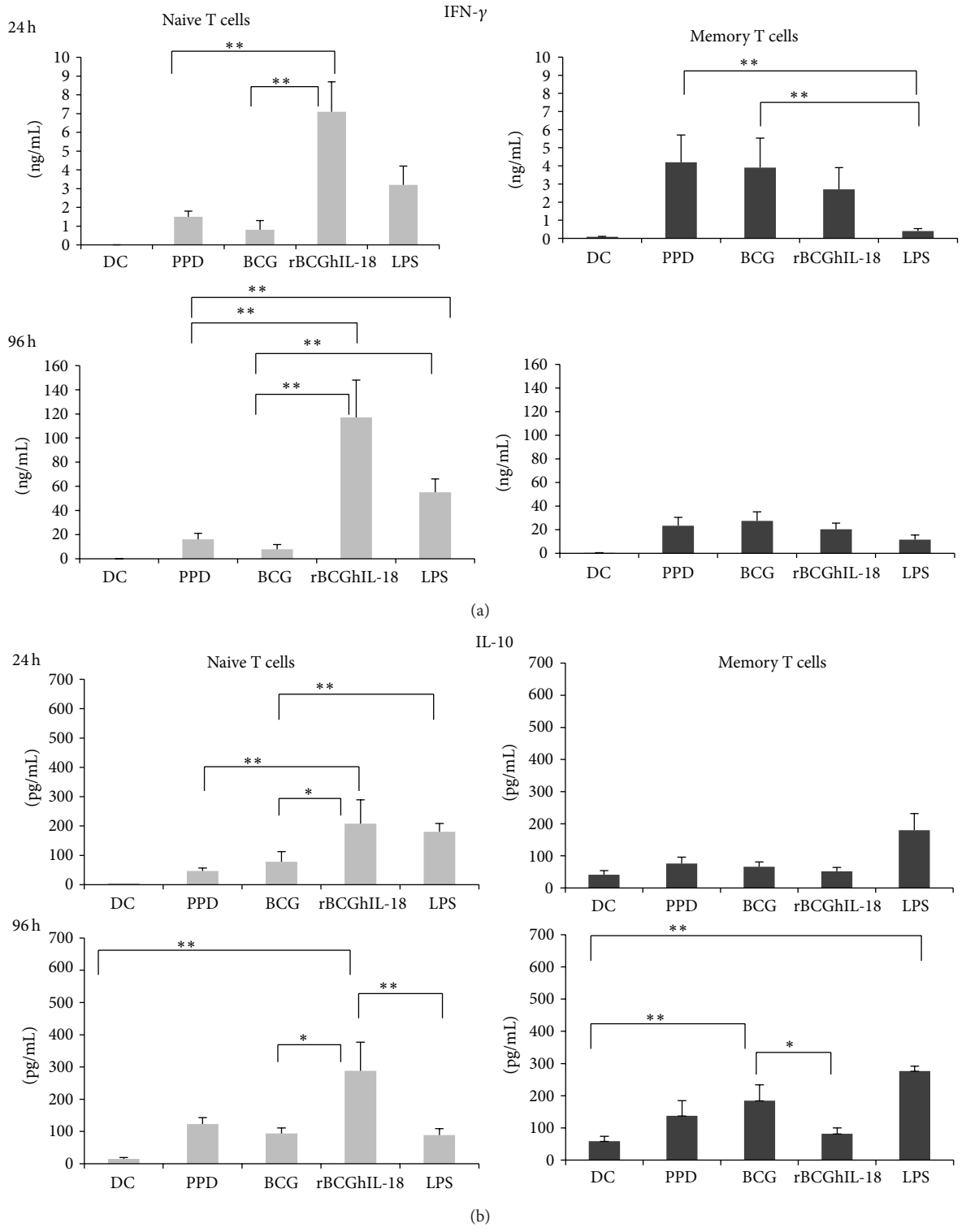

Figure 7: Secretion of IFN-γ (a) and IL-10 (b) by human naive (grey bars) and memory (black bars) T cells following 24 h and 96 h coculture with PPD- (10 μg/mL), BCG- (1 : 1), rBCGIL-18- (1 : 1), or LPS- (1 μg/mL) pulsed autologous MoDCs (ratio MoDCs/T cells, 1 : 10). The cytokine levels in the cocultures were measured by ELISA. Data shown are the mean ± SEM of 20 independent donors. Statistical analyses were performed using the Kruskal-Wallis test and Mann-Whitney U test. $^{*}P < 0.05$; $^{**}P < 0.01$.

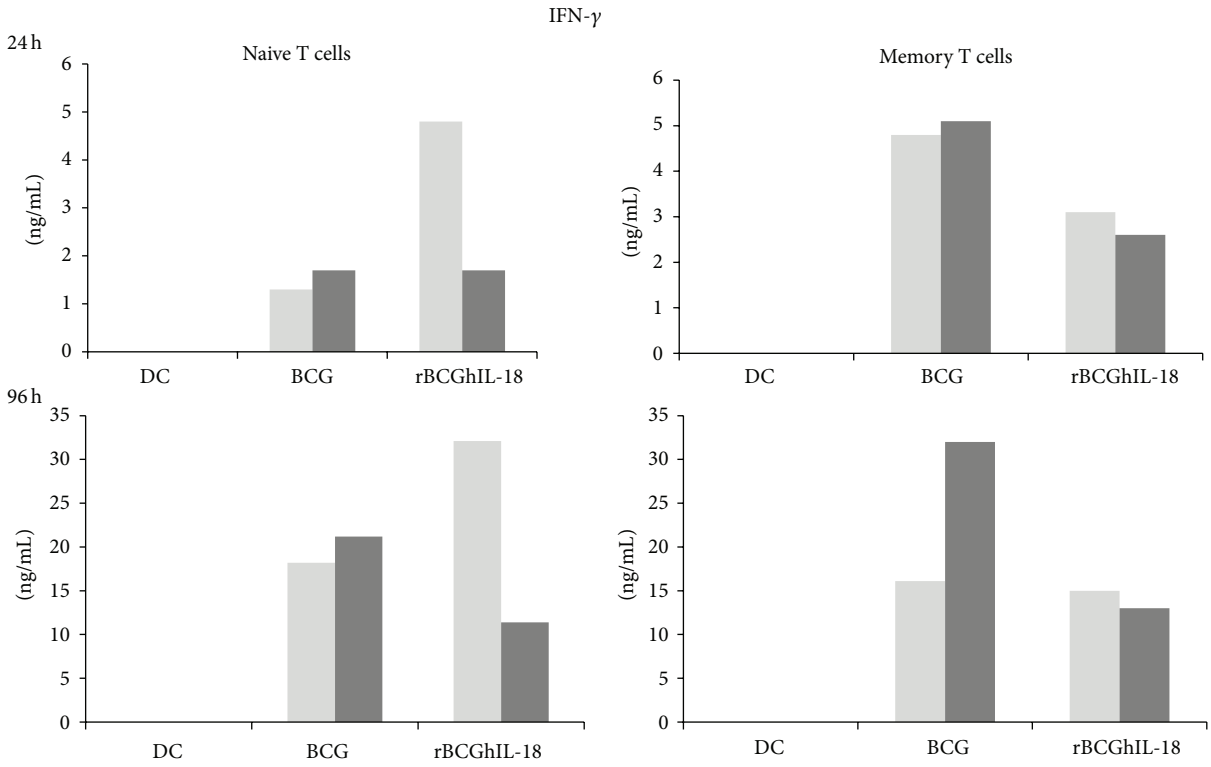

Figure 8: Secretion of IFN-γ by human naive and memory T cells following 24 h and 96 h coculture with BCG- (1 : 1), rBCGIL-18- (1 : 1) pulsed autologous MoDCs (ratio MoDCs/T cells, 1 : 10) in the presence (black bars) of neutralizing human anti-IL-18 antibody or not (grey bars). The cytokine level in the cocultures was measured by ELISA. One representative experiment out of three independent ones is shown.

The use of recombinant BCG producing IL-18 may be an attractive tool to polarize immune responses involved in specific defense mechanisms. Here, we constructed a recombinant BCG strain producing human IL-18 and investigated its effect on DCs and on DC-dependent IFN-γ production by $CD4^+$ T cells in a human *in vitro* model. Live BCG bacilli producing or not producing human IL-18 were used in the study to stimulate human DCs.

First, we examined the effect of rBCGhIL-18 on the expression of cell surface signal transduction receptors on DCs. IL-18 has been reported to promote the expression of costimulatory and adhesion molecules on the macrophages and DCs [30, 31]. Therefore, we examined the effect of rBCGhIL-18 on the expression of DC surface receptors indispensable in the formation of an immune synapse between DCs and T cells. We found that rBCGh-IL-18 upregulated CD86, and to a lesser extent, CD80, while other DC surface molecules (HLA-DR, CD40) were not upregulated. Nonrecombinant BCG also increased the expression of these receptors on DCs, which is in contrast to the results reported by Manickam and Sivanandham [32] showing reduced expression of CD80 but not CD86 on BCG- or PPD-stimulated DCs from patients with cervical cancer. The reasons for the discrepancy between the two studies are not clear and could be due to different experimental conditions, such as different MOIs used in the two studies and the health status of the DCs donors. DC-SIGN surface expression appeared to be decreased upon incubation of the DCs with PPD, BCG, rBCGhIL-18, or LPS as compared to unstimulated DCs. The role of DC-SIGN as an important host ligand in mycobacterial infection seems to be more complex since several DC-SIGN ligands on *M. bovis* BCG have been described [33]. Some studies have shown that *M. tuberculosis, M. avium* subsp. *paratuberculosis* and *M. bovis* BCG can bind to DC-SIGN to promote entry into human DCs and alveolar macrophages, in which these bacteria can survive [34, 35]. A decrease in DC-SIGN expression upon incubation with BCG may thus have an impact on the mycobacterial uptake and intracellular survival of mycobacteria.

In the second part, the examination of the cytokine profile of stimulated DCs revealed no significant effect of live BCG or rBCGhIL-18 and PPD on IL-12 production, although this cytokine was induced by LPS-stimulated DCs. The lack of IL-12 induction is surprising, as *M. tuberculosis* H37Rv, BCG, and *M. bovis* have been described to induce IL-12 production by murine macrophages and DCs [36, 37]. Other studies have shown that *M. tuberculosis* H37Rv and BCG do not induce IL-12 production in human macrophages and DCs [38, 39]. The inability of BCG or rBCGhIL-18 to induce IL-12 by DCs might be related to the IL-10 induction by these mycobacteria, as endogenous IL-10 was shown to suppress BCG-driven IL-12 production in DCs, and, in addition, downregulates the migration of antigen-loaded DCs to the draining lymph nodes, thereby decreasing antimycobacterial cellular response [40, 41]. It has also been suggested that IL-10 is linked with the ability of *M. tuberculosis* to evade host

immune responses and mediates long-term infections [42]. In our experimental conditions, we found that rBCGhIL-18 induced significantly more IL-10 by the DCs compared to nonrecombinant BCG or PPD. Significantly higher levels of IL-10 have also been shown by spleen cells of mice infected with recombinant BCG producing murine IL-18 compared to splenocytes from mice infected with non-recombinant BCG [19].

In contrast to IL-12, DCs stimulated with rBCGhIL-18 produced higher amounts of IL-23, compared to DCs treated with BCG or PPD. IL-23 is a heterodimeric cytokine, which shares the p40 subunit with IL-12, but this subunit is covalently linked to the specific p19 subunit [43, 44]. This cytokine can mediate inflammatory and pathological processes either by activating Th17 cells or by directly stimulating macrophages to secrete IL-1, TNF-α, and IL-6 [45, 46]. Initially, overlapping functions of IL-12 and IL-23 were postulated for IFN-γ production in PHA blast T cells, as well as in $CD45RO^+$ memory T cells [44]. Later studies, both *in vitro* and *in vivo*, revealed that IL-23 may negatively regulate IL-12-induced effector functions. IL-23 strongly reduces IL-12-driven secretion of IFN-γ by $CD8^+$ T cells, with less prominent effects in NK and $CD4^+$ T cells [47]. Zhang et al. [37] showed that *M. bovis* induces preferentially IL-23 rather than IL-12 by murine bone marrow-derived DCs. Our results are consistent with these studies, as we found a slight increase in IL-23 production by BCG-treated DCs compared to control DCs, although this did not reach statistical significance.

Among the chemokines involved in the specific attraction of Th1 cells, CXCL10 (IP-10) was described as the major one [48, 49]. Enhanced production of IP-10 by DCs stimulated with mycobacteria has been reported [50, 51], and IP-10 has even been proposed as a biomarker for *M. tuberculosis* infection [52]. In this study, we found that the production of human IL-18 significantly enhanced the ability of BCG to induce the IP-10 production by DCs, implying that this might lead to enhanced interactions of DCs with the Th1 cell population.

We previously reported that circulating naive $CD45RA^+$ $CD4^+$T cells from BCG-vaccinated volunteers become effector helper cells producing IFN-γ upon stimulation by autologous DC pulsed with PPD or infected with live BCG [28].

The present results extend these observations showing significantly enhanced IFN-γ production by naive $CD4^+$ T cells stimulated by rBCGhIL18-infected DCs. The same DCs induced much weaker production of IFN-γ in memory $CD4^+$ T cells. However, stimulation of DC with rBCGhIL-18 or nonrecombinant BCG led to similar levels of IFN-γ production by memory T cells. The strong induction of IFN-γ secretion by naive T cells incubated with rBCGhIL-18-stimulated DC in the absence of detectable amounts of IL-12 may have been due to the presence of IL-18R on the surface of naive T cells. On the other hand, strong IFN-γ production may lead to the upregulation of IL-18R on DCs [31], which may result in an optimized cytokine environment for DC interactions with naive $CD4^+$ T cells and thus enhance Th1 responses.

In cocultures of naive $CD4^+$ T cells and rBCGhIL18-infected DCs a statistically significant enhancement in IL-10 production was noticed. Much lower levels of IL-10 were present in the cocultures of naive T cells with DCs which were previously exposed to BCG or PPD. This observation is in agreement with the results reported by Madura Larsen et al. [39] showing that the interaction between BCG and DCs leads to the development of naive T cells into IL10-producing T cells. In a murine model, *M. bovis*-stimulated DCs also induced high levels of IL-10 by $CD4^+$ T cells [37]. The discriminating effects of rBCGhIL18-infected DCs on IL-10 production by naive and memory $CD4^+$ T cells, as shown in this study, open potential innovative possibilities for the development of new TB vaccines. In our experimental model recombinant rBCGhIL18-infected DCs preferentially induced IL-10 production in naive $CD4^+$ T cells, whereas DCs infected with non-recombinant BCG effectively induced IL-10 production in memory $CD4^+$ T cells.

In conclusion, in the present report, we demonstrated a remarkable advantage of recombinant rBCGhIL-18 producing human IL-18 over nonrecombinant BCG in stimulating human DC to preferentially trigger strong IFN-γ secretion by naive $CD4^+$ T cells, which is accompanied by moderately elevated IL-10 production. Although IFN-γ responses are clearly required for protection against TB, recent studies have shown a lack of correlation between the degree of immune protection induced by BCG and IFN-γ production by $CD4^+$ T cells [53, 54]. In addition, we have recently observed significantly enhanced IFN-γ responses to specific antigens of *M. tuberculosis* in patients with active tuberculosis [55]. Thus, antigen-specific IFN-γ responses may both play an essential role in protection against mycobacteria and be involved in mycobacteria-driven inflammatory processes. Thus, the concomitant enhancement of IFN-γ and IL-10 production in cocultures of rBCGhIL-18 stimulated DCs and naive $CD4^+$ T cells might provide balanced immunizing effects. Obviously, more work is required to better understand the relationship between the discriminating activities of recombinant rBCGhIL-18 producing human IL-18.

Conflict of Interests

The authors declare that there is no conflict of interests regarding the publication of this paper.

Acknowledgment

This work was supported by Grant of Ministry of Science and Higher Education in Poland no. N N401 015236.

References

[1] S. H. E. Kaufmann, "Fact and fiction in tuberculosis vaccine research: 10 years later," *The Lancet Infectious Diseases*, vol. 11, no. 8, pp. 633–640, 2011.

[2] T. Ulrichs and S. H. E. Kaufmann, "New insights into the function of granulomas in human tuberculosis," *The Journal of Pathology*, vol. 208, no. 2, pp. 261–269, 2006.

[3] A. O'Garra, P. S. Redford, F. W. McNab, C. I. Bloom, R. J. Wilkinson, and M. P. R. Berry, "The immune response in

tuberculosis," *Annual Review of Immunology*, vol. 31, pp. 475–527, 2013.

[4] K. Nakamura, H. Okamura, M. Wada, K. Nagata, and T. Tamura, "Endotoxin-induced serum factor that stimulates gamma interferon production," *Infection and Immunity*, vol. 57, no. 2, pp. 590–595, 1985.

[5] C. A. Dinarello, D. Novick, A. J. Puren et al., "Overview of interleukin-18: more than an interferon-γ inducing factor," *Journal of Leukocyte Biology*, vol. 63, no. 6, pp. 658–664, 1998.

[6] F. Biet, C. Locht, and L. Kremer, "Immunoregulatory functions of interleukin 18 and its role in defense against bacterial pathogens," *Journal of Molecular Medicine*, vol. 80, no. 3, pp. 147–162, 2002.

[7] D. Novick, S. Kim, G. Kaplanski, and C. A. Dinarello, "Interleukin-18, more than a Th1 cytokine," *Seminars in Immunology*, vol. 25, no. 6, pp. 439–448, 2013.

[8] M. Kinoshita, S. Seki, S. Ono, N. Shinomiya, and H. Hiraide, "Paradoxical effect of IL-18 therapy on the severe and mild *Escherichia coli* infections in burn-injured mice," *Annals of Surgery*, vol. 240, no. 2, pp. 313–320, 2004.

[9] M. J. Robertson, J. W. Mier, T. Logan et al., "Clinical and biological effects of recombinant human interleukin-18 administered by intravenous infusion to patients with advanced cancer," *Clinical Cancer Research*, vol. 12, no. 14, pp. 4265–4273, 2006.

[10] M. J. Robertson, J. M. Kirkwood, T. F. Logan et al., "A dose-escalation study of recombinant human interleukin-18 using two different schedules of administration in patients with cancer," *Clinical Cancer Research*, vol. 14, no. 11, pp. 3462–3469, 2008.

[11] A. A. Tarhini, M. Millward, P. Mainwaring et al., "A phase 2, randomized study of SB-485232, rhIL-18, in patients with previously untreated metastatic melanoma," *Cancer*, vol. 115, no. 4, pp. 859–868, 2009.

[12] M. Kinoshita, H. Miyazaki, S. Ono, and S. Seki, "Immunoenhancing therapy with interleukin-18 against bacterial infection in immunocompromised hosts after severe surgical stress," *Journal of Leukocyte Biology*, vol. 93, no. 5, pp. 689–698, 2013.

[13] V. E. García, K. Uyemura, P. A. Sieling et al., "IL-18 promotes type 1 cytokine production from NK cells and T cells in human intracellular infection," *The Journal of Immunology*, vol. 162, no. 10, pp. 6114–6121, 1999.

[14] I. Sugawara, "Interleukin-18 (IL-18) and infectious diseases, with special emphasis on diseases induced by intracellular pathogens," *Microbes and Infection*, vol. 2, no. 10, pp. 1257–1263, 2000.

[15] C.-H. Song, J.-S. Lee, H.-H. Nam et al., "IL-18 production in human pulmonary and pleural tuberculosis," *Scandinavian Journal of Immunology*, vol. 56, no. 6, pp. 611–618, 2002.

[16] B. E. Schneider, D. Korbel, K. Hagens et al., "A role for IL-18 in protective immunity against *Mycobacterium tuberculosis*," *European Journal of Immunology*, vol. 40, no. 2, pp. 396–405, 2010.

[17] L. Kremer, L. Dupré, I. Wolowczuk, and C. Locht, "In vivo immunomodulation following intradermal injection with DNA encoding IL-18," *Journal of Immunology*, vol. 163, no. 6, pp. 3226–3231, 1999.

[18] D. Xu, W. L. Chan, B. P. Leung et al., "Selective expression and functions of interleukin 18 receptor on T helper (Th) type 1 but not Th2 cells," *The Journal of Experimental Medicine*, vol. 188, no. 8, pp. 1485–1492, 1998.

[19] F. Biet, L. Kremer, I. Wolowczuk, M. Delacre, and C. Locht, "*Mycobacterium bovis* BCG producing Interleukin-18 increases antigen-specific gamma interferon production in mice," *Infection and Immunity*, vol. 70, no. 12, pp. 6549–6557, 2002.

[20] Y. Luo, H. Yamada, X. Chen et al., "Recombinant *Mycobacterium bovis bacillus Calmette-Guérin* (BCG) expressing mouse IL-18 augmente Th1 immunity and macrophage cytotoxicity," *Clinical and Experimental Immunology*, vol. 137, no. 1, pp. 24–34, 2004.

[21] F. Biet, C. Duez, L. Kremer et al., "Recombinant *Mycobacterium bovis* BCG producing IL-18 reduces IL-5 production and bronchoalveolar eosinophilia induced by an allergic reaction," *Allergy*, vol. 60, no. 8, pp. 1065–1072, 2005.

[22] C. M. Robinson, D. O'Dee, T. Hamilton, and G. J. Nau, "Cytokines involved in interferon-γ production by human macrophages," *Journal of Innate Immunity*, vol. 2, no. 1, pp. 56–65, 2009.

[23] M. G. Ranes, J. Rauzier, M. Lagranderie, M. Gheorghiu, and B. Gicquel, "Functional analysis of pAL5000, a plasmid from *Mycobacterium fortuitum*: construction of a "mini" mycobacterium—*Escherichia coli* shuttle vector," *Journal of Bacteriology*, vol. 172, no. 5, pp. 2793–2797, 1990.

[24] L. Kremer, A. Baulard, J. Estaquier, J. Content, A. Capron, and C. Locht, "Analysis of the *Mycobacterium tuberculosis* 85A antigen promoter region," *Journal of Bacteriology*, vol. 177, no. 3, pp. 642–653, 1995.

[25] A. Baulard, C. Jourdan, A. Mercenier, and C. Locht, "Rapid mycobacterial plasmid analysis by electroduction between *Mycobacterium* spp. and *Escherichia coli*," *Nucleic Acids Research*, vol. 20, no. 15, article 4105, 1992.

[26] U. K. Laemmli, "Cleavage of structural proteins during the assembly of the head of bacteriophage T4," *Nature*, vol. 227, no. 5259, pp. 680–685, 1970.

[27] B. Thurner, C. Röder, D. Dieckmann et al., "Generation of large numbers of fully mature and stable dendritic cells from leukapheresis products for clinical application," *Journal of Immunological Methods*, vol. 223, no. 1, pp. 1–15, 1999.

[28] M. Kowalewicz-Kulbat, D. Kaźmierczak, S. Donevski, F. Biet, J. Pestel, and W. Rudnicka, "Naive helper T cells from BCG-vaccinated volunteers produce IFN-γ and IL-5 to mycobacterial antigen-pulsed dendritic cells," *Folia Histochemica et Cytobiologica*, vol. 46, no. 2, pp. 153–157, 2008.

[29] L. Kremer, A. Baulard, J. Estaquier, O. Poulain-Godefroy, and C. Locht, "Green fluorescent protein as a new expression marker in mycobacteria," *Molecular Microbiology*, vol. 17, no. 5, pp. 913–922, 1995.

[30] P. Reddy, "Interleukin-18: recent advances," *Current Opinion in Hematology*, vol. 11, no. 6, pp. 405–410, 2004.

[31] R. Gutzmer, K. Langer, S. Mommert, M. Wittmann, A. Kapp, and T. Werfel, "Human dendritic cells express the IL-18R and are chemoattracted to IL-18," *The Journal of Immunology*, vol. 171, no. 12, pp. 6363–6371, 2003.

[32] A. Manickam and M. Sivanandham, "*Mycobacterium bovis* BCG and purified protein derivative-induced reduction in the CD80 expression and the antigen up-take function of dendritic cells from patients with cervical cancer," *European Journal of Obstetrics & Gynecology and Reproductive Biology*, vol. 159, no. 2, pp. 413–417, 2011.

[33] M. V. Carroll, R. B. Sim, F. Bigi, A. Jäkel, R. Antrobus, and D. A. Mitchell, "Identification of four novel DC-SIGN ligands on *Mycobacterium bovis* BCG," *Protein & Cell*, vol. 1, no. 9, pp. 859–870, 2010.

[34] T. Geijtenbeek, S. J. Van Vliet, E. A. Koppel et al., "Mycobacteria target DC-SIGN to suppress dendritic cell function," *Journal of Experimental Medicine*, vol. 197, no. 1, pp. 7–17, 2003.

[35] N. Maeda, J. Nigou, J.-L. Herrmann et al., "The cell surface receptor DC-SIGN discriminates between *Mycobacterium* species through selective recognition of the mannose caps on lipoarabinomannan," *The Journal of Biological Chemistry*, vol. 278, no. 8, pp. 5513–5516, 2003.

[36] K. Higuchi, Y. Sekiya, and N. Harada, "Characterization of *M. Tuberculosis*-derived IL-12-inducing material by alveolar macrophages," *Vaccine*, vol. 22, no. 5-6, pp. 724–734, 2004.

[37] X. Zhang, S. Li, Y. Luo et al., "*Mycobacterium bovis* and BCG induce different patterns of cytokine and chemokine production in dendritic cells and differentiation patterns in $CD4^+$T cells," *Microbiology*, vol. 159, no. 2, pp. 366–379, 2013.

[38] R. F. Silver, J. Walrath, H. Lee et al., "Human alveolar macrophage gene responses to *Mycobacterium tuberculosis* strains H37Ra and H37Rv," *The American Journal of Respiratory Cell and Molecular Biology*, vol. 40, no. 4, pp. 491–504, 2009.

[39] J. Madura Larsen, C. Stabell Benn, Y. Fillie, D. van der Kleij, P. Aaby, and M. Yazdanbakhsh, "BCG stimulated dendritic cells induce an interleukin-10 producing T-cell population with no T helper 1 or T helper 2 bias in vitro," *Immunology*, vol. 121, no. 2, pp. 276–282, 2007.

[40] M. C. Gagliardi, R. Teloni, F. Giannoni et al., "*Mycobacterium bovis* bacillus Calmette-Guérin infects DC-$SIGN^-$ dendritic cell and causes the inhibition of IL-12 and the enhancement of IL-10 production," *Journal of Leukocyte Biology*, vol. 78, no. 1, pp. 106–113, 2005.

[41] C. Demangel, P. Bertolino, and W. J Britton, "Autocrine IL-10 impairs dendritic cell (DC)-derived immune responses to mycobacterial infection by suppressing DC trafficking to draining lymph nodes and local IL-12 production," *European Journal of Immunology*, vol. 32, pp. 994–1002, 2002.

[42] P. S. Redford, P. J. Murray, and A. O'Garra, "The role of IL-10 in immune regulation during *M. tuberculosis* infection," *Mucosal Immunology*, vol. 4, no. 3, pp. 261–270, 2011.

[43] A. L. Croxford, F. Mair, and B. Becher, "IL-23: one cytokine in control of autoimmunity," *European Journal of Immunology*, vol. 42, no. 9, pp. 2263–2273, 2012.

[44] B. Oppmann, R. Lesley, B. Blom et al., "Novel p19 protein engages IL-12p40 to form a cytokine, IL-23, with biological activities similar as well as distinct from IL-12," *Immunity*, vol. 13, no. 5, pp. 715–725, 2000.

[45] D. J. Cua, J. Sherlock, Y. Chen et al., "Interleukin-23 rather than interleukin-12 is the critical cytokine for autoimmune inflammation of the brain," *Nature*, vol. 421, no. 6924, pp. 744–748, 2003.

[46] D. Yen, J. Cheung, H. Scheerens et al., "IL-23 is essential for T cell-mediated colitis and promotes inflammation via IL-17 and IL-6," *Journal of Clinical Investigation*, vol. 116, no. 5, pp. 1310–1316, 2006.

[47] A. N. Sieve, K. D. Meeks, S. Lee, and R. E. Berg, "A novel immunoregulatory function for IL-23: Inhibition of IL-12-dependent IFN-γ production," *European Journal of Immunology*, vol. 40, no. 8, pp. 2236–2247, 2010.

[48] F. Sallusto, P. Schaerli, P. Loetscher et al., "Rapid and coordinated switch in chemokine receptor expression during dendritic cell maturation," *European Journal of Immunology*, vol. 28, no. 9, pp. 2760–2769, 1998.

[49] J. H. Dufour, M. Dziejman, M. T. Liu, J. H. Leung, T. E. Lane, and A. D. Luster, "IFN-γ-inducible protein 10 (IP-10; CXCL10)-deficient mice reveal a role for IP-10 in effector T cell generation and trafficking," *Journal of Immunology*, vol. 168, no. 7, pp. 3195–3204, 2002.

[50] Y. Luo, X. Chen, and M. A. O'Donnell, "Mycobacterium bovis bacillus Calmette-Guérin (BCG) induces human CC- and CXC-chemokines *in vitro* and *in vivo*," *Clinical and Experimental Immunology*, vol. 147, no. 2, pp. 370–378, 2007.

[51] M. Ruhwald and P. Ravn, "Biomarkers of latent TB infection," *Expert Review of Respiratory Medicine*, vol. 3, no. 4, pp. 387–401, 2009.

[52] J. Y. Hong, G. S. Jung, H. Kim et al., "Efficacy of inducible protein 10 as a biomarker for the diagnosis of tuberculosis," *International Journal of Infectious Diseases*, vol. 16, no. 12, pp. e855–e859, 2012.

[53] L. M. Connor, M. C. Harvie, F. J. Rich et al., "A key role for lung-resident memory lymphocytes in protective immune responses after BCG vaccination," *European Journal of Immunology*, vol. 40, no. 9, pp. 2482–2492, 2010.

[54] H. McShane, "Tuberculosis vaccines: beyond bacilli Calmette-Guérin," *Philosophical Transactions of the Royal Society B: Biological Sciences*, vol. 366, no. 1579, pp. 2782–2789, 2011.

[55] M. Druszczynska, M. Wlodarczyk, B. Janiszewska-Drobinska et al., "Monocyte signal transduction receptors in active and latent tuberculosis," *Clinical and Developmental Immunology*, vol. 2013, Article ID 851452, 15 pages, 2013.

Hindawi Publishing Corporation
Journal of Immunology Research
Volume 2015, Article ID 834749, 9 pages
http://dx.doi.org/10.1155/2015/834749

Research Article

Evaluation of Anti-TBGL Antibody in the Diagnosis of Tuberculosis Patients in China

Jingge Zhao,[1] Zhaoqin Zhu,[2] Xiaoyan Zhang,[2,3] Yasuhiko Suzuki,[4] Haorile Chagan-Yasutan,[1,5] Haili Chen,[2] Yanmin Wan,[2,3] Jianqing Xu,[2,3] Yugo Ashino,[1] and Toshio Hattori[1,5]

[1] *Division of Emerging Infectious Diseases, Department of Internal Medicine, Graduate School of Medicine, Tohoku University, Sendai, Miyagi 980-8574, Japan*
[2] *Shanghai Public Health Clinical Center, Fudan University, Shanghai 201508, China*
[3] *Key laboratory of Medical Molecular Virology of the Ministries of Education, School of Basic Medical Science, Fudan University, Shanghai 201508, China*
[4] *Division of Global Epidemiology, Hokkaido University Research Center for Zoonosis Control, Sapporo, Hokkaido 001-0020, Japan*
[5] *Laboratory of Disaster-Related Infectious Disease, International Research Institute of Disaster Science, Tohoku University, Sendai, Miyagi 980-8574, Japan*

Correspondence should be addressed to Toshio Hattori; toshatto@med.tohoku.ac.jp

Received 21 November 2014; Revised 28 April 2015; Accepted 24 May 2015

Academic Editor: Beatrice Saviola

Tuberculous glycolipid (TBGL) is a component of the *Mycobacterium tuberculosis* cell wall, and anti-TBGL antibodies are used for serodiagnosis of tuberculosis. Anti-TBGL IgG and IgA levels were measured in 45 pulmonary TB patients (PTB), 26 extrapulmonary TB patients (ETB), 16 AIDS-TB patients, and 58 healthy controls (HC) including 39 health care workers (HW) and 19 newly enrolled students (ST). Anti-TBGL IgG measurements yielded 68.9% and 46.2% sensitivity in PTB and ETB, respectively, and 81.0% specificity. However, anti-TBGL IgA measurements were significantly less sensitive in detecting ETB than PTB (15.4% versus 46.7% sensitivity) but showed up to 89.7% specificity. Samples from AIDS-TB patients exhibited low reaction of anti-TBGL IgG and IgA with 6.3% and 12.5% sensitivity, respectively. Unlike anti-lipoarabinomannan (LAM) IgG that was found to elevate in sputum smearpositive subjects, anti-TBGL IgG and IgA elevated in those with cavitation and bronchiectasis, respectively. Anti-TBGL IgG in cavitary TB yielded 78.2% sensitivity compared to 57.1% in those otherwise. Meanwhile, higher anti-TBGL IgA titers were observed in HW than in ST, and increasing anti-TBGL IgG titers were observed in HW on follow-up. Therefore, higher anti-TBGL antibody titers are present in patients presenting cavities and bronchiectasis and subjects under TB exposure risk.

1. Introduction

In 2013, tuberculosis (TB) infected 9 million new individuals and caused 1.5 million deaths, making it one of the most critical infectious diseases worldwide. In terms of the number of reported cases, China ranks the second after India [1]. However, conventional microscopy is still widely used to diagnose TB, which renders variable sensitivities of 20–60% in detecting *tubercle bacilli* [2]. Moreover, approximately 20% of active TB cases and all latent TB infection (LTBI) cases cannot be microbiologically proven, even with fluorescence microscopy [3].

The specific IgG response to tuberculous glycolipid antigen (TBGL), a combination of trehalose-6,6′-dimycolate (TDM) and minor glycolipids, has been used to diagnose clinical TB infection in Japan, with approximately 80% sensitivity and specificity [4, 5]. The *WHO Stop TB Strategy* recommends TB screening and diagnostic algorithms should be implemented at a country level [6]. Previous studies performed in Japan have found that anti-TBGL IgG and anti-TBGL IgA titers correlate with cavitation and severities implicated by chest radiography [7]. Therefore, a combination of TBGL antibody detection and other TB clinical findings could further improve the accuracy of TB diagnosis [7, 8].

In a study in the Philippines, elevated anti-TBGL antibody titers were observed in healthcare workers (HW) with LTBI [9]. However, no study has evaluated anti-TBGL antibodies in TB patients or healthy individuals in China. Like TBGL, lipoarabinomannan (LAM), another glycolipid that constitutes mycobacterial cell walls, has been immensely investigated for its important roles in the immune-pathogenesis of TB [8–10], albeit limitations of anti-LAM IgG in TB diagnosis that may mislead diagnosis in about a quarter of cases [10]. Therefore, it is important to evaluate anti-TBGL antibodies in the context of varied TB pathogenesis attributable to pulmonary TB (PTB) patients, extrapulmonary TB (ETB) patients, and AIDS-TB patients.

2. Materials and Methods

2.1. Study Subjects. Blood samples were drawn from adult subjects (age > 18) recruited from Shanghai Public Health Clinical Center (SHAPHC), affiliated with Fudan University, Shanghai, China, between 2008 and 2011, after informed consent was obtained according to the protocol approved by the ethics committees from SHAPHC and the Tohoku University School of Medicine, Japan (20121322). PTB, ETB, and AIDS-TB samples were obtained from hospitalized patients who had undergone less than 2 weeks of anti-TB treatment. Blood was drawn after diagnosis of TB (Table 1). ETB samples included samples from patients with 9 different subtypes of ETB (Table 2). HIV-1 infection in the AIDS-TB patients was confirmed by detecting HIV-1 antibodies. The healthy control subjects (HC) recruited included 19 students (ST) and 39 health care workers (HW). The samples used for follow-up analysis were collected from 16 HW who underwent an annual checkup from 2009 to 2011. All HC subjects were diagnosed as free from active TB based on chest radiography and free from HIV infection at the time of blood collection.

2.2. Anti-TBGL Antibodies. Plasma levels of anti-TBGL IgG and IgA were measured using a Determiner TBGL Antibody ELISA kit (Kyowa Medex Co., Ltd., Tokyo, Japan). This assay uses TBGL antigen which is a combination of trehalose 6,6-dimycolate (TDM) and hydrophobic glycolipids extracted from MTB H37Rv and has been described previously [7]. The cutoff index for anti-TBGL IgG and IgA was set to 2.0 U/mL in accordance with previous studies (Figure 1(a)) [4, 5].

2.3. Anti-LAM IgG ELISA. The anti-LAM IgG ELISA method has been previously described [11]. ELISA Nunc MaxiSorp plates (Thermo Fisher Scientific, Inc., Waltham, MA) [12] were coated with 100 μL per well of 0.5 μg/mL purified lipoarabinomannan (LAM) (NACALAI TESQUE, INC.). A polyclonal antibody from Dr. Makoto Matsumoto (Otsuka Pharmaceutical Co., Ltd., Tokushima, Japan), which was made from a LAM immunized rabbit, was used as a positive control. Serum samples were diluted 100-fold in fetal bovine serum and incubated in coated well for 1 hour. After being washed, HRP-conjugated goat anti-human IgG heavy chain polyclonal antibody (LifeSpan BioSciences, Inc., Seattle, WA) was diluted 1 : 10,000 in 1% (w/v) BSA in PBS and added as the secondary antibody to detect anti-LAM IgG. Reactions were visualized using a TMB HRP substrate kit (KPL, Inc., Gaithersburg, MD). Optical density (OD) values were measured at 450 nm. The cutoff for anti-LAM IgG was set based on Receiver Operating Characteristic (ROC) curve (Figure 3(c)).

2.4. Statistical Analysis. All data were analyzed using GraphPad Prism 6.0 (GraphPad Software, San Diego, CA). A nonparametric t-test was used to determine the significance of differences between 2 groups with non-Gaussian distributions. *Kruskal-Wallis* tests were used to evaluate differences when more than 2 groups were involved. *Dunn's post hoc* tests were used to evaluate the differences between 2 groups following the *Kruskal-Wallis* test. A Chi-square test was used to test the variances among groups. The results were considered significant at $p < 0.05$. Paired nonparametric t-tests were used to compare the differences in the same samples in the three years of follow-up. Estimated optimal cutoff for other antibodies was achieved by Youden's index by MedCalc (MedCalc Software bvba, Belgium).

3. Results

3.1. Anti-TBGL Antibodies and Anti-LAM Antibodies. For anti-TBGL IgG, more samples from PTB patients had elevated titers compared to those with AIDS-TB ($p < 0.05$) or compared to HC ($p < 0.0001$). Amongst ETB samples, more samples had elevated titers of anti-TBGL IgG compared to HC ($p < 0.01$) (Figure 1(a)). Of note, there was no difference in anti-TBGL IgG titers between PTB and ETP samples. For anti-TBGL IgA, significantly higher titers were observed in the PTB samples compared to those of other groups ($p < 0.0001$ for HC, $p < 0.001$ for AIDS-TB, and $p < 0.05$ for ETB). However, there was no difference between ETP and HC samples or between ETP and AIDS-TB samples (Figure 1(b)). For anti-LAM IgG, significantly larger number of samples with higher responses was found amongst those from PTB patients compared to HC ($p < 0.001$) or AIDS-TB ($p < 0.05$) patients. Nevertheless, measurements of ETB samples were not significantly different from those of HC or AIDS-TB samples for anti-LAM IgG. Unlike that for anti-TBGL IgA, no difference was observed between the PTB and ETB samples with respect to anti-LAM IgG (Figure 1(c)).

3.2. Serodiagnosis amongst TB Patients. PTB patients were grouped in correspondence with the clinical findings listed in Table 1. Anti-TBGL IgG titers were significantly higher in patients with cavitation compared to those without such pathology, and significantly elevated anti-TBGL IgA titers were observed in subjects with bronchiectasis compared to those without it (t-test, $p < 0.05$, Figures 2(a) and 2(b)). However, there were no differences between subgroups for anti-LAM IgG with respect to chest radiographic findings ($p > 0.05$, Figure 2(c)), in spite of the fact that there were subjects with positive sputum smears that were higher anti-LAM IgG responses, which was not observed for anti-TBGL IgG or IgA (Figure 2(c)). Similar to PTB patients,

Table 1: Clinical and demographic information of study patients.

Parameter	Value for group			
	PTB	ETB	AIDS-TB	HC
Number of patients	45	26	16	58
Age (years [mean ± SD])	60.47 ± 18.19	46.83 ± 20.30	45.53 ± 8.02	28.43 ± 5.92
Sex (number of males/number of females)	35/10	11/15	12/3	41/17
Classification (number)				
New case	28	21	12	0
Relapsed case	11	4	3	0
Unknown	6	1	1	0
Comorbidities[a]				
Chronic diseases	27/17 (61.4)	9/17 (34.6)	5/9 (33.3)	n.a
Symptoms[a]				
Cough & chest discomfort	38/6 (86.4)	12/12 (50.0)	8/7 (53.3)	0/58 (0.0)
Fever	14/30 (31.8)	15/9 (62.5)	11/4 (73.3)	0/58 (0.0)
Hemoptysis	12/32 (27.3)	1/23 (4.2)	0/16 (0.0)	0/58 (0.0)
Expectoration	23/21 (52.3)	5/20 (20.0)	0/16 (0.0)	0/58 (0.0)
Chest X-ray[a]				
Cavitation	24/20 (54.5)	0/26 (0.0)	0/16 (0.0)	0/58 (0.0)
Pleural effusion	15/29 (34.1)	10/15 (40.0)	5/9 (35.7)	0/58 (0.0)
Lymphadenopathy (BHL)	3/41 (6.8)	3/22 (12.0)	3/11 (21.4)	0/58 (0.0)
Bronchiectasis	13/31 (29.5)	2/23 (8.0)	0/14 (0.0)	0/58 (0.0)
TB screening test[a]				
Smear	23/18 (56.1)	7/14 (33.3)	9/4 (69.2)	0/58 (0.0)
TST	11/6 (64.7)	7/3 (70.0)	1/0 (100.0)	0/58 (0.0)
TB antibody[a]				
Anti-TBGL IgG[b,c,e]	31/14 (68.9)	12/14 (46.2)	1/15 (6.3)	11/47 (19.0)
Anti-TBGL IgA[b,c,d]	21/23 (46.7)	4/22 (15.4)	2/14 (12.5)	6/52 (10.3)
Others mean ± std				
Blood IgA (g/L)	3.41 ± 1.76	3.13 ± 0.75	n.a	n.a
Blood IgG (g/L)	14.82 ± 4.64	16.50 ± 2.84	n.a	n.a
Blood IgM (g/L)	1.11 ± 0.50	1.49 ± 0.62	n.a	n.a
CRP (mg/L)	26.07 ± 27.64	28.95 ± 26.87	n.a	n.a
CD4 count	n.a	n.a	159.75 ± 177.16	n.a
CD8 count	n.a	n.a	636.38 ± 438.26	n.a

PTB = pulmonary TB; ETB = extrapulmonary TB; HC = healthy control. [a]The number of positive subjects/the number of negative subjects (percentage of positive subjects). [b]Significant difference between PTB and HC samples ($p < 0.05$). [c]Significant difference between PTB and AIDS-TB samples ($p < 0.05$). [d]Significant difference between PTB and ETB samples ($p < 0.05$). [e]Significant difference between ETB and HC samples ($p < 0.05$).

Table 2: Anti-TBGL IgG, anti-TBGL IgA, and anti-LAM IgG in ETB patients.

Subtypes of ETB ($n = 26$)	Number	TB related Biomarkers					
		Anti-TBGL IgG		Anti-TBGL IgA		Anti-LAM IgG	
Tuberculous pleurisy	7	2 (28.6%)[a]	1.2 [0.4–7.0][b]	1 (14.3%)	0.4 [0–4.0]	2 (28.6%)	0.06 [0.02–0.50]
Tuberculous meningitis	4	1 (25%)	0.65 [0.6–8.2]	0 (0%)	0.05 [−0.1–0.7]	1 (25%)	0.05 [0.03–0.08]
Miliary TB	3	2 (66.7%)	2.9 [1.3–5.6]	1 (33.3%)	0.6 [0–2.1]	3 (100%)	0.10 [0.01–0.14]
Intestinal TB	3	3 (100%)	15.9 [3.9–27.9]	1 (33.3%)	1.7 [0.2–428.8]	3 (100%)	0.14 [0.12–0.33]
Lymph node TB	3	1 (33.3%)	0.5 [0.4–11]	0 (0%)	0.2 [0.2–0.2]	2 (66.7%)	0.12 [0.06–0.39]
Renal TB	2	1 (50%)	20.4 [0.3–40.5]	0 (0%)	0.45 [0.2–0.7]	1 (50%)	0.12 [0.06–0.19]
Bone TB	2	1 (50%)	12.85 [0.4–25.3]	0 (0%)	0.2 [0–0.4]	2 (100%)	0.11 [0.10–0.12]
Endometrial TB	1	1 (100%)	3.5 [3.5]	1 (100%)	3.3 [3.3]	0 (0%)	0.06 [0.06]
Extrarenal TB	1	0 (0%)	0.8 [0.8]	0 (0%)	0.1 [0.1]	1 (100%)	0.13 [0.13]

ETB = extrapulmonary TB. [a]positive number (percentage) in compariso with the cut off of anti-TBGL IgG (cut off = 2), anti-TBGL IgA (cut off = 2), and anti-LAM IgG (cut off = 0.07), respectively; [b]median [range].

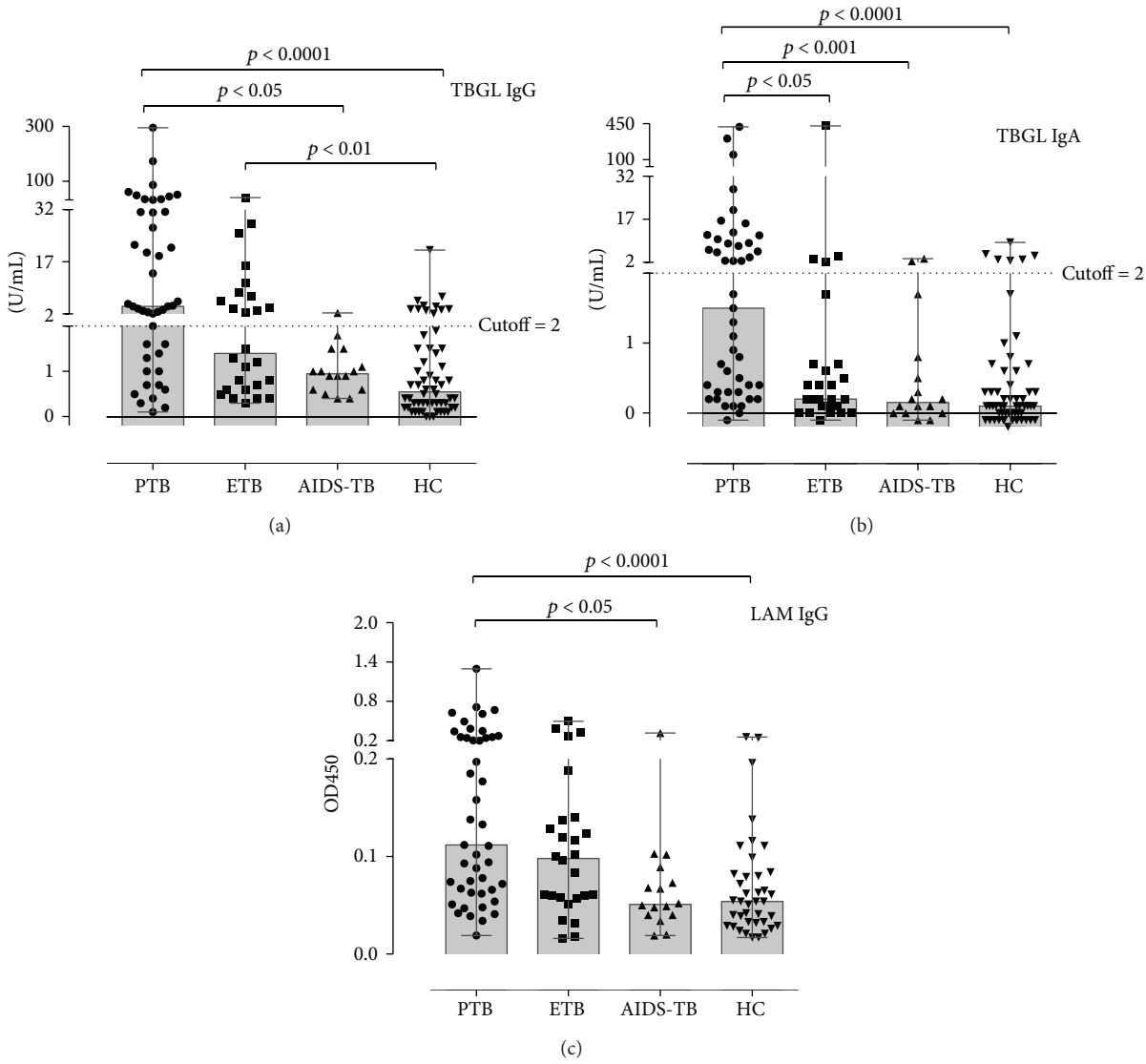

Figure 1: Detection of anti-TBGL IgG, anti-TBGL IgA, and anti-LAM IgG in TB patients and HC. PTB = pulmonary TB; ETB = extrapulmonary TB; HC = healthy control. Anti-TBGL antibody titers were evaluated in U/mL, and the anti-LAM IgG reactivity was assessed as OD values.

ETB patients showed relatively high anti-TBGL IgG titers in contrast to anti-TBGL IgA titers which were lower in ETB samples. Remarkably, all 3 intestinal TB subjects were anti-TBGL IgG positive (Median 15.9 Range [3.9–27.9]), while only 2 out of 7 TB pleurisy subjects showed positive in anti-TBGL IgG (Median 1.2 Range [0.4–7.0]). Samples from AIDS-TB patients had considerably lower titers for anti-TBGL antibodies compared to other TB groups (Figures 1(a) and 1(b)).

3.3. Anti-TBGL Antibody and Anti-LAM IgG in Healthy Controls (HC). We examined HC and HW anti-TBGL antibody titers. There are two subgroups of HC in this study, HW who worked in environments with higher risk to TB exposure and ST who had merely enrolled less than 1 year in the lab. The age of HW (30.51 ± 0.99, $n = 39$) was significantly higher than that of ST (24.16 ± 1.38, $n = 19$) (Table 1). Age did not correlate with either anti-TBGL antibody or anti-LAM IgG titers within HC or ST (Spearman, $p > 0.05$). The difference between ST and HW for anti-TBGL IgG and anti-LAM IgG titers was not statistically significant (nonparametric t-test, $p > 0.05$ for both), while such difference for anti-TBGL IgA titers was significant ($p < 0.01$, Figure 4(b)). We also performed a follow-up study of anti-TBGL antibodies in 16 HW. In the three-year follow-up, we observed a trend of HW subjects with increasing positive for anti-TBGL IgG but not for anti-TBGL IgA ($p < 0.05$, Figures 4(c) and 4(d)).

4. Discussion

The findings that the highest levels of anti-TBGL IgG were associated with cavitation in Chinese PTB patients were

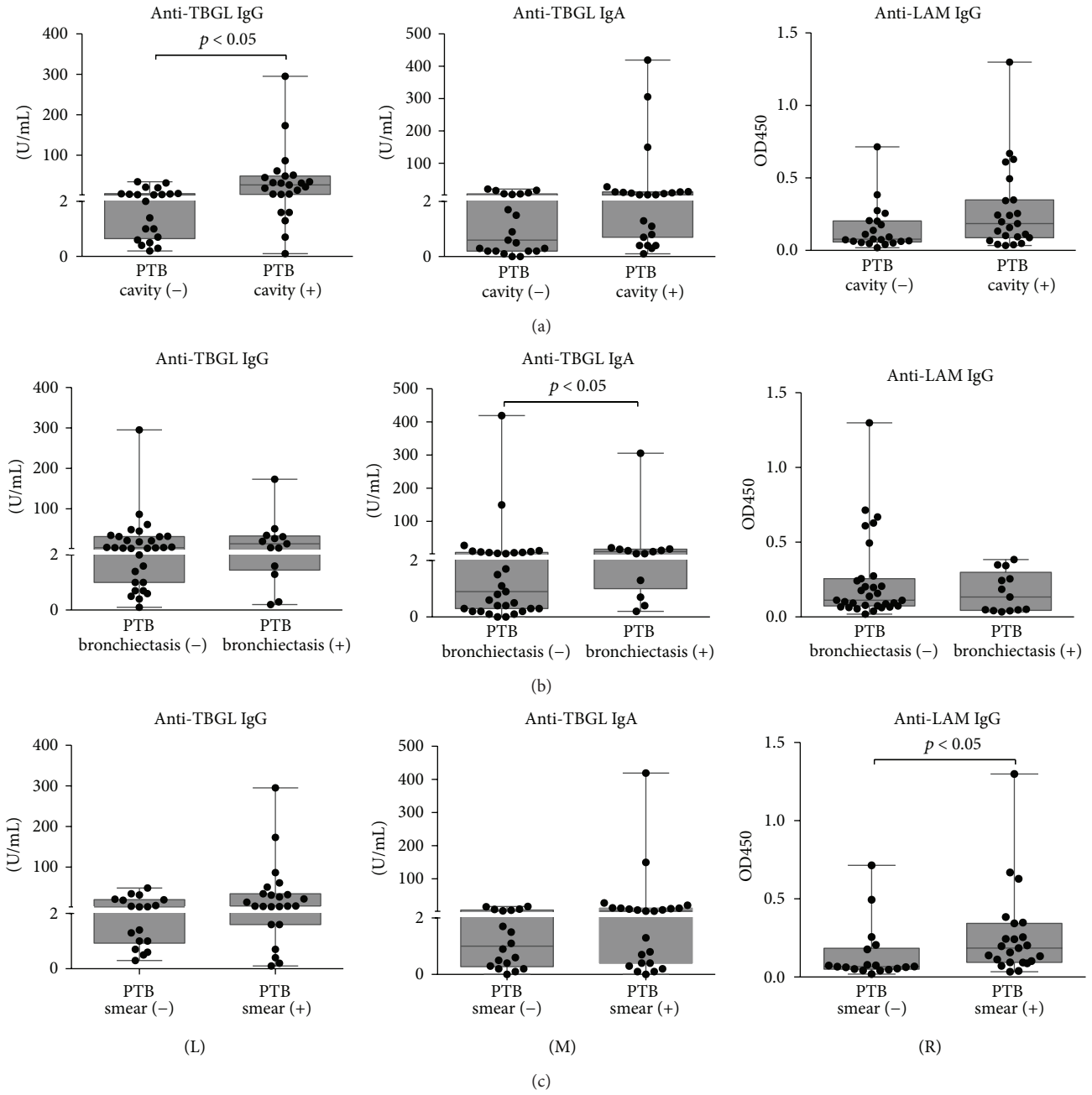

Figure 2: Elevated titers in association with different clinical findings. (a), (b), and (c) display findings of PTB-cavity versus PTB-noncavity, PTB-bronchiectasis versus PTB-nonbronchiectasis, and PTB-smear-negative versus PTB-smear-positive, respectively. A p value less than 0.05 indicates a significant difference between 2 groups by nonparametric t-test. (L), (M), and (R) referred to anti-TBGL IgG, anti-TBGL IgA, and anti-LAM IgG, respectively.

consistent with a previous study on Japanese subjects [7], a trend that was not observed for anti-LAM IgG. In contrast, higher anti-LAM IgG responses were observed in patients who are sputum smear positive, in agreement with a previous study [10, 13]. LAM-Anti-LAM complex may be formed in the serum of the sputum negative samples, reducing the sensitivity of anti-LAM antibody detection [14]. On the other hand, LAM was found more frequently in the urine of smear-positive patients, suggesting a constant stimulus for anti-LAM antibodies existing in such patients [15]. LAM may not associate with cavitation, while TBGL contained TDM, a cord factor, which has been reported to induce cavitation and granulomatous responses [16, 17]. CD1d targets TDM, which may play a critical role in hypersensitive granulomatous response to mycobacterial cord factor [18]. Therefore, in spite of the elevated titers of anti-TBGL IgG and anti-LAM IgG in PTB patients (Figures 1(a) and 1(c)), results of the clinical factor analysis for PTB suggested

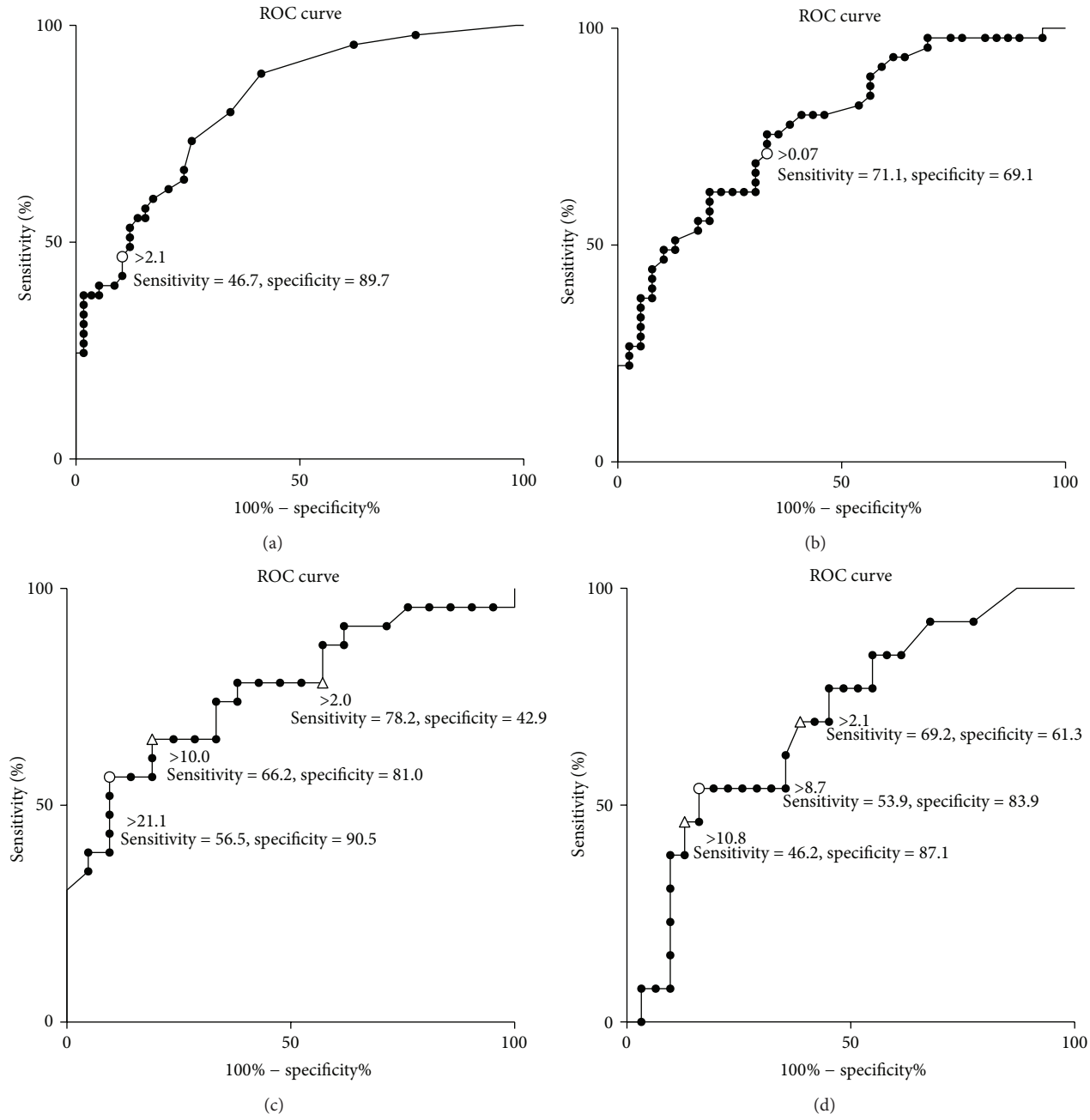

Figure 3: ROC analysis for different antibodies. (a) and (b) ROC analysis between PTB patients and HC for anti-TBGL IgA and anti-LAM IgG, respectively; (c) ROC analysis between cavities positive and negative subjects for anti-TBGL IgG; (d) ROC analysis between bronchiectasis positive and negative subjects for anti-TBGL IgA. *Circle*: estimated optimal cutoff according to Youden's index; *triangle*: arbitrary cutoff.

that anti-TBGL antibody responses are associated with a pathogenesis different from that associated with anti-LAM antibody. Although anti-TBGL IgA showed a higher titer in bronchiectasis PTB patients, 9 out of 13 patients presented with cavitation. In China, TB antibody measurements serving as a suggestive reference must be in combination with a third TB specific clinical reference for TB diagnosis. Amongst clinical findings, smear positive appears less challenging compared to cavitation and bronchiectasis to diagnose TB [19] that can be found not only in TB but also in other lung infections, such as *Aspergillus fumigatus* infection, or in lung cancer; therefore measurement of anti-TBGL antibody may benefit confirmation of PTB infection with cavitation or bronchiectasis radiography and avoid being compromised by sputum smear results [5, 8].

Elevated anti-TBGL IgG titers but low anti-TBGL IgA and anti-LAM IgG titers were observed in ETB patients (Figures 1(a) and 1(b)). Although higher anti-TBGL IgG titers were detected in all the ETB subtypes combined, anti-TBGL IgG titers varied with different sites of ETB.

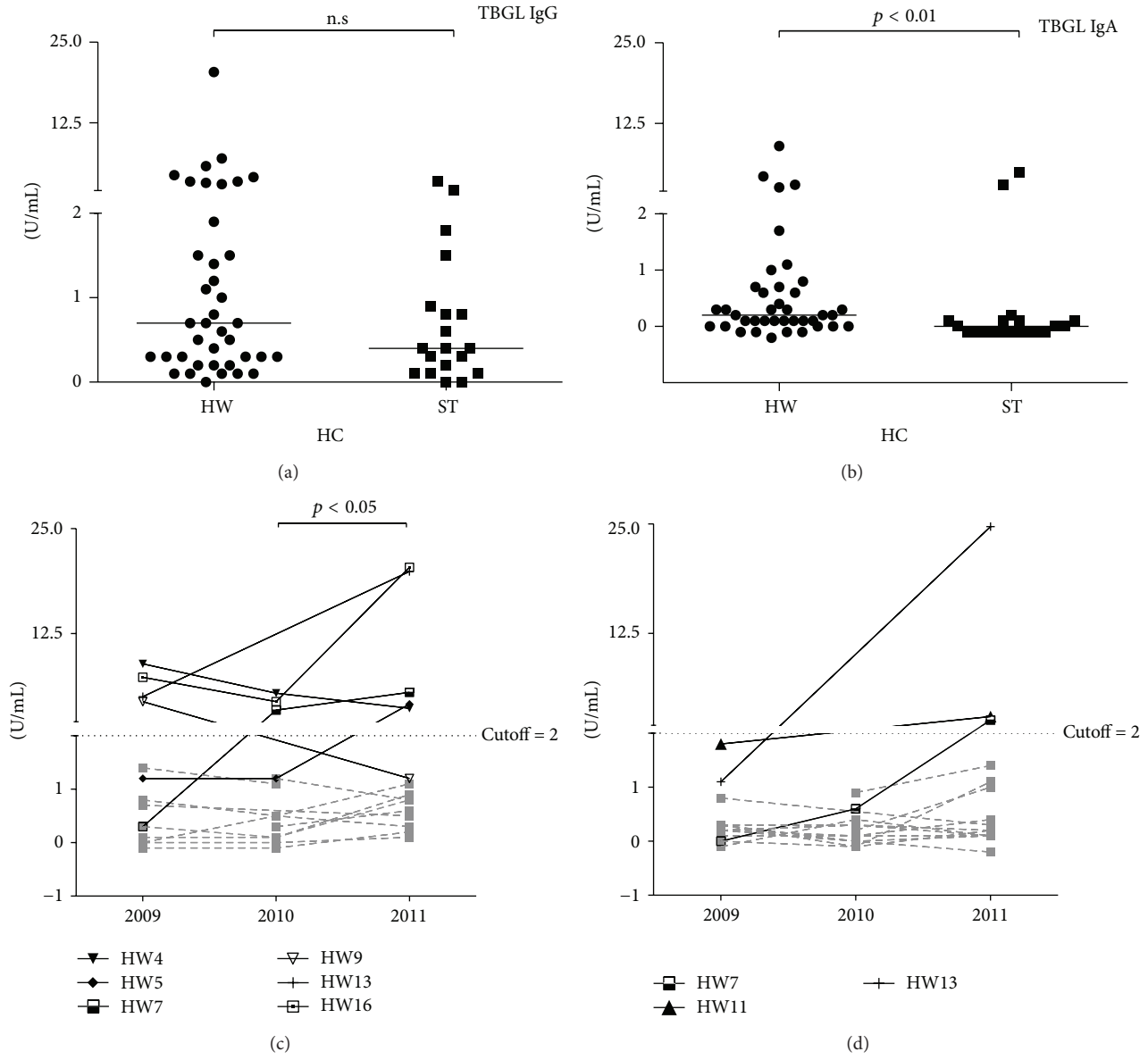

Figure 4: Detection of anti-TBGL antibodies and anti-LAM IgG among HC including HW and ST and follow-up study of HW. HW refers to health care workers; ST refers to new enrolled students (a and b); 2009, 2010, and 2011 refer to different years of sample collection (c and d).

Of note, tuberculous pleurisy showed relatively lower anti-TBGL IgG titers as compared to intestinal TB ($p < 0.05$, data not shown), suggesting an association between anti-TBGL antibody and specific sites of ETB where gastrointestinal mucosal may participate in responding to TBGL [20], as anti-TBGL antibody titer was found to decrease significantly in gastrectomized TB patients in our previous study [21]. Low titers of TB related antibody have been found in TB pleurisy in previous studies, but the reason is still unclear [22]. Low anti-TBGL antibodies and anti-LAM IgG titers were observed in AIDS-TB patients (Figure 1) due to failure in the development of potent humoral responses [23] and a malfunctioning gastrointestinal immune system [24].

The possibility of health care workers developing latent TB infection (LTBI) was 2.02–2.76 times higher than that of those in low-risk workplaces, and the LTBI incidence rate in HW was reported to be up to 43.4% in China [25]. In our previous study in the Philippines, we found elevated titers of both anti-TBGL IgG and IgA in HC subjects with diagnosed LTBI [9]. Of note, the follow-up study on 16 HW showed significant increase in anti-TBGL IgG titers over 3 years in the current study, though the significance of the data is not clear because LTBI was not confirmed.

The strength of this study, performed in a TB-prevalent country, is that anti-TBGL antibody detection could be sensitive and specific for PTB and ETB patients and HC in the context of clinical manifestation. In PTB, high anti-TBGL IgG and IgA titers were found to be associated with cavitation and bronchiectasis, respectively. In ETB, elevated anti-TBGL IgG titer in the absence of anti-TBGL IgA titer may serve as a pair

of biomarkers to diagnose ETB from PTB. TBGL antibody titers may be high in those who have been at risk of TB exposure, thereby raising cautions for low sensitivity of anti-TBGL antibodies test for healthy individuals. The limitation of this study includes the lack of the prognostic observation for PTB subjects, insufficient samples from each subgroup of ETB, and the inability to confirm LTBI infection in HW.

Disclosure

Jingge Zhao and Zhaoqin Zhu are the co-first authors for this work.

Conflict of Interests

The authors declare that there is no conflict of interests regarding the publication of this paper.

Acknowledgments

This work was supported by the Scientific Research Expenses for Health and Welfare program from the Ministry of Health, Labour and Welfare, Japan (TH), International Collaborative Study Grants from Human Science Foundation, and the grant from the Ministry of Education, Culture, Sports, Science, and Technology, Japan (MEXT) for the Joint Research Program of the Research Center for Zoonosis Control, Hokkaido University. This study was also supported by Shanghai Health Bureau project, Nongovernmental International Cooperation Project from the Shanghai Municipal Science and Technology Commission, National Natural Science Funds of China, and the Twelfth-Five-Major-Project of the Ministry of Science and Technology of China. The authors thank Dr. Yanqing Xiong and Dr. Shuihua Lu from SHAPHC for providing samples. TBGL kits were kindly provided by Kyowa Medex Co., Ltd., Japan. Anti-LAM antibodies were kindly provided by Dr. Makoto Matsumoto from Otsuka Pharmaceutical Co., Ltd., Tokushima, Japan.

References

[1] WHO, "Global tuberculosis report 2014," Tech. Rep. WHO/HTM/TB/2014.08, World Health Organization, Geneva, Switzerland, 2014, http://www.who.int/tb/publications/global_report/en/.

[2] S. S. S. Lima, W. T. Clemente, M. Palaci, R. V. Rosa, C. M. D. F. Antunes, and J. C. Serufo, "Conventional and molecular techniques in the diagnosis of pulmonary tuberculosis: a comparative study," *Jornal Brasileiro de Pneumologia*, vol. 34, no. 12, pp. 1056–1062, 2008.

[3] K. R. Steingart, M. Henry, V. Ng et al., "Fluorescence versus conventional sputum smear microscopy for tuberculosis: a systematic review," *The Lancet Infectious Diseases*, vol. 6, no. 9, pp. 570–581, 2006.

[4] T. Kishimoto, O. Moriya, J.-I. Nakamura, T. Matsushima, and R. Soejima, "Evaluation of the usefulness of a serodiagnosis kit, the determiner TBGL antibody for tuberculosis: setting reference value," *Kekkaku*, vol. 74, no. 10, pp. 701–706, 1999.

[5] R. Maekura, Y. Okuda, M. Nakagawa et al., "Clinical evaluation of anti-tuberculous glycolipid immunoglobulin G antibody assay for rapid serodiagnosis of pulmonary tuberculosis," *Journal of Clinical Microbiology*, vol. 39, no. 10, pp. 3603–3608, 2001.

[6] World Health Organization (WHO), *The Stop TB Strategy*, World Health Organization (WHO), Geneva, Switzerland, 2014, http://www.who.int/tb/strategy/stop_tb_strategy/en/.

[7] M. Mizusawa, M. Kawamura, M. Takamori et al., "Increased synthesis of anti-tuberculous glycolipid immunoglobulin G (IgG) and IgA with cavity formation in patients with pulmonary tuberculosis," *Clinical and Vaccine Immunology*, vol. 15, no. 3, pp. 544–548, 2008.

[8] R. Maekura, H. Kohno, A. Hirotani et al., "Prospective clinical evaluation of the serologic tuberculous glycolipid test in combination with the nucleic acid amplification test," *Journal of Clinical Microbiology*, vol. 41, no. 3, pp. 1322–1325, 2003.

[9] U. R. Siddiqi, P. S. A. Leano, H. Chagan-Yasutan et al., "Frequent detection of anti-tubercular-glycolipid-IgG and -IgA antibodies in healthcare workers with latent tuberculosis infection in the Philippines," *Clinical and Developmental Immunology*, vol. 2012, Article ID 610707, 10 pages, 2012.

[10] T. A. Tessema, G. Bjune, B. Hamasur, S. Svenson, H. Syre, and B. Bjorvatn, "Circulating antibodies to lipoarabinomannan in relation to sputum microscopy, clinical features and urinary anti-lipoarabinomannan detection in pulmonary tuberculosis," *Scandinavian Journal of Infectious Diseases*, vol. 34, no. 2, pp. 97–103, 2002.

[11] J. A. D. Navoa, S. Laal, L.-A. Pirofski et al., "Specificity and diversity of antibodies to *Mycobacterium tuberculosis* arabinomannan," *Clinical and Diagnostic Laboratory Immunology*, vol. 10, no. 1, pp. 88–94, 2003.

[12] J. Nowak, C. Watala, and M. Boncler, "Antibody binding, platelet adhesion, and protein adsorption on various polymer surfaces," *Blood Coagulation and Fibrinolysis*, vol. 25, no. 1, pp. 52–60, 2014.

[13] X. Yu, R. Prados-Rosales, E. R. Jenny-Avital, K. Sosa, A. Casadevall, and J. M. Achkar, "Comparative evaluation of profiles of antibodies to mycobacterial capsular polysaccharides in tuberculosis patients and controls stratified by HIV status," *Clinical and Vaccine Immunology*, vol. 19, no. 2, pp. 198–208, 2012.

[14] A. Raja, P. R. Narayanan, R. Mathew, and R. Prabhakar, "Characterization of mycobacterial antigens and antibodies in circulating immune complexes from pulmonary tuberculosis," *Journal of Laboratory and Clinical Medicine*, vol. 125, no. 5, pp. 581–587, 1995.

[15] S. D. Lawn, A. D. Kerkhoff, M. Vogt, and R. Wood, "Clinical significance of lipoarabinomannan detection in urine using a low-cost point-of-care diagnostic assay for HIV-associated tuberculosis," *AIDS*, vol. 26, no. 13, pp. 1635–1643, 2012.

[16] T. V. Guidry, R. L. Hunter Jr., and J. K. Actor, "Mycobacterial glycolipid trehalose 6,6′-dimycolate-induced hypersensitive granulomas: contribution of $CD4^+$ lymphocytes," *Microbiology*, vol. 153, no. 10, pp. 3360–3369, 2007.

[17] K. J. Welsh, R. L. Hunter, and J. K. Actor, "Trehalose 6,6′-dimycolate—a coat to regulate tuberculosis immunopathogenesis," *Tuberculosis*, vol. 93, supplement, pp. S3–S9, 2013.

[18] M. S. Vincent, J. E. Gumperz, and M. B. Brenner, "Understanding the function of CD1-restricted T cells," *Nature Immunology*, vol. 4, no. 6, pp. 517–523, 2003.

[19] L. B. Gadkowski and J. E. Stout, "Cavitary pulmonary disease," *Clinical Microbiology Reviews*, vol. 21, no. 2, pp. 305–333, 2008.

[20] P. D. Smith, L. E. Smythies, R. Shen, T. Greenwell-Wild, M. Gliozzi, and S. M. Wahl, "Intestinal macrophages and response to microbial encroachment," *Mucosal Immunology*, vol. 4, no. 1, pp. 31–42, 2011.

[21] J. Ashino, Y. Ashino, H. Guio, H. Saitoh, M. Mizusawa, and T. Hattori, "Low antibody response against tuberculous glycolipid (TBGL) in elderly gastrectomised tuberculosis patients," *International Journal of Tuberculosis and Lung Disease*, vol. 9, no. 9, pp. 1052–1053, 2005.

[22] K. R. Steingart, M. Henry, S. Laal et al., "A systematic review of commercial serological antibody detection tests for the diagnosis of extrapulmonary tuberculosis," *Thorax*, vol. 62, no. 10, pp. 911–918, 2007.

[23] J. M. Achkar and E. R. Jenny-Avital, "Incipient and subclinical tuberculosis: defining early disease states in the context of host immune response," *Journal of Infectious Diseases*, vol. 204, supplement 4, pp. S1179–S1186, 2011.

[24] J. M. Brenchley and D. C. Douek, "HIV infection and the gastrointestinal immune system," *Mucosal Immunology*, vol. 1, no. 1, pp. 23–30, 2008.

[25] X. Zhang, H. Jia, F. Liu et al., "Prevalence and risk factors for latent tuberculosis infection among health care workers in China: a cross-sectional study," *PLoS ONE*, vol. 8, no. 6, Article ID e66412, 2013.

Research Article

Multifunctional Analysis of CD4$^+$ T-Cell Response as Immune-Based Model for Tuberculosis Detection

Miriam Lichtner,[1,2] Claudia Mascia,[1] Ilaria Sauzullo,[1] Fabio Mengoni,[1] Serena Vita,[1] Raffaella Marocco,[2] Valeria Belvisi,[2] Gianluca Russo,[1] Vincenzo Vullo,[1] and Claudio M. Mastroianni[1,2]

[1]*Department of Public Health and Infectious Diseases, Istituto Pasteur-Fondazione Cenci Bolognetti, Sapienza University, Piazzale Aldo Moro 5, 00185 Rome, Italy*
[2]*Infectious Diseases Unit, Sapienza University, Corso della Repubblica 79, 04100 Latina, Italy*

Correspondence should be addressed to Claudio M. Mastroianni; claudio.mastroianni@uniroma1.it

Received 17 September 2014; Revised 30 December 2014; Accepted 30 December 2014

Academic Editor: Vishwanath Venketaraman

Mono- and multifunctional specific CD4$^+$ and CD8$^+$ T-cell responses were evaluated to improve the immune-based detection of active tuberculosis (TB) and latent infection (LTBI). We applied flow cytometry to investigate cytokines profile (IFN-γ, TNF-α, and IL-2) of T cells after stimulation with TB antigens in 28 TB-infected subjects (18 active TB and 10 LTBI) and 10 uninfected controls. Cytokines production by CD4$^+$ T cells at single-cell levels was higher in TB-infected subjects than uninfected controls ($P < 0.0001$). Assigning to activated CD4$^+$ T cells, producing any of the three cytokines, a cut-off >0.45%, it was possible to differentiate TB-infected (>0.45%) by uninfected subjects (<0.45%). Among TB-infected subjects, the frequencies of multifunctional CD4$^+$ T cells, simultaneously producing all 3 cytokines, are lower in active TB than LTBI subjects ($P = 0.003$). Thus, assigning to triple-positive CD4$^+$ T cells a cut-off <0.182%, TB-infected individuals could be classified as active TB subjects (<0.182%) or LTBI subjects (>0.182%). The magnitude of CD8$^+$ T-cell responses showed no differences between active TB and LTBI. Multifunctional CD4$^+$ T-cell responses could have the potential to identify at single time point subjects without TB infection and patients having active or latent TB.

1. Introduction

Mycobacterium tuberculosis (*Mtb*) infects more than 2 billion people worldwide; 90% of *Mtb*-infected individuals are able to resist overt tuberculosis (TB) disease determining the state of latency of infection (LTBI) [1]. Although latent and active TB disease are likely part of a dynamic spectrum [2, 3], individuals with LTBI are classically considered to be asymptomatic and not infectious; thus, the accurate classification of TB status is essential since treatment and prevention approaches are entirely different.

All existing tests for LTBI diagnosis, the tuberculin skin test (TST) and the newer interferon-gamma release assays (IGRAs), are acceptable but remain imperfect tests [4]. They represent indirect markers of *Mtb* exposure and provide immunological evidence of host sensitization to TB antigens. Both tests depend on cell-mediated immunity, and neither test can accurately differentiate between active TB and LTBI, distinguish reactivation from reinfection, or discriminate the various stages within the spectrum of *Mtb* infection [5, 6]. Thus, there is a need for newer biomarkers to classify patients at a single time point as having active TB, LTBI, or no infection.

Alternative immunological methods have been investigated in recent years [7–11]. In particular, multifunctional T cells, defined by their ability to coexpress two or more cytokines, have showed a better diagnostic yield than IGRA to detect TB infection [12–14] and have improved discrimination between active TB and LTBI [7–11, 15].

However, currently there is no consensus whether multifunctional T cells represent a marker of protective immunity or disease activity. Studies in animal models revealed a potential association of multifunctional Th1 cells with protective

immunity to TB [16], but some recent studies in humans have implicated multifunctional Th1 cells in protective immunity against pulmonary disease [10, 17], while others have shown that these cells might merely reflect the presence of active disease [7, 9].

In the present study, we applied an intracellular cytokine flow cytometry (ICCFC) to investigate monofunctional and multifunctional *Mtb*-specific $CD4^+$ and $CD8^+$ T cells in active TB and LTBI adults. Based on our findings, we propose an immune-based approach, which could improve the identification at single time point of subjects with no TB infection or patients having active or latent TB.

2. Materials and Methods

2.1. Study Subjects. The study population included 38 subjects enrolled at the Department of Public Health and Infectious Diseases, "Sapienza" University, Rome, Italy. The subjects were firstly classified into 2 main groups: TB infected and uninfected subjects. TB infected people were subsequently classified as active TB and latent TB. In summary, 18 patients with active TB (age range, 26–61 years); 10 patients with LTBI (age range, 41–60 years); and 10 healthy subjects (age range, 27–43 years) were recruited.

Diagnosis of active TB was made on the basis of clinical and radiological findings and was confirmed by identification of *M. tuberculosis* with microbiological methods and/or histological examination of affected tissues. All patients presented tubercular lung involvement.

We classified as LTBI the subjects who tested positive for both TST and QFT-GIT. All subjects classified as LTBI had also one of the following risk factors: chest X-ray suggestive of prior TB infection (apical pleural thickening, pulmonary nodules, upper lobe bronchiectasis, interstitial granulomatous calcification, cavitation, and lymph node or pericardial calcification) and a history of exposure to a case of active TB, originating from an area with a high prevalence of TB infection. None of the individuals had clinical, radiologic, and microbiological evidence of active TB, and none had received prior TB treatment. The healthy subjects were unexposed individuals with no previous history of TB, no know TB contact and tested negative for TST and QFT-GIT.

Measurement of IFN-γ levels by IGRA and multifunctional analysis of $CD4^+$ and $CD8^+$ T cells were performed on the same blood samples collected from all patients.

The study received approval from the Local Ethics Committee (reference number 2669), and informed consent was provided by all subjects.

2.2. Tuberculin Skin Test and QuantiFERON TB Gold-In Tube (QFT-GIT). After blood was drawn for the QFT-GIT assay, a TST (Biocine Test PPD, Chiron, Siena, Italy) was performed according to the Mantoux method by the same experienced operator, considering an induration of ≥10 mm as positive. The QFT-GIT assay (Cellestis Limited, Carnegie, Australia) was carried out and interpreted by the same trained technician, as per the manufacturer's instructions. Both operators were blind to the clinical status of the patients.

2.3. Intracellular Cytokine Flow Cytometry (ICCFC). For intracellular cytokine flow cytometry, heparinized peripheral blood was collected, and 0.5 mL of whole blood was added to 3 test tubes containing, respectively, saline (negative control), phytohaemagglutinin (PHA), and TB antigens (ESAT-6, CFP-10, and TB 7.7) [18]. The test tubes were supplied with the QFT-GIT. The TB antigens are pools of overlapping peptides and are pooled together as a single stimulation condition.

Whole blood was costimulated with anti-CD28 plus anti-CD49d (5 μL/mL, BD Bioscience, Pharmingen, Italy) as indicated by several authors [9, 10, 19], and Brefeldin A (10 μg/mL) (Sigma-Aldrich) was immediately added to each tube as previously described [20]. In order to avoid aspecific stimulation related to CD28/CD49d costimulation, we added anti-CD28/CD49d antibodies to both negative (saline) and positive (PHA) control tubes and to TB antigens tubes (ESAT-6, CFP-10, and TB 7.7) and we further subtracted the background values (in terms of IL-2, IFN-γ, and TNF-α) from TB antigens tubes.

In brief, after 18 hrs of incubation, the cell surface staining was performed with the following markers, anti-CD45-VioBlue, anti-CD4 PE-Vio770, and anti-CD8 PerCP (Miltenyi Biotec, Germany), and the red cells were lysed with 1 mL FACS lysing solution (BD Bioscience). Cells were then permeabilized with 0.5 mL FACS permeabilizing solution (BD Bioscience) and intracellularly stained with anti-IFN-γ FITC, anti-TNF-α APC, and anti-IL-2 PE (Miltenyi Biotec). Cells were fixed in 1% paraformaldehyde and analysed within 1 hr using a MACSQuant Analyzer flow cytometer (Miltenyi Biotec) after calibration and automatic compensation. We acquired at least 100,000 cells in the lymphocyte gate. FlowJo Software version 7.6.5 was used to perform a "combination gates" analysis. Seven different population cells were detected in $CD4^+$ and in $CD8^+$ cell gate on the basis of IFN-γ, IL-2, and TNF-α produced by $CD4^+$ and $CD8^+$ T cells (Figure 1). Background cytokine production in negative control (saline buffer) was subtracted from each stimulated condition. Intra-assay coefficient of variation and interassay coefficient variation were estimated and were <5% and <10%, respectively.

We classed T cells producing any of the 3 cytokines (IFN-γ or IL-2 or TNF-α) as "activated T cells," those producing IFN-γ alone or in combination with IL-2 and/or TNF-α as "total IFN-γ^+ T cells," those producing IL-2 alone or in combination with IFN-γ and/or TNF-α as "total IL-2^+ T cells," and those producing TNF-α alone or in combination with IL-2 and/or IFN-γ as "total TNF-α^+ T cells." Similarly, we classed polyfunctional T cells (those simultaneously producing all 3 cytokines) as "IFN-γ^+ IL-2^+ TNF-α^+ T cells."

2.4. Statistical Analysis. GraphPad Prism Software version 5 (Software MacKiev) was used. Nonparametric Kruskal-Wallis ANOVA with Dunn's posttest comparison and nonparametric Mann-Whitney test was applied to compare T-cell frequencies and the percentage of cytokine-secreting cells between 3 or 2 groups of patients, respectively. Receiver operating characteristic (ROC) analysis was performed to calculate optimal cut-off values for both activated $CD4^+$ T cells and polyfunctional $CD4^+$ T cells. ROC curves were

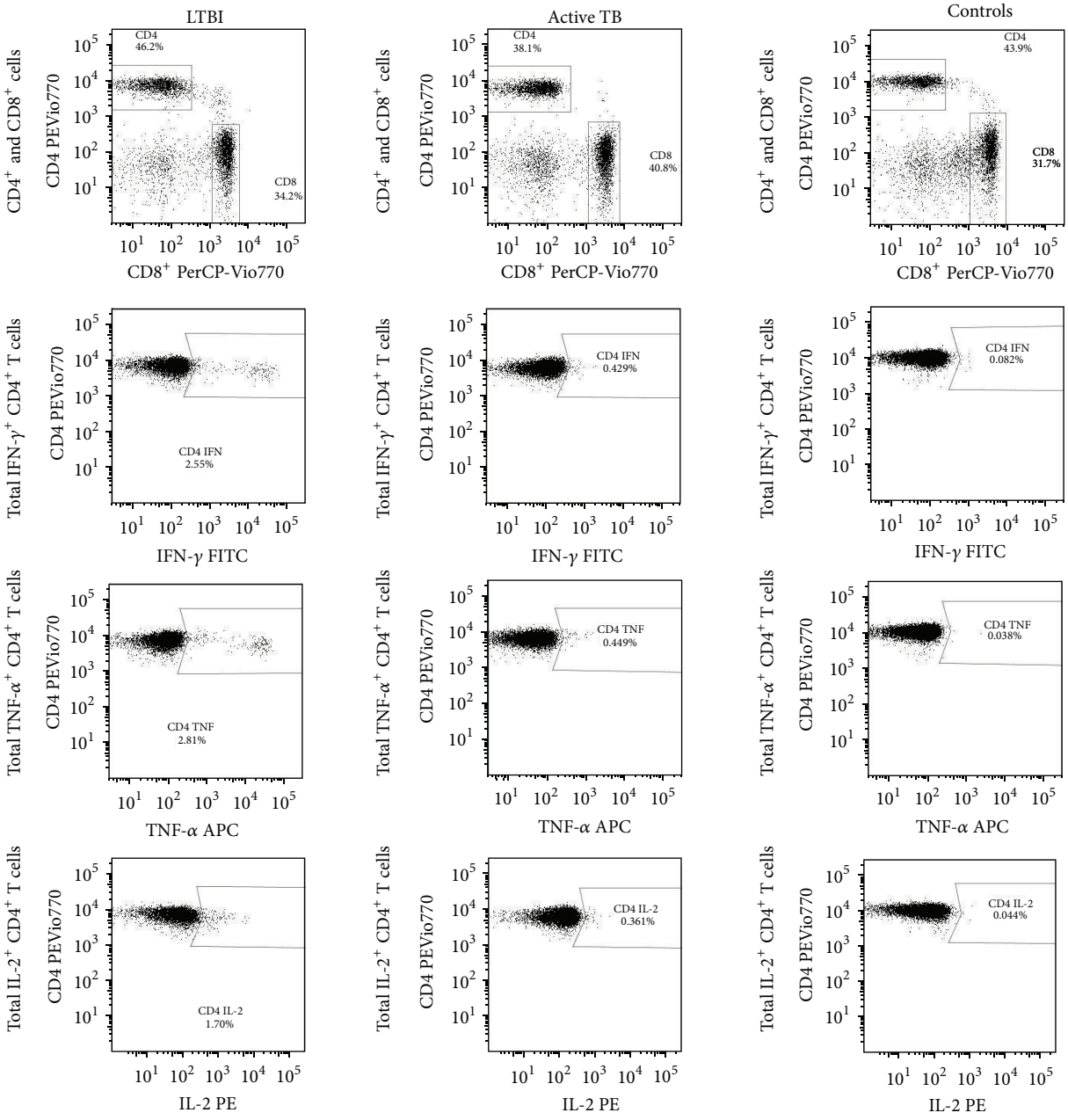

Seven population cells			
CD4 IFN$^+$ CD4 IL-2$^+$ CD4 TNF$^+$	1.28	0.078	0.006
CD4 IFN$^+$ CD4 IL-2$^+$ CD4 TNF$^-$	0.291	0.195	0.031
CD4 IFN$^+$ CD4 IL-2$^-$ CD4 TNF$^+$	0.542	0.02	0.006
CD4 IFN$^+$ CD4 IL-2$^-$ CD4 TNF$^-$	0.436	0.137	0.038
CD4 IFN$^-$ CD4 IL-2$^+$ CD4 TNF$^+$	0.04	0.02	0
CD4 IFN$^-$ CD4 IL-2$^+$ CD4 TNF$^-$	0.092	0.068	0.006
CD4 IFN$^-$ CD4 IL-2$^-$ CD4 TNF$^+$	0.951	0.332	0.025

Figure 1: Representative flow cytometry "combination gates" analysis of CD4$^+$ T cells of LTBI, active TB, and control subject under stimulation of TB antigens. Whole blood was analysed using a gating strategy to exclude debris and to identify CD4$^+$ and CD8$^+$ T cells on CD45$^+$ lymphocytes. The subsequent analysis was on CD4$^+$ gate to describe IFN-γ, IL-2, and TNF-α producing T cells. The percentages of the seven different population cells were showed at bottom and were defined in CD4$^+$ cell gate on the basis of total IFN-γ, IL-2, and TNF-α producing cells.

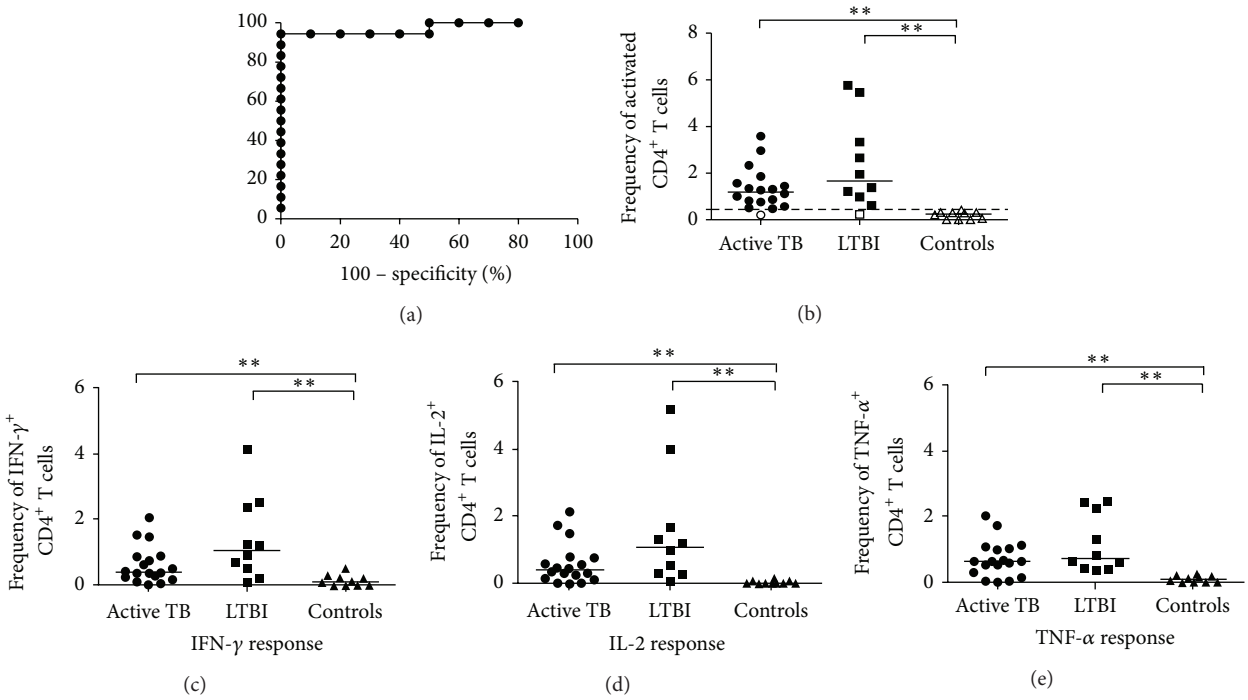

Figure 2: Analysis of cytokine production by $CD4^+$ cells at the single-cell level. (a) ROC curve (plotting sensitivity versus 1 − specificity) to discriminate infected (active TB and LTBI) from uninfected patients. The area under curve (AUC) was 0.9722. (b) Analysis of activated *M. tuberculosis*-specific $CD4^+$T cells producing any of the 3 cytokines (IFN-γ, IL-2, or TNF-α), using a cut-off to score responses as either positive or negative. The subjects were considered as positive (black) whether the frequency of $CD4^+$ T cells was >0.45% and negative (white) when the frequency was <0.45%. Horizontal bars represent the median values and horizontal dashed line indicates the cut-off of 0.45%. ((c), (d), and (e)) Frequency of "total IFN-γ^+," "total IL-2^+," and "total TNF-α^+" *Mtb*-specific $CD4^+$T cells in active TB patients ($n = 18$), in LTBI patients ($n = 10$), and in healthy controls ($n = 10$) is shown. Horizontal bars represent the median values. Statistical analysis was performed using Kruskal-Wallis ANOVA with Dunn's posttest comparison and significant differences are indicated by asterisks ($^{**}P < 0.01$).

generated by plotting the sensitivity against 1 − specificity, and the area under the curve (AUC) with 95% confidence intervals (95% CIs) was calculated. All statistical analyses were two-sided and considered significant at P values < 0.05.

3. Results

3.1. TST and QFT-GIT Results. QFT-GIT was positive in 13/18 (72%), negative in 3/18 (17%), and indeterminate in 2/18 (11%) of active TB patients. As expected, QFT-GIF was positive in all 10 (100%) LTBI patients and in none of the healthy controls. The TST was positive in all LTBI and negative in all healthy controls, whereas it was positive in 11/18 (61%) and 7/18 (39%) of active TB patients.

3.2. Cytokine Flow Cytometry Analysis of Mtb-Specific $CD4^+$ T Cells at the Single-Cell Level. The expression of $CD4^+$ T cells producing any of the 3 cytokines (IFN-γ or IL-2 or TNF-α) was assessed in patients with active TB, LTBI, and healthy controls, after simulation with *Mtb*-specific antigens. A significantly higher frequency of these $CD4^+$ T cells was found in active TB patients (median 1.197%, range 0.219%–3.59%) and in LTBI patients (1.666%, 0.234–5.762%) if compared to healthy controls (0.246%, 0–0.423%; $P < 0.0001$ by Kruskal-Wallis test); on the other hand, no significant differences were found between the 2 infected group subjects. Following this observation, we performed a ROC analysis (Figure 2(a)) and a cut-off >0.45% for activated $CD4^+$ T cells was found as the value allowing the best combination of sensitivity (94.44%, 95% CI: 72.2–99.8%) and specificity (100%, 95% CI: 69.15–100%; AUC 0.9722; 95% CI: 0.9141–1.030%, $P < 0.0001$) to differentiate *Mtb*-infected patients (active TB and LTBI) from healthy controls. Using this cut-off, we scored as positive 17/18 (95%) of active TB patients, 9/10 (90%) of LTBI patients, and none of 10 healthy controls (Figure 2(b)). Thus, the analysis of *Mtb*-specific $CD4^+$ T cells allowed the discrimination between *Mtb*-infected and uninfected patients.

In another set of analyses, we compared the frequency of "total IFN-γ^+ $CD4^+$ T cells," "total IL-2^+ $CD4^+$ T cells," and "total TNF-α^+ $CD4^+$ T cells" (as defined in Section 2) in our 3 groups of the subjects. The frequencies of "total IFN-γ^+ $CD4^+$ T cells" and "total IL-2^+ $CD4^+$ T cells" were higher in LTBI patients compared to those with active TB and healthy controls, although these differences attained statistical significance only between *Mtb*-infected (active TB and LTBI) and healthy subjects ($P = 0.0014$ for IFN-γ; $P = 0.0001$ for IL-2 by Kruskal-Wallis test)

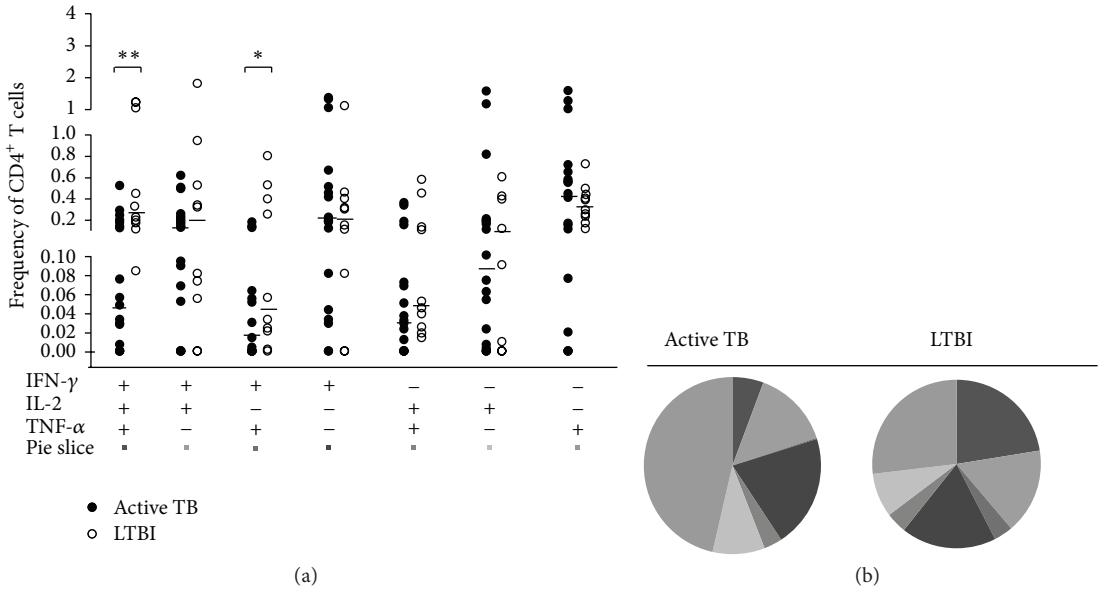

Figure 3: Multifunctional cytokine analysis of *M. tuberculosis*-specific $CD4^+$ T cells. (a) Frequency of *Mtb*-specific $CD4^+$ T cells producing all combinations of IFN-γ, IL-2, and TNF-α in active TB patients ($n = 18$, black circles) and in LTBI patients ($n = 10$, white circles). Horizontal bars represent the median values. Statistical analysis was performed using Mann-Whitney test and significant differences are indicated by asterisks ($^{**}P < 0.01$, $^{*}P < 0.05$). (b) Pie charts represent the relative proportions of cytokine-producing T-cell subsets in each group after *Mtb*-specific stimulation. A key to colours used in the pie charts is shown at the bottom of the panel (a).

(Figures 2(c) and 2(d)). The frequency of "TNF-α^+ $CD4^+$ T cells" was higher in patients with active and latent TB than in healthy controls ($P = 0.0003$ by Kruskal-Wallis test; Figure 2(e)).

Thus, the analysis of cytokine production by *Mtb*-specific $CD4^+$ T cells at the single-cell level was unable to indicate TB status among the studied subjects not allowing a distinction between active TB and LTBI.

3.3. Multifunctional Cytokine Analysis of Mtb-Specific $CD4^+$ T Cells. We analysed our samples for all possible combinations of intracellular expression of IFN-γ, IL-2, and TNF-α in cytokine-producing $CD4^+$ T cells in subjects with active and latent TB. Significantly greater frequencies of both "IFN-γ^+ TNF-α^+" and "IFN-γ^+ IL-2^+ TNF-α^+" $CD4^+$ T-cell subsets were observed in LTBI patients compared to active TB patients ($P = 0.003$ and $P = 0.034$, respectively; by Mann-Whitney test) (Figure 3(a)). Conversely, the frequency of other single- or double-cytokine-secreting $CD4^+$ T cells did not differ significantly between these two groups.

However, the cytokine profile (Figure 3(b)) revealed that in LTBI patients the proportion of polyfunctional $CD4^+$ T cells producing the 3 cytokines simultaneously was greater (23%) compared to other double-cytokine-producing $CD4^+$ T cells (IFN-γ^+ TNF-α^+ = 4%; IL-2^+ TNF-α^+ = 4%; IFN-γ^+ IL-2^+ = 16%), but similar to single-cytokine-producing $CD4^+$ T cells (TNF-α^+ = 27%, IFN-γ^+ = 18%). In contrast, subjects with active TB showed a smaller proportion of polyfunctional $CD4^+$ T cells (8%) and a predominance of $CD4^+$ T-cell subset secreting TNF-α alone which constituted 46% of the total cytokine response.

Based on these differences, we performed a ROC analysis (Figure 4(a)) and cut-off < 0.182% for polyfunctional $CD4^+$ T cells allowed the best combination of sensitivity (77.78%, 95% CI: 52.36–93.59) and specificity (70%, 95% CI: 34.75–93.33%; AUC 0.8444; 95% CI: 0.7021–0.9868%, $P = 0.0002$) to differentiate between active TB and LTBI subjects. Using this cut-off to score ICCFC responses as either positive or negative, we observed a positive response (>0.182%) in 4 out of 18 (22%) active TB patients and in 7 out of 10 (70%) LTBI patients (Figure 4(b)). In our hands, the frequency of polyfunctional $CD4^+$ T cells which simultaneously produced IFN-γ, IL-2, and TNF-α may be indicative of LTBI status.

3.4. Specific $CD8^+$ T-Cell Responses to Mtb Antigens in Intracellular Cytokine Flow Cytometry. The analysis of activated $CD8^+$ T cells, producing any of the 3 cytokines (IFN-γ or IL-2 or TNF-α) showed similar results to $CD4^+$ T cells, revealing a significant greater frequency of activated $CD8^+$ T cells in both active TB (median 0.599%, range 0–4.55%) and LTBI patients (0.489%, 0–1.796%) compared to healthy controls (0%, range 0–0.249%, $P < 0.0020$ by Kruskal-Wallis test), but no difference was found between two groups of infected individuals (Figure 5(a)). Likewise, the frequency of "total IFN-γ^+ $CD8^+$ T cells" (Figure 5(b)), "total IL-2^+ $CD8^+$ T cells" (Figure 5(c)), and "total TNF-α^+ $CD8^+$ T cells" (Figure 5(d)) was significantly higher in active TB patients compared to the other 2 groups of patients. These differences were only statistically significant between active TB subjects and healthy controls ($P = 0.0045$ for IFN-γ^+; $P = 0.0033$ for IL-2; $P = 0.0078$ for TNF-α by Kruskal-Wallis test).

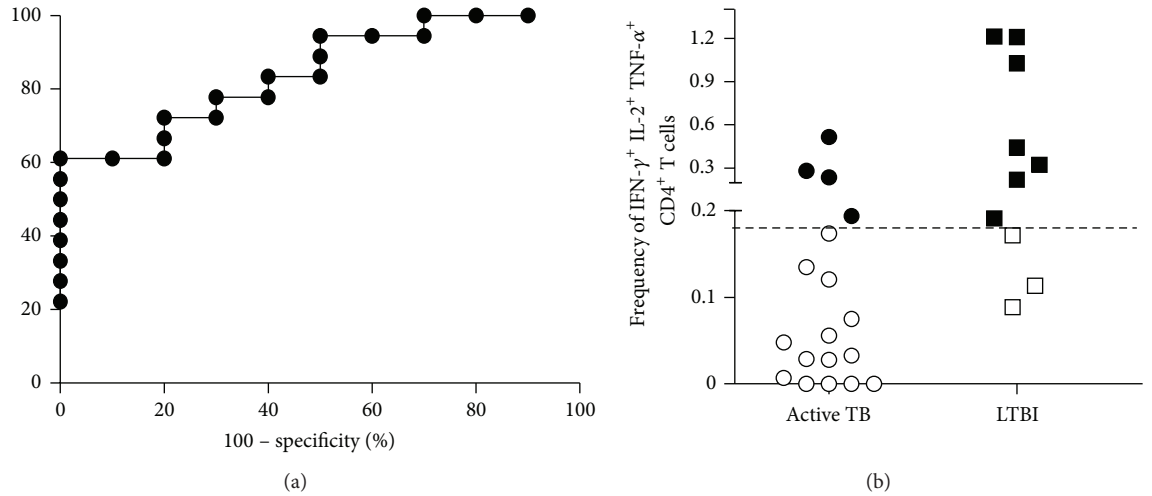

Figure 4: Differentiation between active and latent *Mtb*-infected subjects. (a) ROC curve (plotting sensitivity versus 1 – specificity) to discriminate active TB from LTBI patients. The area under curve (AUC) was 0.8444. (b) Analysis of triple-positive IFN-γ^+ IL-2^+ TNF-α^+ $CD4^+$ T cells, using a cut-off to score responses as either positive or negative. The subjects were considered as positive (black) whether the frequency of $CD4^+$ T cells was >0.182% and negative (white) when the frequency was <0.182%. Horizontal bars represent the median values and horizontal dashed line indicates the cut-off of 0.182%.

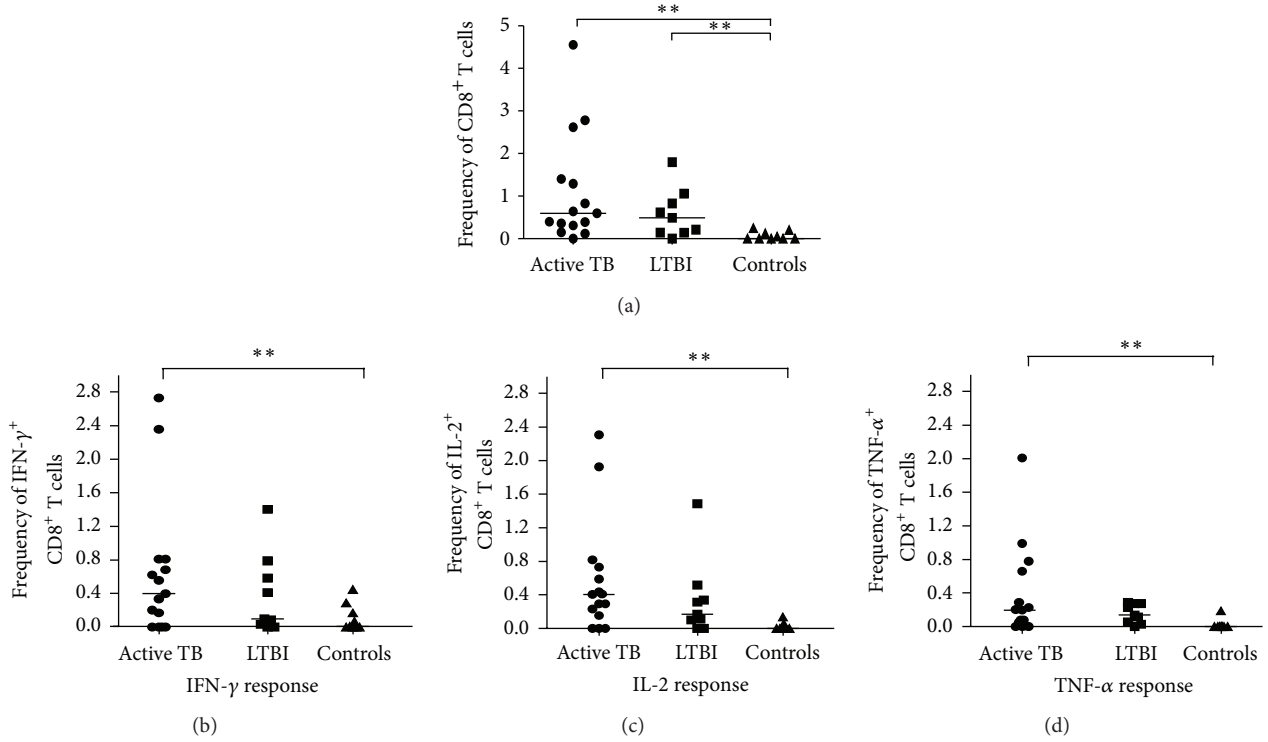

Figure 5: Analysis of cytokine production by $CD8^+$ T cells at the single-cell level. (a) Frequencies of activated *Mtb*-specific $CD8^+$T cells producing any of the 3 cytokines (IFN-γ, IL-2, or TNF-α) cells in active TB patients (n = 18), in LTBI patients (n = 10), and in healthy controls (n = 10) are show. ((b), (c), and (d)) Frequency of "total IFN-γ^+," "total IL-2^+," and "total TNF-α^+" *Mtb*-specific $CD8^+$T in active TB patients (n = 18), in LTBI patients (n = 10), and in healthy controls (n = 10) is shown. Horizontal bars represent the median values. Statistical analysis was performed using Kruskal-Wallis ANOVA with Dunn's posttest comparison and significant differences are indicated by asterisks ($^{**}P < 0.01$).

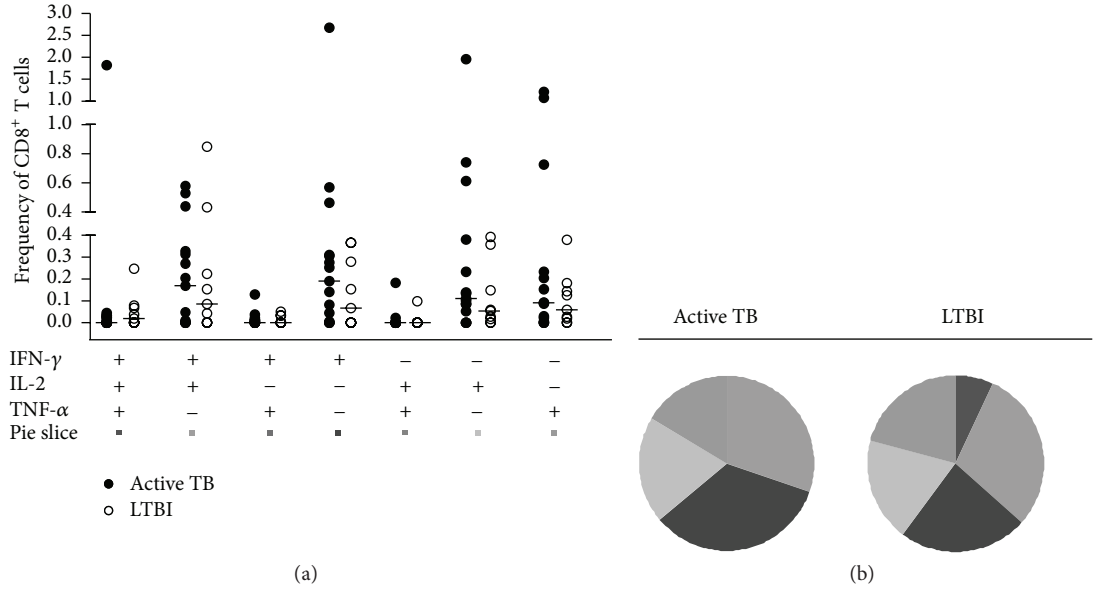

Figure 6: Multifunctional cytokine analysis of *Mtb*-specific $CD8^+$ T cells. (a) Frequency of *Mtb*-specific $CD8^+$ T cells producing all combinations of IFN-γ, IL-2, and TNF-α in active TB patients ($n = 18$, black circles) and in LTBI patients ($n = 10$, white circles). Horizontal bars represent the median values. Statistical analysis was performed using Mann-Whitney test. (b) Pie charts represent the relative proportions of cytokine-producing T-cell subsets in each group after *Mtb*-specific stimulation. A key to colours used in the pie charts is shown at the bottom of the panel (a).

As regards the cytokine profiles of *Mtb*-specific $CD8^+$ T cells, we found no significant differences between active TB and LTBI subjects ($P > 0.05$ for each $CD8^+$ T-cell subset by Mann-Whitney test; Figure 6(a)). Still, observing the pie charts (Figure 6(b)) the proportions of single-, double-, or triple-cytokine-secreting $CD8^+$ T-cell subsets were comparable between two groups of individuals.

Hence, the evaluation of the *Mtb*-specific $CD8^+$ T-cell responses in both monofunctional and polyfunctional analyses did not allow the distinction between active TB and LTBI subjects.

4. Discussion

In recent years, immunological response to *Mtb* has been extensively studied with the purpose of not only better understanding the TB pathogenesis but also improving diagnosis. The more recent IGRA offer some improvements over the TST, showing an excellent specificity for LTBI diagnosis and correlating well with the magnitude of exposure to *M. tuberculosis* [21]. Nevertheless, they have several known limitations including the reduced accuracy in immunocompromised subjects [22–24], the presence of conversions and reversions of results when serially applied in the same individuals [25–27], the inability to distinguish reactivation from reinfection, and the inability to accurately differentiate between LTBI and active TB [5, 6].

In the present study, using IGRA assay as a tool for TB detection, no significant differences in the average IFN-γ responses were observed among our TB and LTBI subjects, since similar percentages of positive IFN-γ responses were present in both of the 2 groups.

With a view to improving discrimination between active TB and LTBI, we applied an intracellular cytokine flow cytometry (ICCFC) to investigate monofunctional and multifunctional *Mtb*-specific $CD4^+$ and $CD8^+$ T cells.

Multifunctional T cells simultaneously secreting IFN-γ, TNF-α, and IL-2 play a critical role in the control of chronic bacterial and viral infections [28]. Changes in cytokine profiles could be a general feature of *Mtb*-specific T cells in TB infection, but limited and controversial data have made it difficult to define the role of these cells in TB [29]. Some studies support the concept that a higher proportion of triple-positive $CD4^+$ T cells correlates with LTBI when comparing active TB and latent subjects, suggesting that this T-cell subset may be a surrogate marker of *Mtb* load and consequently of active replication control in LTBI subjects [10, 15, 17]. In contrast, others indicate a higher proportion of triple-positive $CD4^+$ T cells in active TB than in LTBI subjects [7, 9], but the methodology used was different and so was the definition of LTBI.

The present study provides a detailed analysis of the frequency of cytokine-producing $CD4^+$ and $CD8^+$ T cells in *Mtb*-infected (active TB and LTBI) and uninfected subjects.

Regarding the $CD4^+$ T-cell compartment, the first finding was that analysis of activated cells producing any of the 3 cytokines (IFN-γ or IL-2 or TNF-α) may help to differentiate *Mtb*-infected (active TB and LTBI) and uninfected subjects. In fact with a cut-off > 0.45% for activated $CD4^+$ T cells, we scored as positive the 95% of active TB patients, the 90%

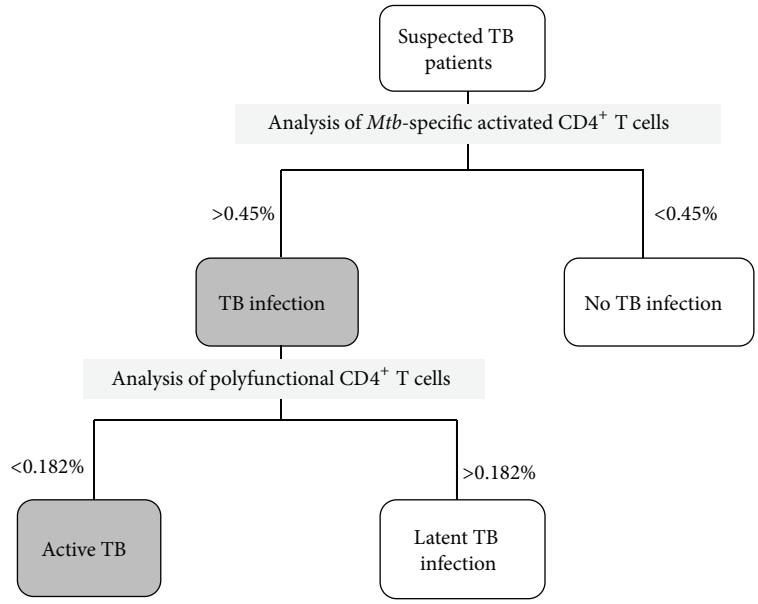

Figure 7: Proposed immune-based model for detection of active and latent TB. Taking into account the analysis of activated $CD4^+$ T cells, it is possible to differentiate *Mtb*-infected subjects (>0.45%) by uninfected subjects (<0.45%). With the analysis of multifunctional $CD4^+$ T cells, simultaneously producing all 3 cytokines, infected individuals may be classified as active TB subjects (<0.182%) or as LTBI subjects (>0.182%).

of LTBI patients, and none of healthy controls, clearly differentiating *Mtb*-infected patients from healthy controls. It is interesting to note that active TB patients showed a low response using TST and QFT (only 61% and 72%, resp.) confirming that routinely immunological tests were not useful in diagnosis of active disease. Our data suggest that analysis of activated $CD4^+$ T cells has a good sensitivity in active TB.

Also the analysis of $CD4^+$ T cells secreting IFN-γ alone, IL-2 alone, and TNF-α alone, revealed a prevalent frequency of all these T cells in infected compared to uninfected subjects. Still, it is interesting to note a slightly higher frequency of both "all IFN-γ^+" and "all IL-2^+" $CD4^+$ T cells in LTBI patients with respect to active TB patients, in line with recent studies showing that $CD4^+$ T cells producing IFN-γ and IL-2 have been implicated in protective immunity to TB [30, 31]. Taken together, monofunctional analysis was able to distinguish infected and uninfected subjects but was unable to indicate TB status not allowing a clear distinction between active and latent infection.

Moreover searching for a difference between active and latent TB, we performed a broad characterization of the functional profiles of *Mtb*-specific $CD4^+$ T cells to determine all combinations of intracellular expression of IFN-γ, IL-2, and TNF-α. These findings revealed that latent infection is associated with an increased frequency of two $CD4^+$ T-cell subsets, those producing IFN-γ, IL-2, and TNF-α simultaneously (triple-positive) and those producing IFN-γ in combination with TNF-α, indicating a possible protective role of these cells population in maintaining latent inflection. Indeed, we found that multifunctional $CD4^+$ T cells, in particular those producing 3 cytokines simultaneously, provided the best discrimination between active and latent infection. In fact using a cut-off of 0.182% for triple-positive $CD4^+$ T cells, most LTBI subjects (70%) showed a positive response, whereas the majority of active TB patients (78%) have a response below the cut-off.

Taken together, the detection of less than 0.182% of triple-positive $CD4^+$ T cells is strongly indicative of active TB with a specificity of 70%, whereas frequencies of these cells above 0.182% could be indicative of LTBI with sensitivity of 77.7%.

Most notably and in contrast with latent infection, our subjects with active TB disease had a predominance of $CD4^+$ T cells secreting TNF alone which constituted 46% of the total cytokine response. This is in agreement with previous studies showing that TNF production is a major component of the immune response to *Mtb*-antigen in active disease and thus the most reliable marker for diagnosing TB disease [7, 10, 11, 32, 33]. TNF expansion could be responsible for a high degree of inflammation, which could be linked to tissue damage and lung lesions rather than protection and control of the pathogen.

According to what has been assumed to be the hallmark of a protective $CD4^+$ T-cell response in various models of human viral infections [28, 34, 35], we found a significantly higher proportion of multifunctional IFN-γ^+ IL-2^+ TNF-α^+ $CD4^+$ T cells in subjects with LTBI, which are able to control *Mtb* replication compared with those with current TB disease, in which $CD4^+$ T cells secreting TNF alone dominated the *Mtb*-specific response.

As regards the $CD8^+$ T-cell compartment, Rozot et al. [36, 37] recently indicated that *Mtb*-specific $CD8^+$ T-cell responses can be detected predominantly in patients with active TB as compared to LTBI subjects, suggesting

a correlation between $CD8^+$ T-cell responses and high antigen burden [19, 38]. This hypothesis is supported by a recent study performed in children showing that *Mtb*-specific $CD8^+$ T cells were detected in active TB disease but not in healthy children recently exposed to *Mtb*, despite the fact that similar frequencies of $CD4^+$ T cells were present in both groups [39].

Moreover, little is known about the size, quality, and specificity of *Mtb*-specific $CD8^+$ T-cell responses during active and latent infection. In our study, the monofunctional analysis allowed a distinction between infected and uninfected subjects, following the same trend as in $CD4^+$ T cells. Conversely, the polyfunctional analysis of $CD8^+$ T-cell responses showed no significant differences between active and latent infected patients.

The present study has some limitations, such as the relatively small number of patients within each clinical group and the lack of a prospective analysis. Nevertheless, the ICCFC assessment of multifunctional *Mob*-specific $CD4^+$ T cells enabled us to determine the different clinical stage of TB infection. In this respect we propose an immune model (Figure 7) which, with a cut-off of 0.45% for activated $CD4^+$ T cells, may initially discriminate *Mtb*-infected (active TB and LTBI) patients (>0.45%) from uninfected subjects (<0.45%) with a specificity of 100%. Then, the infected individuals may be classified as active TB subjects if they showed frequencies of triple-positive T cells less than 0.182% and as LTBI subjects if the frequencies of triple-positive T cells are instead above 0.182% with a sensitivity of 77.78% and a specificity of 70%.

5. Conclusion

Multifunctional flow cytometry analysis of specific $CD4^+$ T-cell response may represent a simple and rapid immune-based approach to distinguish between *Mtb*-infected and uninfected subjects. The more interesting result of the study is the increased number of active TB patients detected with multifunctional analysis of $CD4^+$ T-cell response in comparison to QTF-GIT or TST. As general use as a clinical diagnostic test in order to identify patients with active versus latent TB infection, this immunological approach needs to be validated in a larger and prospective study and to be extended to other forms of active tuberculosis.

Conflict of Interests

The authors declare that they have no conflict of interests in publishing this paper.

Acknowledgments

The authors gratefully acknowledge the contributions to this research by the study participants and staff.

References

[1] World Health Organization, *Global Tuberculosis Control: WHO Report 2013*, WHO, Geneva, Switzerland, 2013, http://www.who.int/tb/publications/global_report/en/.

[2] C. E. Barry Jr., H. I. Boshoff, V. Dartois et al., "The spectrum of latent tuberculosis: rethinking the biology and intervention strategies," *Nature Reviews Microbiology*, vol. 7, no. 12, pp. 845–855, 2009.

[3] K. Dheda, S. K. Schwander, B. Zhu, R. N. Van Zyl-Smit, and Y. Zhang, "The immunology of tuberculosis: from bench to bedside," *Respirology*, vol. 15, no. 3, pp. 433–450, 2010.

[4] M. Pai, C. M. Denkinger, S. V. Kik et al., "Gamma interferon release assays for detection of *Mycobacterium tuberculosis* infection," *Clinical Microbiology Reviews*, vol. 27, no. 1, pp. 3–20, 2014.

[5] M. Sester, G. Sotgiu, C. Lange et al., "Interferon-γ release assays for the diagnosis of active tuberculosis: a systematic review and meta-analysis," *European Respiratory Journal*, vol. 37, no. 1, pp. 100–111, 2011.

[6] J. Z. Metcalfe, C. K. Everett, K. R. Steingart et al., "Interferon-γ release assays for active pulmonary tuberculosis diagnosis in adults in low-and middle-income countries: systematic review and meta-analysis," *Journal of Infectious Diseases*, vol. 204, no. 4, supplement, pp. S1120–S1129, 2011.

[7] J. S. Sutherland, I. M. Adetifa, P. C. Hill, R. A. Adegbola, and M. O. C. Ota, "Pattern and diversity of cytokine production differentiates between *Mycobacterium tuberculosis* infection and disease," *European Journal of Immunology*, vol. 39, no. 3, pp. 723–729, 2009.

[8] V. Sargentini, S. Mariotti, S. Carrara et al., "Cytometric detection of antigen-specific IFN-γ/IL-2 secreting cells in the diagnosis of tuberculosis," *BMC Infectious Diseases*, vol. 9, article 99, 2009.

[9] N. Caccamo, G. Guggino, S. A. Joosten et al., "Multifunctional $CD4^+$ T cells correlate with active *Mycobacterium tuberculosis* infection," *European Journal of Immunology*, vol. 40, no. 8, pp. 2211–2220, 2010.

[10] A. Harari, V. Rozot, F. B. Enders et al., "Dominant TNF-α^+*Mycobacterium tuberculosis*-specific $CD4^+$ T cell responses discriminate between latent infection and active disease," *Nature Medicine*, vol. 17, no. 3, pp. 372–377, 2011.

[11] M. Streitz, S. Fuhrmann, D. Thomas et al., "The phenotypic distribution and functional profile of tuberculin-specific CD4 T-cells characterizes different stages of TB infection," *Cytometry Part B, Clinical Cytometry*, vol. 82, no. 6, pp. 360–368, 2012.

[12] W. L. Leung, K. L. Law, V. S. S. Leung et al., "Comparison of intracellular cytokine flow cytometry and an enzyme immunoassay for evaluation of cellular immune response to active tuberculosis," *Clinical and Vaccine Immunology*, vol. 16, no. 3, pp. 344–351, 2009.

[13] D. I. Won and J. R. Park, "Flow cytometric measurements of TB-specific T cells comparing with quantiFERON-TB gold," *Cytometry Part B—Clinical Cytometry*, vol. 78, no. 2, pp. 71–80, 2010.

[14] J. Lee, S. Y. Lee, D. I. Won, S. I. Cha, J. Y. Park, and C. H. Kim, "Comparison of whole-blood interferon-γ assay and flow cytometry for the detection of tuberculosis infection," *Journal of Infection*, vol. 66, no. 4, pp. 338–345, 2013.

[15] E. Petruccioli, L. Petrone, V. Vanini et al., "IFNγ/TNFα specific-cells and effector memory phenotype associate with active tuberculosis," *Journal of Infection*, vol. 66, no. 6, pp. 475–486, 2013.

[16] E. K. Forbes, C. Sander, E. O. Ronan et al., "Multifunctional, high-level cytokine-producing Th1 cells in the lung, but not spleen, correlate with protection against *Mycobacterium tuberculosis* aerosol challenge in mice," *The Journal of Immunology*, vol. 181, no. 7, pp. 4955–4964, 2008.

[17] C. L. Day, D. A. Abrahams, L. Lerumo et al., "Functional capacity of *Mycobacterium tuberculosis*-specific T cell responses in humans is associated with mycobacterial load," *The Journal of Immunology*, vol. 187, no. 5, pp. 2222–2232, 2011.

[18] B. M. Kagina, N. Mansoor, E. P. Kpamegan et al., "Qualification of a whole blood intracellular cytokine staining assay to measure mycobacteria-specific CD4 and CD8 T cell immunity by flow cytometry," *Journal of Immunological Methods*, vol. 22, no. 14, pp. 356–361, 2014.

[19] S. Commandeur, K. E. Van Meijgaarden, C. Prins et al., "An unbiased genome-wide *Mycobacterium tuberculosis* gene expression approach to discover antigens targeted by human T cells expressed during pulmonary infection," *Journal of Immunology*, vol. 190, no. 4, pp. 1659–1671, 2013.

[20] I. Sauzullo, R. Scrivo, F. Mengoni et al., "Multi-functional flow cytometry analysis of $CD4^+$ T cells as an immune biomarker for latent tuberculosis status in patients treated with tumour necrosis factor (TNF) antagonists," *Clinical and Experimental Immunology*, vol. 176, no. 3, pp. 410–417, 2014.

[21] R. Diel, D. Goletti, G. Ferrara et al., "Interferon-γ release assays for the diagnosis of latent *Mycobacterium tuberculosis* infection: a systematic review and meta-analysis," *European Respiratory Journal*, vol. 37, no. 1, pp. 88–99, 2011.

[22] I. Sauzullo, F. Mengoni, R. Scrivo et al., "Evaluation of QuantiFERON-TB gold in-tube in human immunodeficiency virus infection and in patient candidates for anti-tumour necrosis factor-alpha treatment," *The International Journal of Tuberculosis and Lung Disease*, vol. 14, no. 7, pp. 834–840, 2010.

[23] M. Santin, L. Muñoz, and D. Rigau, "Interferon-gamma release assays for the diagnosis of tuberculosis and tuberculosis infection in HIV-infected adults: a systematic review and meta-analysis," *PLoS ONE*, vol. 7, no. 3, Article ID e32482, 2012.

[24] R. Scrivo, I. Sauzullo, F. Mengoni et al., "Serial interferon-γ release assays for screening andmonitoring of tuberculosis infection during treatment with biologic agents," *Clinical Rheumatology*, vol. 31, no. 11, pp. 1567–1575, 2012.

[25] R. Scrivo, I. Sauzullo, F. Mengoni et al., "Mycobacterial interferon-γ release variations during longterm treatment with tumor necrosis factor blockers: lack of correlation with clinical outcome," *The Journal of Rheumatology*, vol. 40, no. 2, pp. 157–165, 2013.

[26] I. Sauzullo, F. Mengoni, R. Marocco et al., "Interferon-γ release assay for tuberculosis in patients with psoriasis treated with tumour necrosis factor antagonists: in vivo and in vitro analysis," *British Journal of Dermatology*, vol. 169, no. 5, pp. 1133–1140, 2013.

[27] K. H. Kim, S. W. Lee, W. T. Chung et al., "Serial interferon-gamma release assays for the diagnosis of latent tuberculosis infection in patients treated with immunosuppressive agents," *The Korean Journal of Laboratory Medicine*, vol. 31, no. 4, pp. 271–278, 2011.

[28] S. Kannanganat, C. Ibegbu, L. Chennareddi, H. L. Robinson, and R. R. Amara, "Multiple-cytokine-producing antiviral CD4 T cells are functionally superior to single-cytokine-producing cells," *Journal of Virology*, vol. 81, no. 16, pp. 8468–8476, 2007.

[29] J. T. Mattila, C. R. Diedrich, P. Ling Lin, J. Phuah, and J. L. Flynn, "Simian immunodeficiency virus-induced changes in T cell cytokine responses in cynomolgus macaques with latent *Mycobacterium tuberculosis* infection are associated with timing of reactivation," *Journal of Immunology*, vol. 186, no. 6, pp. 3527–3537, 2011.

[30] K. A. Millington, J. A. Innes, S. Hackforth et al., "Dynamic relationship between IFN-gamma and IL-2 profile of Mycobacterium tuberculosis-specific T cells and antigen load," *The Journal of Immunology*, vol. 178, no. 8, pp. 5217–5226, 2007.

[31] K. A. Millington, S. Gooding, T. S. C. Hinks, D. J. M. Reynolds, and A. Lalvani, "*Mycobacterium tuberculosis*-specific cellular immune profiles suggest bacillary persistence decades after spontaneous cure in untreated tuberculosis," *The Journal of Infectious Diseases*, vol. 202, no. 11, pp. 1685–1689, 2010.

[32] M. Streitz, S. Fuhrmann, F. Powell et al., "Tuberculin-specific T cells are reduced in active pulmonary tuberculosis compared to LTBI or status post BCG vaccination," *The Journal of Infectious Diseases*, vol. 203, no. 3, pp. 378–382, 2011.

[33] C. H. Kim, K. J. Choi, S. S. Yoo et al., "Comparative analysis of whole-blood interferon-γ and flow cytometry assays for detecting post-treatment Immune responses in patients with active tuberculosis," *Cytometry B: Clinical Cytometry*, vol. 86, no. 4, pp. 236–243, 2014.

[34] G. Pantaleo and A. Harari, "Functional signatures in antiviral T-cell immunity for monitoring virus-associated diseases," *Nature Reviews Immunology*, vol. 6, no. 5, pp. 417–423, 2006.

[35] M. R. Betts, M. C. Nason, S. M. West et al., "HIV nonprogressors preferentially maintain highly functional HIV-specific $CD8^+$ T cells," *Blood*, vol. 107, no. 12, pp. 4781–4789, 2006.

[36] V. Rozot, S. Vigano, J. Mazza-Stalder et al., "*Mycobacterium tuberculosis*-specific $CD8^+$ T cells are functionally and phenotypically different between latent infection and active disease," *European Journal of Immunology*, vol. 43, no. 6, pp. 1568–1577, 2013.

[37] V. Rozot, A. Patrizia, and S. Vigano, "Combined use of *Mycobacterium tuberculosis*-specific CD4 and CD8 T-cell responses is a powerful diagnostic tool of active tuberculosis," *Clinical of Infectious Diseases*, vol. 60, no. 3, pp. 432–437, 2015.

[38] D. A. Lewinsohn, A. S. Heinzel, J. M. Gardner, L. Zhu, M. R. Alderson, and D. M. Lewinsohn, "*Mycobacterium tuberculosis*-specific $CD8^+$ T cells preferentially recognize heavily infected cells," *The American Journal of Respiratory and Critical Care Medicine*, vol. 168, no. 11, pp. 1346–1352, 2003.

[39] C. Lancioni, M. Nyendak, S. Kiguli et al., "$CD8^+$ T cells provide an immunologic signature of tuberculosis in young children," *The American Journal of Respiratory and Critical Care Medicine*, vol. 185, no. 2, pp. 206–212, 2012.

Hindawi Publishing Corporation
Journal of Immunology Research
Volume 2014, Article ID 196124, 9 pages
http://dx.doi.org/10.1155/2014/196124

Research Article

Dose of Incorporated Immunodominant Antigen in Recombinant BCG Impacts Modestly on Th1 Immune Response and Protective Efficiency against *Mycobacterium tuberculosis* in Mice

Hui Ma,[1] Kang Wu,[1] Fang Liu,[1] Hua Yang,[1] Han Kang,[1,2] Ning-Ning Chen,[1] Qin Yuan,[1] Wen-Jiang Zhou,[1] and Xiao-Yong Fan[1,2]

[1] *Shanghai Public Health Clinical Center Affiliated to Fudan University, Shanghai 201508, China*
[2] *Key Laboratory of Medical Molecular Virology of MOE/MOH, Shanghai Medical College, Fudan University, Shanghai 200032, China*

Correspondence should be addressed to Xiao-Yong Fan; xyfan008@fudan.edu.cn

Received 15 May 2014; Accepted 9 July 2014; Published 23 July 2014

Academic Editor: Vishwanath Venketaraman

One approach for improving BCG efficacy is to utilize BCG as vehicle to develop recombinant BCG (rBCG) strains overexpressing *Mycobacterium tuberculosis (M. tb)* antigens. Also expression level of a candidate antigen should impact the final T cell responses conferred by rBCG. In this study, based on our previously constructed differential expression system, we developed two rBCG strains overexpressing *M. tb* chimeric antigen Ag856A2 (coding a recombinant *ag85a* with 2 copies of *esat-6* inserted at *Acc* I site of *ag85a*) at differential levels under the control of the subtly modified *furA* promoters. These two rBCG strains were used to vaccinate C57BL/6 mice and exploit dose of incorporated antigen in rBCG to optimize immune response and protective efficiency against *M. tb* challenge in mouse model. The results showed that rBCG strains overexpressing Ag856A2 at differential levels induced different antigen-specific IFN-γ production and comparable number of *M. tb*-specific CD4 T cells expressing IL-2. *M. tb* challenge experiment showed that rBCG strains afforded enhanced but comparable immune protection characterized by reduced bacillary load, lung pathology, and inflammation. These results suggested that the dose of antigens incorporated in rBCG can impact T cell immune responses but imposed no significantly differential protective efficacies.

1. Introduction

Tuberculosis (TB) caused by *Mycobacterium tuberculosis (M. tb)* continues to be a significant global health problem, affecting millions of people worldwide [1, 2]. Approximately 95% of all TB cases occur in the developing world [3]. It is a prevalent infectious disease in China, with 250,000 deaths from TB annually and 6 million active TB patients at present [4]. The global incidence of TB is raising due to coinfection with the human immunodeficiency virus (HIV) and the emergence of multidrug-resistant (MDR) *M. tb* strains [5, 6]. According to the report of World Health Organization (WHO), *M. tb* will cause 1 billion new cases and about 35 million deaths worldwide by 2020 [7]. Therefore, effective treatment and control strategies are urgently needed to counteract the global threat of TB.

The current vaccine against TB, *M. bovis* Bacilli-Calmette-Guérin (BCG), is a live attenuated vaccine which has been widely used throughout the world for many decades. BCG protects children efficiently against miliary and meningeal TB, but protective efficiency against pulmonary TB in adults has been found to vary highly from 0% to 80% [8]. Much effort has been devoted to improving BCG efficacy by genetic engineering technology because of its strong immunostimulatory properties and proven safety for human use [9, 10]. Recombinant BCG (rBCG) expressing different immunodominant antigens of *M. tb*, such as secreted antigens (Ag85B, Ag85C, ESAT-6, etc.) or latency associated antigens

(α-Crystallin, Rv2659c, Rv3407 and Rv1733c, etc.), have been tested as candidate vaccines against TB and are demonstrated to have an enhanced ability to induce Th1 immune response and protection against *M. tb* challenge in animal models [11, 12]. Also, it is definitely no doubt that doses of antigens could subtly influence the magnitude of host immune response as well as protection efficacy, no matter antigen is administered in the form of rBCG [13], protein [14], DNA [15], or RNA [16].

We have previously reported the construction of a *M. tb furA* gene operator/promoter (p*furA*)-based differential expression system, from which it is feasible to express target antigens of interest in a modular fashion [4]. This system will facilitate the development of novel recombinant BCG vaccine candidates. *M. tb* chimeric antigen Ag856A2, which is coded by a recombinant *ag85a* gene with 2 copies of *esat-6* gene inserted at the *Acc* I site of *ag85a* (see Figure S1 in Supplementary Material available online at http://dx.doi.org/10.1155/2014/196124), shows improved immunogenicity in mice when it is inoculated intramuscularly as a DNA vaccine [17]. For the current study, we selected two rBCG strains overexpressing the same chimeric antigen Ag856A2 at the maximum difference: rBCG186 and rBCG486 overexpressing the fusion protein under control of the wild-type or the optimized double-mutated *furA* promoters, respectively [4]. We tested their efficacy as vaccines in C57BL/6 mice, comparing immune response and protection against *M. tb* challenge. The results showed that mice vaccinated with rBCG186 or rBCG486 generally induced higher antigen-specific effector and memory immune responses, as well as protective efficacies compared to mice vaccinated with the parent BCG strain. However, the two rBCG strains between themselves, which expressed the chimeric antigen Ag856A2 at different levels, induced different antigen-specific IFN-γ production and comparable number of *M. tb*-specific CD4 T cells expressing IL-2. And the protective efficacies imposed by the two rBCG strains displayed no significant differences although higher protection was observed in rBCG486 vaccinated mice than that in rBCG186 vaccinated mice.

2. Materials and Methods

2.1. Experimental Animals and Ethics Statement. Female specific pathogen-free (SPF) C57BL/6 mice aged 6–8 wks were purchased from Shanghai SLAC Laboratory Animal Co., Ltd. (Shanghai, China) and kept under SPF conditions with food and water *ad libitum* until challenge. Infected mice were maintained in a biosafety level 3 (BSL-3) biocontainment animal facility. All animal experiment protocols were approved by Chinese Science Academy Committee on Care and Use of Laboratory Animals and were performed according to the guidelines of the Laboratory Animal Ethical Board of Shanghai Public Health Clinical Center.

2.2. Bacterial Strains and Growth Conditions. *E. coli* DH5α was cultured in liquid or solid LB medium. *M. bovis* BCG-Danish was kindly gifted from Shanghai Institute of Biological Products. BCG and its derivative recombinant strains were grown in liquid Middlebrook 7H9 broth (BD Difco, USA) supplemented with 10% oleic acid-albumin-dextrose-catalase enrichment (OADC, BD Difco, USA), 0.2% glycerol, and 0.05% Tween 80. Cultures in the exponential phase were frozen and stored at −80°C. When required, kanamycin was added at a final concentration of 50 or 20 μg/mL for *E. coli* or mycobacteria, respectively.

2.3. Plasmid Construction and Recombinant BCG Strains Preparation. Two rBCG strains overexpressing *M. tb* chimeric immunodominant antigen Ag856A2 at different levels were constructed as previously described [4]. Briefly, the Ag856A2 coding gene, which is a recombinant *ag85a* gene with 2 copies of *esat-6* gene inserted in its *Acc* I site [17], was amplified from the plasmid template of DNA vaccine HG856A and then cloned into mycobacterial differential expression vectors pMFA11 and pMFA41 under control of the prototypical and double-mutated (mutations: initial codon change from GTG to AUG and 6 bp substitution at upstream AT-rich region) *furA* promoter, respectively. The resulting constructs were electroporated into BCG-Danish competent cells and selected on Middlebrook 7H11 agar with kanamycin. The rBCG transformants were grown to midexponential phase in complete Middlebrook 7H9 broth and then verified the recombinant protein expression by routine Western-blotting assay.

2.4. Mouse Immunization and M. tb Challenge. Mice were vaccinated subcutaneously (*s.c.*) with 2×10^6 colony-forming units (CFU) of BCG or rBCGs in 100 μL saline. Eight weeks after vaccination, groups of 6 mice were either sacrificed for assessment of antigen-specific T cell responses in splenocytes or exposed to an aerosol of virulent *M. tb* H37Rv strain to deposit an inhaled dose of 100–200 CFU per lung by an inhalation exposure system (Glas-Col, USA) [18].

2.5. Ex Vivo IFN-γ ELISPOT Assay. IFN-γ ELISPOT assay kit (BD Biosciences, USA) was used as described by the manufacturer. Plates were coated with anti-IFN-γ mAb overnight at 4°C and then blocked with RPMI 1640 medium containing 10% fetal bovine serum (FBS) for 1 h at room temperature. Splenocytes (2.5×10^5 cells/well) from immunized mice were isolated, plated, and cultured with 10 μg/mL PPD (Statens Serum Institute, Denmark) or 2 μg/mL recombinant Ag85A, 6 μg/mL recombinant ESAT-6 to provide stimulation at 37°C, 5% CO_2 for 20 h. After washing the plates with PBS-T20 (1 × PBS, pH 7.4, 0.05% Tween 20), biotinylated anti-IFN-γ was added for 2 h at room temperature. Streptavidin-HRP was added for 45 min, and the color was developed with 3-amino-9-ethylcarbazole (AEC) substrate (BD Biosciences). An immunospot analyzer (Cellular Technology, USA) was used to count the spots.

2.6. Flow Cytometric Analysis of Intracellular Cytokine Production. Splenocytes (2×10^6 cells/well) isolated at 8 weeks after immunization were plated in 96-well plates and stimulated with 10 μg/mL PPD for 14 h in the presence of 1 μg/mL anti-CD28 (BD Biosciences) and subsequently incubated for an additional 5 h at 37°C following the addition of 0.5 μL/mL monensin/GolgiStop (BD Biosciences). Following overnight

incubation at 4°C, the cells were washed in FACS buffer (PBS containing 0.1% sodium azide and 1% FBS) and subsequently stained for 30 min at 4°C for surface markers with mAbs as indicated using anti-CD3-Pacific Blue, anti-CD8-FITC, and anti-CD44-V500 (all from BD Biosciences). Cells were then washed in FACS buffer, fixed, permeabilized using the Cytofix/Cytoperm kit (BD Biosciences) according to the manufacturer's instructions and stained intracellularly for 30 min at 4°C using anti-IFN-γ-APC-Cy7, anti-TNF-α-Percp-Cy5.5, and anti-IL-2-APC mAbs (all from BD Biosciences). Cells were subsequently washed, resuspended in FACS buffer, and then analyzed by multiparameter flow cytometry using a BD FACSAria flow cytometer (BD Biosciences). For each sample, at least 300,000 events were collected and responses were analyzed using FlowJo software (Tree Star, USA).

2.7. Bacterial CFU Assay. Five weeks after infection, mice were sacrificed and the mycobacterial burden was determined by plating homogenates of lung, excluding right postcaval lobe, and entire spleen onto Middlebrook 7H11 agar plates supplemented with 10% OADC enrichment and a 4-antibiotic mixture (40 U/mL polymycin B, 4 μg/mL amphotericin, 50 μg/mL carbenicillin, 2 μg/mL trimethoprim) that prevents growth of contaminating microorganisms. Plates were incubated at 37°C for 3 weeks in semisealed plastic bags and then CFU were counted and expressed as $\log_{10}$ CFU per organ.

2.8. Histopathological Analysis. The right postcaval lobes were fixed in formalin and embedded in paraffin. Then, the embedded lung lobes were sectioned in thickness of 5 μm, stained with haematoxylin and eosin (H & E) and photographed using a Olympus CKX41 microscope (Olympus, Japan) fitted with an Olympus DP20 camera connected to a computer. The Image Pro Plus program (Media Cybernetics, USA) was utilized to objectively assess the level of inflammation present in each image. The inflamed areas stained a more intense purple than the noninflamed areas. The mean percent of area inflamed was quantified averaging from three to five lung sections of each of the different groups of mice.

2.9. Immunohistochemistry. Immunohistochemistry of lung sections was performed as previously described [19]. The antibodies were rabbit polyclonal anti-mouse TNF-α (Abcam, UK), rabbit polyclonal IFN-γ antibodies (Invitrogen, USA), and rabbit polyclonal anti-mouse iNOS antibody (Cayman Chemical, USA). All sections were examined by light microscopy, and the expression of TNF-α, IFN-γ, or iNOS was semiquantified by intensity of positive signal using Image Pro Plus software.

2.10. Statistical Analysis. Immune responses, protective efficacies, and histopathological staining were tested by one-way ANOVA followed by Tukey's multiple comparison tests of the means. Immunohistochemistry staining was compared by a nonparametric Mann-Whitney U test. $^{*}P < 0.05$ $^{**}P < 0.01$, or $^{***}P < 0.001$.

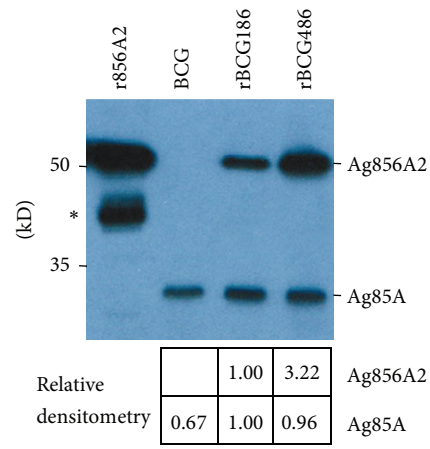

Figure 1: Expression of chimeric antigen Ag856A2 in rBCG strains by Western blotting. Equal amounts of lysates supernatant from cell crude extracts of (r)BCGs were run in SDS-PAGE and then probed with mouse antiserum to Ag85A. The origin of the lysate is marked in the top. Band intensities of Ag856A2 and Ag85A from BCG, rBCG186, and rBCG486 were quantified by densitometry (Image-J software) and divided by cognate band intensity from rBCG186 (relative densitometry). Lane "r856A2" represents rAg856A2 purified after expression in *E. coli* and serving as the positive control. The staining intensity of native Ag85A was roughly at the same level in all lanes, indicating that equal amounts of whole cell lysates were loaded. The result is representative of two independent experiments. *The degradative form of rAg856A2.

3. Results

3.1. rBCG Strains Overexpress Different Levels of Fusion Protein Ag856A2. We have previously developed a novel mycobacterial differential expression system (pMFA series) based on the *M. tb furA* gene operator/promoter (p*furA*) or its derivatives. Ag856A2 was cloned into two of these plasmids, pMFA11 and pMFA41, which drives low and high gene expression under the control of the wild-type and modified *fur*A promoters, respectively [4]. By transformation of BCG, we obtained two strains, rBCG186 and rBCG486, which drove correspondingly low and high expression of chimeric immunodominant antigen Ag856A2 (Figure 1, upper panel). Quantification of the band intensities of Western-blot indicated that rBCG486 roughly expressed > 3-fold of Ag856A2 than rBCG186 did (Figure 1, lower panel).

3.2. Higher Expression of Ag856A2 in rBCG Strains Induces Higher Antigen-Specific IFN-γ Response. Eight weeks after vaccination, ELISPOT assay of splenocytes showed that more cells in the rBCG486-vaccinated mice expressed Ag85A-specific IFN-γ compared to those of rBCG186- and BCG-vaccinated mice (Figure 2, left panel). Also, significantly elevated numbers of splenocytes expressed ESAT-6-specific IFN-γ in both rBCG186- and rBCG486-vaccinated mice compared to that of BCG-vaccinated mice (Figure 2, middle panel). Additionally, ESAT-6-specific IFN-γ was induced at much higher level in rBCG486-vaccinated mice compared to rBCG186 group (Figure 2, middle panel). A similar pattern of PPD-specific IFN-γ responses as Ag85A-specific response

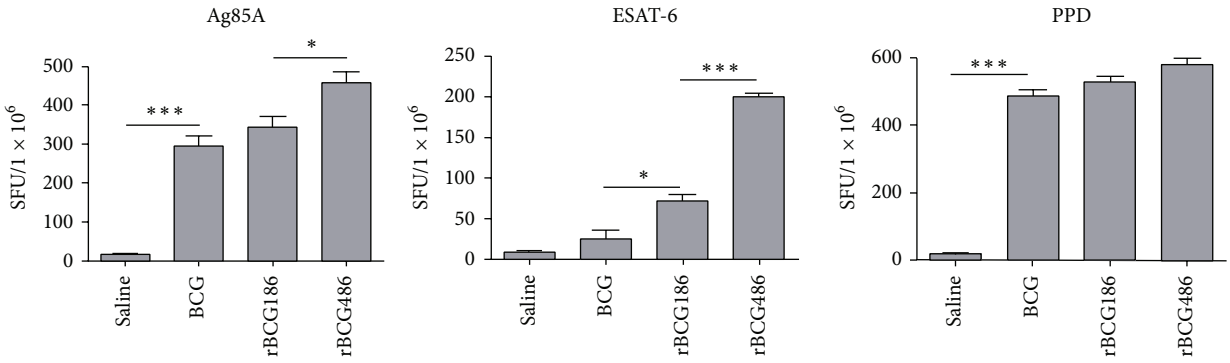

Figure 2: ELISPOT assays of *M. tb*-specific IFN-γ producing splenocytes in (r)BCGs-vaccinated mice. Eight weeks after vaccination, splenocytes were isolated and then incubated with purified Ag85A, ESAT-6, or PPD for *ex vivo* IFN-γ ELISPOT assay. Column diagram for mean number of spot-forming units (SFU) ± SD ($n = 6$) were shown. $^{*}P < 0.05$ or $^{***}P < 0.001$ (one-way ANOVA).

was also observed but the difference was not statistically significant, regarding to the comparisons of rBCG486-vaccinated mice and other immunized groups (Figure 2, right panel).

3.3. rBCG Vaccination Induce Higher IL-2-Producing CD4 T Cell Responses. We used flow cytometry to measure the capacity of *M. tb*-specific CD4 T cells from spleens of vaccinated mice producing cytokines IFN-γ, TNF-α, and IL-2 at single cell level after stimulation *in vitro* with PPD. The cytokine-producing $CD3^{+}CD4^{+}$ cells were classified into seven subpopulations based on their production of IFN-γ, TNF-α, and IL-2 in any combination (Figure 3(a)).

Significantly increased frequencies of PPD-specific IL-2^{+} CD4 T cells were identified in rBCG-vaccinated mice, whereas increased frequencies of IFN-γ^{+} cells were identified in BCG-vaccinated mice even though statistically insignificant (Figure 3(a)). The pie chart of this data clarified the dominance of IL-2^{+} CD4 T cells in rBCG-vaccinated mice, while IFN-γ^{+} CD4 T cells dominated the responses of BCG-vaccinated mice (Figure 3(b)). rBCG and BCG-vaccination did not differ in their ability to induce *M. tb*-specific CD4 T cells producing other combinations of cytokines ($P > 0.05$). In accordance, we also observed higher integrated mean fluorescence intensities (iMFI = %frequency × MFI) of IL-2 in IL-2-producing CD4 T cells, even though it is statistically insignificant (Figure 3(c)).

3.4. Enhanced Protection Conferred by rBCG Vaccination. In general, rBCG induced higher antigen-specific cytokine responses as compared to BCG (Figures 2 and 3), and rBCG486 induced higher antigen-specific IFN-γ response (Figure 2) and comparable frequency of *M. tb*-specific CD4 T cells expressing IL-2 (Figure 3). Then, we further compared the protective efficacies of rBCG486, rBCG186, and BCG against *M. tb*-challenge. As shown in Figure 4(a), 5 weeks after challenge all vaccinated mice had a significantly reduced bacillary load in lungs, when compared to the saline-treated mice. Vaccination with BCG and rBCG186 resulted in a comparable reduction in bacillary load (Figure 4). However, even though rBCG486 vaccination induced a significantly greater protection when compared to the BCG-vaccinated mice, it showed no difference of protection when compared to the rBCG186-vaccinated mice (Figure 4(a)). The bacillary loads in spleens shared the similar pattern as those in lungs, with rBCG486-vaccinated mice having far fewer bacilli when compared to the saline-treated or BCG-vaccinated mice and having comparable bacilli compared to the rBCG186-vaccinated mice (Figure 4(b)).

3.5. Reduced Pulmonary Inflammation following rBCG Vaccination. Five weeks after challenge, *M. tb* infection caused severe pathology changes in saline-treated mice, with about 24.3% of the tissue showing extensive multifocal granulomatous infiltration, characterized by numerous foamy macrophages surrounded by inflammatory cells (Figure 5). However, all the vaccinated groups of mice had significantly reduced pulmonary granulomatous consolidation compared to the unvaccinated mice (i.e., 13.42% consolidation in BCG-vaccinated group, 7.24% in rBCG186-vaccinated group, and 4.87% in rBCG486-vaccinated group). The rBCG-vaccinated mice showed the mildest pathology, and all of the mice in these two groups had mainly well-preserved alveolar spaces with only a few scattered areas of diffused infiltration (Figure 5).

3.6. Localization of TNF-α, IFN-γ, and Inducible Nitric Oxide Synthase (iNOS) in M. tb Infected Lung. Immunohistochemical staining of the lung tissues showed the presence of TNF-α, IFN-γ, and iNOS in all groups of infected mice and staining was strongest in the granulomatous lesions compared to that in the nongranulomatous areas. However, the extent of staining varied among the groups. Five weeks after infection, a very high level of TNF-α was observed in the lungs of saline-treated mice (Figure 6(a)); TNF-α staining was extensive in necrotic areas within the advanced coalescent granulomas. Vaccination with BCG resulted in the reduced amounts of TNF-α expression, even though statistically insignificant. In contrast, rBCG-vaccinated mice, especially rBCG486-vaccinated mice, showed only a little weak staining for TNF-α and this was restricted primarily to the granuloma core (Figure 6(a)). Similar patterns of IFN-γ and iNOS staining

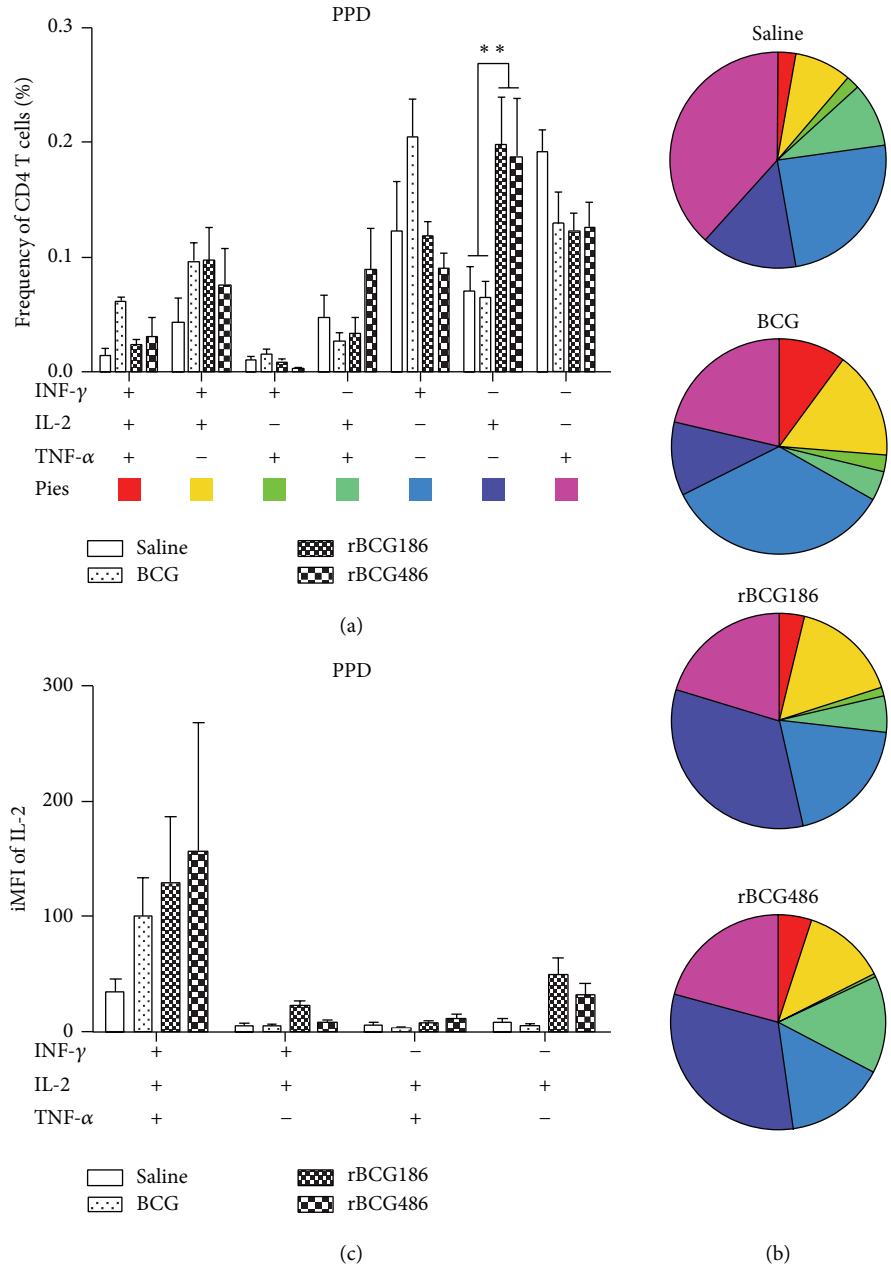

Figure 3: Flow cytometric analysis of intracellular cytokine production after immunization. Eight weeks after vaccination, splenocytes from 6 mice were isolated, pooled and stimulated with PPD for 14 h, and then analyzed for cytokine production by intracellular cytokine staining (ICS) assay. $CD3^+CD4^+$ T cells producing IFN-γ, TNF-α, and IL-2 were distinguished as seven distinct subpopulations based on their production of these cytokines in any combination. The subpopulation proportions as components of the total $CD4^+$ T cell population are shown (a) and their proportions as components of the seven subpopulations are shown in pie chart form (b). Integrated mean fluorescence intensities (iMFI) of IL-2 in four cytokine profiles (c). Data are shown as mean ± SEM. $^{**}P < 0.01$ (one-way ANOVA).

were also observed except that there was relatively much weaker staining in the lungs of (r)BCG-vaccinated mice compared to the saline-treated mice (Figures 6(b) and 6(c)). Similar pattern of TNF-α, IFN-γ, and iNOS staining was also observed in the infected spleens of vaccinated mice, with the highest staining in saline-treated mice, moderate staining in BCG-vaccinated mice, and the lowest staining in rBCG-vaccinated mice (Figure S2).

4. Discussion

During the past decades, great efforts have been focused on modifications of the current BCG vaccine to develop new anti-TB vaccine candidates [20]. Some modified rBCG strains, such as rBCG30 and rBCGΔ*UreC*::*Hly*, have been demonstrated to yield improved protection against *M. tb* infection in experimental animal model compared to the

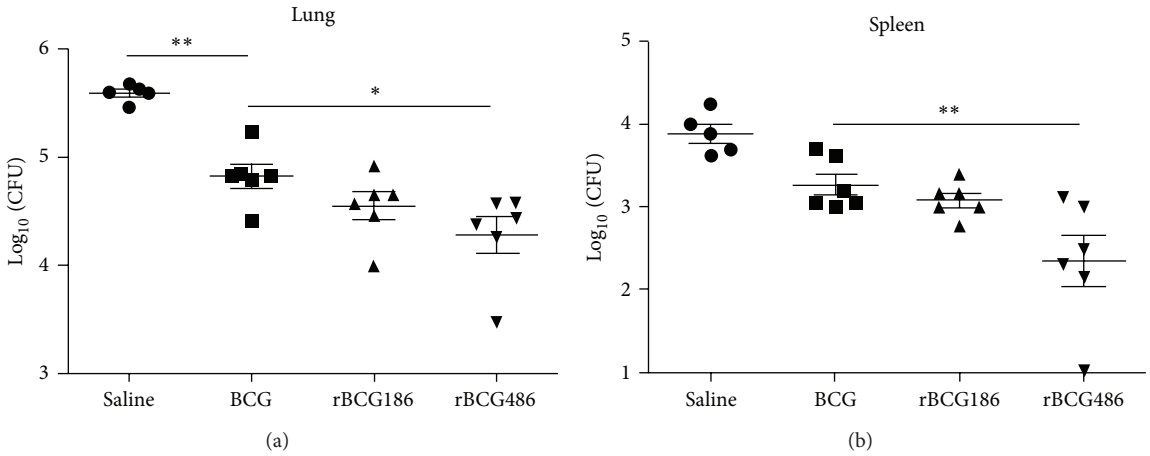

Figure 4: Enhanced protection against *M. tb* challenge by rBCGs vaccination. Eight weeks after vaccination, mice ($n = 5$ or 6) were challenged with *M. tb* H37Rv; bacillary loads in lung (a) and spleen (b) were determined at 5 weeks after infection and expressed as Log_{10} CFU per organ. Representative data from one of two experiments were shown. $^{*}P < 0.05$ or $^{**}P < 0.01$ (one-way ANOVA).

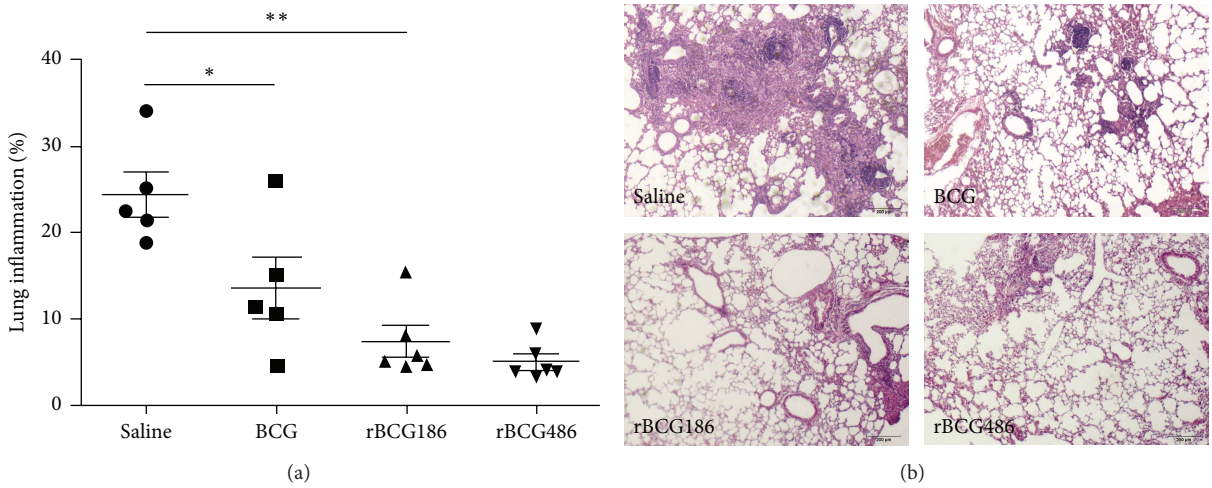

Figure 5: Reduced pathology in vaccinated mice after infection. The percentage of lung area showing infiltration and consolidation was determined by H & E staining 5 weeks after infection (a), and representative histological appearances of lung tissue are shown in the right panel (b). $^{*}P < 0.05$ or $^{**}P < 0.01$ (one-way ANOVA).

existing BCG vaccine and have entered into clinical trial. Nevertheless, it is promising to keep on optimization of BCG protective immune if two points are being issued. One is the fact that the best immunodominant antigen for TB should be precisely defined. Another is that the expression levels of such antigens should be optimal enough to elicit effective immune responses [21]. Here, we constructed two rBCG strains overexpressing immunodominant chimeric antigen Ag856A2 at varying levels depending upon the strengths of the different *furA* promoters [4] and then compared the cellular immune response and protection in mice induced by these two rBCG strains.

One way to improve BCG efficacy is to overexpress mycobacterial immunodominant antigens to induce optimal host immune responses in the life cycle of BCG within host [12, 19]. This kind of strategy reflects that the doses of antigens are one of pivotal factors influencing the protective efficacies of vaccines. Aagaard et al. demonstrated that protective efficiency of TB subunit vaccines is highly dependent on the antigen dose [14]. They vaccinated mice with different doses of fusion protein Ag85B-TB10.4 which were emulsified in adjuvant IC31, and the higher immune response and protective efficacy were only observed when the antigen was administered in proper doses, and decreasing or increasing of the antigen dose would dramatically dwarf the protection efficacies of the antigens [14]. In our study, the cognate antigen Ag856A2 in rBCG186 and rBCG486 was expressed under the control of promoters p*furA* and p*furAma* (Figure S1) [4]. These two promoters, by their nature, were verified to have varied promoter activities, with p*furA* the lower one and p*furAma* the higher one [4], and were consequently used to develop the rBCG strains

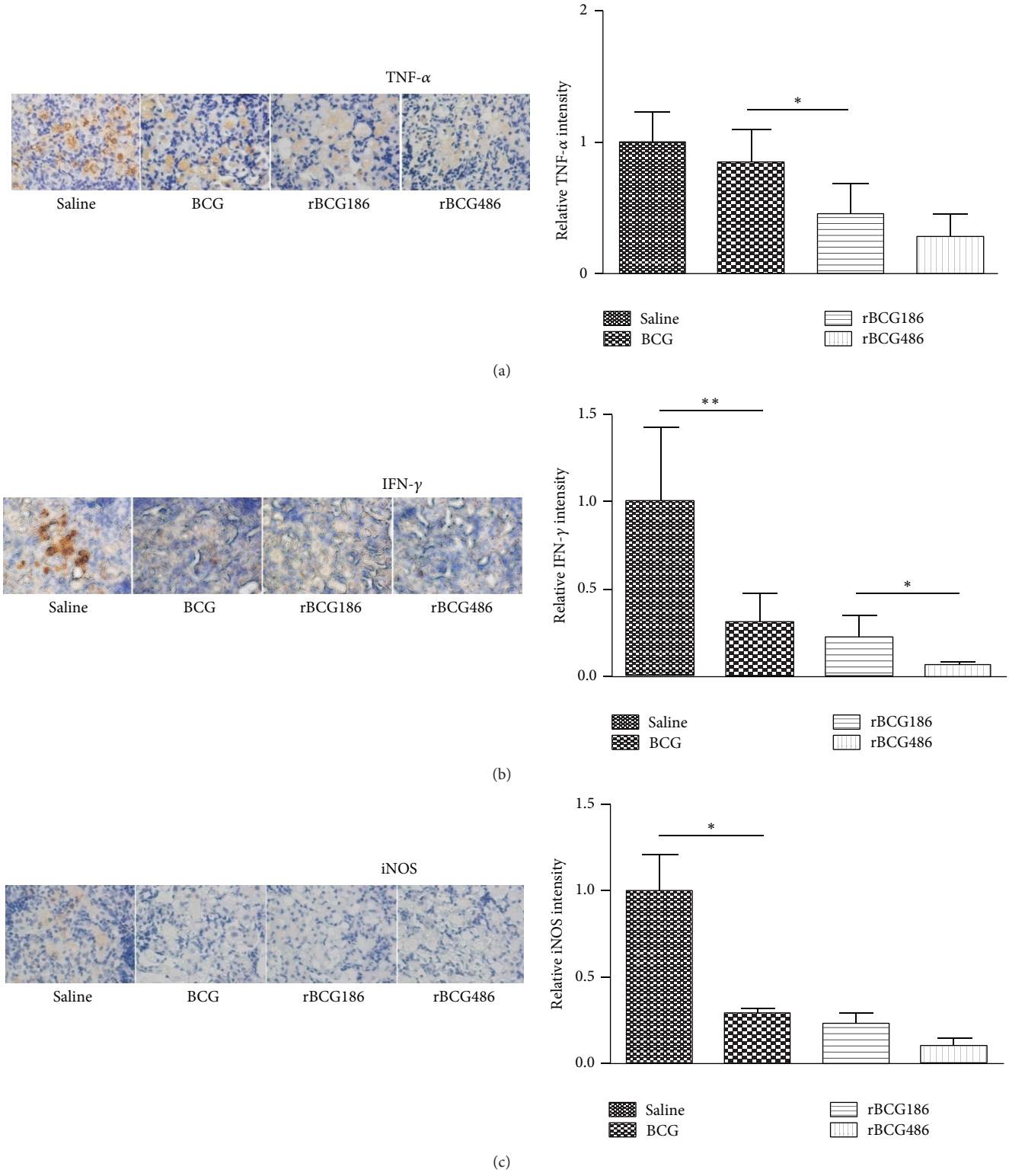

Figure 6: Localization of TNF-α, IFN-γ, and iNOS in infected lungs of mice 5 weeks after infection. Representative photomicrographs show immunohistochemical staining (brown color) for TNF-α (a), IFN-γ (b), and iNOS (c) in pulmonary granulomas (left panel). Quantification of staining (intensity × area of staining) is displayed as mean ± SD. $^{*}P < 0.05$ or $^{**}P < 0.01$ (Mann-Whitney U test).

overexpressing chimeric antigen Ag856A2 at different levels, with lower expression in rBCG186 and higher expression in rBCG486 (Figure 1). And different Ag856A2 antigen loading in rBCGs resulted in differential host immune responses, with the higher antigen-specific effector immune response in the rBCG486-vaccinated mice as validated through *in vitro* IFN-γ ELISPOT assay (Figure 2). However, we did not observe the significant differences in the qualities of *M. tb*-specific CD4 T cells coexpressing IFN-γ, TNF-α, and IL-2 (Figure 3), nor the protection efficacies and lung inflammations, between the two groups of rBCGs-vaccinated mice (Figures 4 and 5). Interestingly, subtly higher percent of polyfunctional CD4 T cells (IFN-γ^+IL-2$^+$TNF-α^+) was observed in BCG-vaccinated mice compared to other groups of mice (Figure 3(a)); however, the protective efficacy elicited by BCG vaccination is not that effective as rBCGs (Figure 4). This contradictory result could be explained with the fact that the lower iMFI values of IFN-γ, IL-2, and TNF-α in BCG-vaccinated mice were observed (see the case of IL-2 in Figure 3(c) as representative). MFI provides one measure of the quality of the immune response since the cells that are more actively producing cytokine stain more brightly [22], thus the lower iMFI values of cytokines reflected poor quality although mildly higher frequency of polyfunctional CD4 T cells was seen in BCG-vaccinated mice, and this further emphasizes that not only the magnitude but also the quality of vaccine-induced T cells responses are critical to guide development of effective immunization strategies [23]. In addition, higher IL-2 secretion, both in the levels of percentage and iMFI, were seen in the rBCG486-vaccinated mice than that of BCG group; this data support our recent findings that IL-2 production in the spleens of vaccinated mice after vaccination can predict vaccine efficacy (Kang H, et al. Immunology, 2014; in press). The same explanation might also be used to account for the fact that although the saline-treated mice showed high numbers of cells producing TNF-α, the iMFI is relative low (data not shown).

The quality of T cell response has significant effect on the establishment of protective memory [23]. As with the phenotypic heterogeneous nature of T cells, these cells are definitely functional heterogeneous. Thus, in addition to monitoring exclusively the IFN-γ response after vaccination, researchers have been focusing on the coexpression of more cytokines at single cell level through flow cytometry technique [24, 25]. The rBCG186 or rBCG486, at least at the time we tested, induced much higher frequencies of IL-2$^+$ CD4 T cells responding to PPD stimulation in splenocytes compared to the saline-treated or BCG-vaccinated mice after vaccination, which was further confirmed by higher IL-2 production when cytokine concentration was measured as iMFI value (Figure 3). Although IL-2 has little direct effector function, it has the ability to expand effector functions of other T cells [23]. In the linear model of differentiation for CD4$^+$ Th1 cells, IL-2$^+$ CD4 T cells belong to memory cells and have the potential to differentiate into IFN-γ-producing cells after recalling by the relevant antigens [23]. Thus, rBCG186 and rBCG486, because of the incorporation of chimeric antigen Ag856A2, enhance the memory capacity of host to *M. tb* pathogen. However, we did not detect any differences of CD4 T cells between rBCG186-vaccinated and rBCG486-vaccinated mice. This may attribute to the short vaccination time window we chose, or the real differences lies in other functions of T cells which is beyond the scope of the T cell functions currently tested and may need to be further exploited in the future.

Effective and coordinated participation of cytokines contribute to the TB control. Those relevant Th1 cytokines (e.g., TNF-α and IFN-γ), in a larger extent, function through activation of macrophages [26]. TNF-α and IFN-γ synergistically inhibit the growth of *M. tb* in macrophages through stimulating the production of reactive nitrogen intermediates (RNIs) [27, 28]. As for RNIs, iNOS is the vital enzyme involved for the production of RNIs [29, 30]. TNF-α, IFN-γ, and iNOS give proper containment of *M. tb* in the early stage [31]. At later stage of infection when inhibition or killing of *M. tb* is well established, their levels of expression will go down to a reasonable value; otherwise immune-pathological response would happen [32]. rBCGs, especially rBCG486, induced enhanced protection against *M. tb* infection in this study (Figure 4). Consistent with the protective efficacy, the inflammation responses in the infected lungs alleviated greatly in rBCGs-vaccinated mice after infection (Figure 5). When measuring the expression levels of inflammatory molecules, the rBCGs-vaccinated mice also displayed reduced levels of expression which were in accordance with the remissive granulomatous inflammation (Figures 5 and 6).

Conflict of Interests

The authors declare that there is no conflict of interests regarding the publication of this paper.

Authors' Contribution

Hui Ma and Kang Wu contributed equally to this work.

Acknowledgments

This work was supported by grants from Chinese National Mega Science & Technology Program on Infectious Diseases (2013ZX10003007-003), National Science Foundation of China (81273328, 31170876, 81301407, and 81101213), Shanghai Rising-Star Program (12QH1401900), Shanghai Health Bureau (20114013), Shanghai Science and Technology Commission (10411962700 and 134119a5200), and Shanghai Natural Science Fund for Youth Scholars (12ZR1448200).

References

[1] M. A. Aziz and A. Wright, "The World Health Organization/International Union against Tuberculosis and Lung Disease Global Project on Surveillance for anti-tuberculosis drug resistance: a model for other infectious diseases," *Clinical Infectious Diseases*, vol. 41, supplement 4, pp. S258–S262, 2005.

[2] P. F. Barnes and M. D. Cave, "Molecular epidemiology of tuberculosis," *The New England Journal of Medicine*, vol. 349, no. 12, pp. 1149–1156, 2003.

[3] L. Grode, P. Seiler, S. Baumann et al., "Increased vaccine efficacy against tuberculosis of recombinant *Mycobacterium bovis*

bacille Calmette-Guérin mutants that secrete listeriolysin," *The Journal of Clinical Investigation*, vol. 115, no. 9, pp. 2472–2479, 2005.

[4] X. Fan, H. Ma, J. Guo et al., "A novel differential expression system for gene modulation in Mycobacteria," *Plasmid*, vol. 61, no. 1, pp. 39–46, 2009.

[5] D. Maher, "Re-thinking global health sector efforts for HIV and tuberculosis epidemic control: promoting integration of programme activities within a strengthened health system," *BMC Public Health*, vol. 10, article 394, 2010.

[6] N. R. Gandhi, P. Nunn, K. Dheda et al., "Multidrug-resistant and extensively drug-resistant tuberculosis: a threat to global control of tuberculosis," *The Lancet*, vol. 375, no. 9728, pp. 1830–1843, 2010.

[7] M. Opravil, "Epidemiological and clinical aspects of mycobacterial infections," *Infection*, vol. 25, no. 1, pp. 56–59, 1997.

[8] P. W. Roche, J. A. Triccas, and N. Winter, "BCG vaccination against tuberculosis: past disappointments and future hopes," *Trends in Microbiology*, vol. 3, no. 10, pp. 397–401, 1995.

[9] A. S. Pym, P. Brodin, L. Majlessi et al., "Recombinant BCG exporting ESAT-6 confers enhanced protection against tuberculosis," *Nature Medicine*, vol. 9, no. 5, pp. 533–539, 2003.

[10] M. A. Horwitz, G. Harth, B. J. Dillon, and S. Maslesa-Galic, "Recombinant bacillus Calmette-Guerin (BCG) vaccines expressing the Mycobacterium tuberculosis 30-kDa major secretory protein induce greater protective immunity againts tuberculosis than conventional BCG vaccines in a highly susceptible animal model," *Proceedings of the National Academy of Sciences of the United States of America*, vol. 97, no. 25, pp. 13853–13858, 2000.

[11] S. H. E. Kaufmann, "Tuberculosis vaccine development: strength lies in tenacity," *Trends in Immunology*, vol. 33, no. 7, pp. 373–379, 2012.

[12] T. H. M. Ottenhoff and S. H. E. Kaufmann, "Vaccines against tuberculosis: Where are we and where do we need to go?" *PLoS Pathogens*, vol. 8, no. 5, Article ID e1002607, 2012.

[13] N. Dhar, V. Rao, and A. K. Tyagi, "Skewing of the Th1/Th2 responses in mice due to variation in the level of expression of an antigen in a recombinant BCG system," *Immunology Letters*, vol. 88, no. 3, pp. 175–184, 2003.

[14] C. Aagaard, T. T. K. T. Hoang, A. Izzo et al., "Protection and polyfunctional T cells induced by Ag85B-TB10.4/IC31 against Mycobacterium tuberculosis is highly dependent on the antigen dose," *PLoS ONE*, vol. 4, no. 6, Article ID e5930, 2009.

[15] S. Tollefsen, T. E. Tjelle, J. Schneider et al., "Improved cellular and humoral immune responses against *Mycobacterium tuberculosis* antigens after intramuscular DNA immunisation combined with muscle electroporation," *Vaccine*, vol. 20, no. 27-28, pp. 3370–3378, 2002.

[16] D. X. Johansson, K. Ljungberg, M. Kakoulidou, and P. Liljeström, "Intradermal electroporation of naked replicon rna elicits strong immune responses," *PLoS ONE*, vol. 7, no. 1, Article ID e29732, 2012.

[17] Z. Li, D. Song, H. Zhang et al., "Improved humoral immunity against tuberculosis ESAT-6 antigen by chimeric DNA prime and protein boost strategy," *DNA and Cell Biology*, vol. 25, no. 1, pp. 25–30, 2006.

[18] J. Wu, H. Ma, Q. Qu et al., "Incorporation of immunostimulatory motifs in the transcribed region of a plasmid DNA vaccine enhances Th1 immune responses and therapeutic effect against *Mycobacterium tuberculosis* in mice," *Vaccine*, vol. 29, no. 44, pp. 7624–7630, 2011.

[19] R. Jain, B. Dey, N. Dhar et al., "Enhanced and enduring protection against tuberculosis by recombinant BCG-Ag85C and its association with modulation of cytokine profile in lung," *PLoS ONE*, vol. 3, no. 12, Article ID e3869, 2008.

[20] P. Andersen, "TB vaccines: progress and problems," *Trends in Immunology*, vol. 22, no. 3, pp. 160–168, 2001.

[21] V. Rao, N. Dhar, and A. K. Tyagi, "Modulation of host immune responses by overexpression of immunodominant antigens of *Mycobacterium tuberculosis* in bacille Calmette-Guérin," *Scandinavian Journal of Immunology*, vol. 58, no. 4, pp. 449–461, 2003.

[22] B. Dey, R. Jain, U. D. Gupta, V. M. Katoch, V. D. Ramanathan, and A. K. Tyagi, "A booster vaccine expressing a latency-associated antigen augments bcg induced immunity and confers enhanced protection against tuberculosis," *PLoS ONE*, vol. 6, no. 8, Article ID e23360, 2011.

[23] R. A. Seder, P. A. Darrah, and M. Roederer, "T-cell quality in memory and protection: implications for vaccine design," *Nature Reviews Immunology*, vol. 8, no. 4, pp. 247–258, 2008.

[24] C. Aagaard, T. Hoang, J. Dietrich et al., "A multistage tuberculosis vaccine that confers efficient protection before and after exposure," *Nature Medicine*, vol. 17, no. 2, pp. 189–195, 2011.

[25] S. C. De Rosa, F. X. Lu, J. Yu et al., "Vaccination in humans generates broad T cell cytokine responses," *Journal of Immunology*, vol. 173, no. 9, pp. 5372–5380, 2004.

[26] Y. V. N. Cavalcanti, M. C. A. Brelaz, J. K. D. A. L. Neves, J. C. Ferraz, and V. R. A. Pereira, "Role of TNF-alpha, IFN-gamma, and IL-10 in the development of pulmonary tuberculosis," *Pulmonary Medicine*, vol. 2012, Article ID 745483, 10 pages, 2012.

[27] K. Yu, C. Mitchell, Y. Xing, R. S. Magliozzo, B. R. Bloom, and J. Chan, "Toxicity of nitrogen oxides and related oxidants on mycobacteria: *M. tuberculosis* is resistant to peroxynitrite anion," *Tubercle and Lung Disease*, vol. 79, no. 4, pp. 191–198, 1999.

[28] C. A. Scanga, V. P. Mohan, K. Yu et al., "Depletion of $CD4^+$ T cells causes reactivation of murine persistent tuberculosis despite continued expression of interferon γ and nitric oxide synthase 2," *The Journal of Experimental Medicine*, vol. 192, no. 3, pp. 347–358, 2000.

[29] J. L. Flynn, M. M. Goldstein, J. Chan et al., "Tumor necrosis factor-α is required in the protective immune response against *Mycobacterium tuberculosis* in mice," *Immunity*, vol. 2, no. 6, pp. 561–572, 1995.

[30] A. S. Davis, I. Vergne, S. S. Master, G. B. Kyei, J. Chua, and V. Deretic, "Mechanism of inducible nitric oxide synthase exclusion from mycobacterial phagosomes," *PLoS Pathogens*, vol. 3, no. 12, article e186, 2007.

[31] A. Raja, "Immunology of tuberculosis," *Indian Journal of Medical Research*, vol. 120, no. 4, pp. 213–232, 2004.

[32] A. M. Cooper and S. A. Khader, "The role of cytokines in the initiation, expansion, and control of cellular immunity to tuberculosis," *Immunological Reviews*, vol. 226, no. 1, pp. 191–204, 2008.

Hindawi Publishing Corporation
Journal of Immunology Research
Volume 2014, Article ID 395626, 8 pages
http://dx.doi.org/10.1155/2014/395626

Research Article

A *Mycobacterium bovis* BCG-Naked DNA Prime-Boost Vaccination Strategy Induced $CD4^+$ and $CD8^+$ T-Cell Response against *Mycobacterium tuberculosis* Immunogens

Miao Lu, Zhi Yang Xia, and Lang Bao

Laboratory of Infection and Immunity, School of Basic Medical Science, West China Center of Medical Sciences, Sichuan University, No. 17, Third Section, Ren Min Nan Road, Chengdu, Sichuan 610041, China

Correspondence should be addressed to Lang Bao; baolang@scu.edu.cn

Received 11 November 2013; Revised 2 January 2014; Accepted 6 February 2014; Published 11 March 2014

Academic Editor: Beatrice Saviola

Mycobacterium tuberculosis infection is still a major global public health problem. Presently the only tuberculosis (TB) vaccine available is Bacille Calmette-Guérin (BCG), although it fails to adequately protect against pulmonary TB in adults. To solve this problem, the development of a new effective vaccine is urgently desired. BCG-prime DNA-booster vaccinations strategy has been shown to induce greater protection against tuberculosis (TB) than BCG alone. Some studies have demonstrated that the two genes (Rv1769 and Rv1772) are excellent T-cell antigens and could induce T-cell immune responses. In this research, we built BCG-C or BCG-P prime-recombination plasmid PcDNA3.1-Rv1769 or PcDNA3.1-Rv1772 boost vaccinations strategy to immunize BALB/c mice and evaluated its immunogenicity. The data suggests that the BCG-C+3.1-72 strategy could elicit the most long-lasting and strongest Th1-type cellular immune responses and the BCG-C+3.1-69 strategy could induce the high level CD8+ T-cell response at certain time points. These findings support the ideas that the prime-boost strategy as a combination of vaccines may be better than a single vaccine for protection against tuberculosis.

1. Introduction

Today tuberculosis (TB) still remains a major infectious cause of morbidity and mortality worldwide, one-third of the world's population is latently infected with *Mycobacterium tuberculosis*. Bacille Calmette-Guérin (BCG) is the only available vaccine against tuberculosis presently, and the protective efficacy of it is variable from 0 to 80% in many field trials and is unclear in pulmonary TB in adults [1], but it prevents miliary tuberculosis in newborns and toddlers [2, 3]. The cause of these large differences in vaccine-induced protection is poorly understood, and some of its limitations may involve short-lived BCG-induced immune reactivity. This raises an issue that a novel TB vaccine which can protect adults against tuberculosis is urgently needed [3, 4], while BCG vaccination of newborns should be continued as it is effective. Previous TB vaccines are classified into 4 main groups: (1) DNA vaccines, (2) recombinant BCG vaccines, (3) subunit vaccines, and (4) attenuated vaccines, and currently most efforts to improve the protective immunity of BCG are focused on strategies that incorporate priming with BCG, recombinant BCG, or other attenuated mycobacteria followed by a heterologous booster immunization that aims to improve the duration and efficacy of the responses [5–7]. Considering all kinds of reasons, we decide to choose the heterologous prime-boost vaccination strategy comprised of priming with BCG and boosting with a novel vaccine candidate [8, 9].

Cellular immune responses are critical for the control of *Mycobacterium tuberculosis* infection, which depends on polyfunctional $CD4^+$ and $CD8^+$ T-cell responses [10, 11]. T helper type 1 (Th1) $CD4^+$ T cell can primarily secrete interferon-γ (IFN-γ), which is important in *M. tuberculosis* infection and disease prevention [12]. $CD8^+$ cytolytic T lymphocytes (CTLs) are essential for clearance of intracellular *M. tuberculosis* infection [13] by secreting perforin, granulysin,

Table 1: Heterologous prime-boost immunization schedule.

Group	Prime	Boost1	Boost2
PBST	PBST	PBST	PBST
BCG-C	BCG-China	PBST	PBST
BCG-P	BCG-Pasteur1173	PBST	PBST
BCG-C+pcDNA3.1	BCG-China	Plasmid pcDNA3.1	Plasmid pcDNA3.1
BCG-P+pcDNA3.1	BCG-Pasteur1173	Plasmid pcDNA3.1	Plasmid pcDNA3.1
BCG-C+3.1-69	BCG-China	Plasmid pc-Rv1769	Plasmid Pc-Rv1769
BCG-P+3.1-69	BCG-Pasteur1173	Plasmid pc-Rv1769	Plasmid Pc-Rv1769
BCG-C+3.1-72	BCG-China	Plasmid pc-Rv1772	Plasmid Pc-Rv1772
BCG-P+3.1-72	BCG-Pasteur1173	Plasmid pc-Rv1772	Plasmid Pc-Rv1772
Timeline in weeks	0 ↓	3 ↓	6 ↓

and extracellular enzymes into the immunological synapse [14]. Heterologous prime-boost strategy has been used in many models of pathogenic infections [15], and some studies demonstrate that prime-boost strategies using BCG as prime and heterologous constructs such as recombinant DNA, recombinant adenovirus, and recombinant poxviruses as boosting immunogens can enhance $CD4^+$ and $CD8^+$ T-cell responses against TB [6, 7, 16–18].

To search for a novel effective vaccine candidate to improve the protection of BCG, many strategies have been attempted and a number of antigens have been studied. In our research, we choose two BCG substrains (BCG-Pasteur1173 and BCG-China) which are different in two deletions called RD14 and N-RD18 [19, 20], which are present in BCG-China, but absent in BCG-Pasteur1173. We notice two genes (Rv1769 and Rv1772) in RD14 deletion, which have been studied superficially, and some research has indicated that Rv1769 and Rv1772 should be considered for potential subunit vaccines [21, 22].

In previous work, researchers paid much attention to ESAT-6, CFP-10, and Ag85 [7, 16, 23–25], and little attention has been paid to the RD14 deletion. Maybe the genes located in this deletion are responsible for different immunogenicity between the BCG-Pasteur and BCG-China. Based on all of the reasons above, we have constructed several vaccination strategies primed with BCG-C or BCG-P and boosted with recombination plasmid pcDNA3.1-Rv1769 or pcDNA3.1-Rv1772 to immunize BALB/c mice and evaluated its immunogenicity. This study shows that this strategy can elicit potent humoral and cellular immune responses comprising both $CD4^+$ and $CD8^+$ T cells against TB in mice, but its protective efficacy was not to be demonstrated in this study.

2. Materials and Methods

2.1. Bacterial Strains, Media, and Plasmids. *M. bovis* BCG-Pasteur and BCG-China were kindly provided by the Chengdu Biological Products Institute. BCGs were maintained in Sauton's medium ($MgSO_4$ 0.5 g, K_2HPO_4 0.5 g, citric acid 2 g, sodium glutamate 8 g, glycerol 60 mL, $ZnSO_4$ 0.01 g, and ferrum-ammonium citrate 0.05 g in 1000 mL, pH1.4–7.5). The plasmid was originally conserved in our laboratory.

2.2. Plasmid Construction. The Rv1769 and Rv1772 genes were amplified from the BCG-China genome and cloned into pcDNA3.1(+) plasmid to generate recombinant pcDNA3.1-Rv1769 and pcDNA3.1-Rv1772. The sequences were confirmed by sequencing by Invitrogen (Shanghai, China). Endotoxin-free plasmids were prepared using an EndoFree plasmid purification kit (OMEGA, USA). Plasmids were adjusted to a final concentration of 1 mg/mL in PBS and stored at −20°C.

2.3. Animals and Immunization Protocol. 4-5-week-old pathogen-free BALB/c male mice were purchased from the Laboratory of Animals Institute in Sichuan University (Chengdu, China). The vaccination schedules of mice are shown in Table 1. Groups of BALB/c ($n = 18$) were primed with PBST, BCG-China, or BCG-Pasteur1173 at week 0 and boosted with plasmid DNA or control plasmid at week 3 and week 6. Mice were immunized subcutaneously with $5 * 10^6$ CFU of BCG in a volume of 0.1 mL per mouse and intramuscularly with 50 μg DNA in a volume of 0.1 mL each time per mouse. Mice were put to death at 10, 14, 18, and 22 weeks (four mice for each group at each time point). Blood was collected from retroorbital sinus and the sera were stored at −20°C after separation until used.

2.4. ELISA for Antibody Response. Specific antibodies against TB were determined by an indirect ELISA method. The method was described as previous [22, 26]. Each sera sample was tested in three replicates, and the results are expressed as mean ± standard errors.

2.5. Proliferation of Splenocytes. The animals were sacrificed as previously described and the spleens were removed aseptically. The proliferation of lymphocyte were tested by

MTT assay [3-(4,5-dimethylthiazol-2-yl)-2,5-diphenyl tetrazoliumbromide]. The method was described as previous [22, 27]. The results are expressed as the value of stimulation index (SI). SI = OD of stimulated well/OD of unstimulated well.

2.6. Flow Cytometry. The splenocytes were prepared and cultured as previously described [27, 28], and the splenocytes were plated in 6-well flat-bottom plates ($5 * 10^6$ cells in 2 mL of cRPMI per well) with 100 μL TB-PPD (1 μg/mL; XiangRui Biotech, Ltd., Beijing, China) in each well and incubated for 72 h (37°C, 5%CO_2). The cells were collected and washed three times with 0.1 M PBS (PH = 7.2), and then rabbit anti-Mouse $CD4^+$-PE and anti-Mouse $CD8^+$-FITC (eBioscience, USA) were added into EP tube for a 30 min incubation in an ice-bath keep out of the sun. Finally, the cells were washed twice again and the proportions of $CD4^+$ and $CD8^+$ T cells were determined by flow cytometry (FACSCalibur, BD).

2.7. Cytokine Release Assay. The splenocytes were dealt with in the same way as flow cytometry assay previously described, and concentrations of IFN-γ and IL-4 in the medium were measured by an ELISA kit (eBioscience, USA) according to the manufacture's protocol.

2.8. Statistical Analysis. Measurements of these data are expressed as the mean ± standard errors (S.E.). We used one-way ANOVA to analyze the differences among the groups and post hoc test to analyze the differences between two groups. When P value < 0.05, the differences were considered statistically significant.

3. Results

3.1. Antibodies in the Serum. The antibody titers were detected by ELISA assay to reflect the humoral immune response against TB. The levels of antibody response in the sera of the immunized mice at different time points are shown in Figure 1. The results show that firstly the titers of IgG and IgG2a antibodies in the group immunized with BCG-C+3.1-69 and BCG-C+3.1-72 were higher than those in the other 7 groups at the 8th week ($P < 0.01$); secondly the IgG titers in group BCG-C+3.1-69 were higher than those in the BCG-P+3.1-72, PBST, plasmid controls, and positive controls at the 4th and 12th weeks ($P < 0.05$) and were higher than those in the other 8 groups at the 16th week ($P < 0.05$); thirdly the titers of IgG2a antibodies in the group immunized with BCG-C+3.1-69 and BCG-C+3.1-72 were higher than those in the BCG-P+3.1-72, PBST, plasmid controls, and positive controls at the 12th week ($P < 0.05$). Besides, the titers of IgG1 antibodies in the group immunized with BCG-C+3.1-69 were higher than those in the other 8 groups at the 4th, 8th, and 16th weeks ($P < 0.05$). Figure 1(d) shows that groups BCG-C+3.1-69, BCG-C+3.1-72, BCG-P+3.1-69, and BCG-P+3.1-72 all indicated a shift towards a Th1 immune response at the 12th week.

3.2. Lymphoproliferation Assay. To detect the cell-mediated immune response, the splenic lymphocyte proliferation was assessed by MTT assay. The results show that the proliferation of splenocytes in the BCG-C+3.1-69, BCG-C+3.1-72, BCG-P+3.1-69, and BCG-P+3.1-72 groups were higher than those in the PBST, plasmid controls, and positive controls at the 12th week ($P < 0.01$), but there were no significative statistical differences between the above four groups (BCG-C+3.1-69, BCG-C+3.1-72, BCG-P+3.1-69, and BCG-P+3.1-72), while the group BCG-C+3.1-69 showed greater proliferation of splenocytes than the other 8 groups at the 4th week ($P < 0.05$) and than the BCG-C+3.1-72, PBST, plasmid controls, and positive controls groups at the 8th week ($P < 0.05$). The SI value in the BCG-C+3.1-69 and BCG-C+3.1-72 groups peaked at the 12th week, and the proliferation level decreased after this time. Importantly, the proliferation reaction of group BCG-C+3.1-72 still maintains at a high level at the 16th week (Figure 2).

3.3. Percentages of Splenocyte Subsets. The proportions of splenocyte subsets were measured by flow cytometry. As Figure 3 shows, the BCG-C+3.1-72 group induced a significantly greater ratio of $CD4^+$ T cells at the 8th week compared with BCG-P+3.1-69, BCG-P+3.1-72, PBST, plasmid controls, and positive controls groups ($P < 0.05$). In addition, the BCG-C+3.1-69, BCG-C+3.1-72, BCG-P+3.1-69, and BCG-P+3.1-72 groups induced a significantly greater ratio of $CD4^+$ T cells at the 12th week compared with PBST, plasmid controls, and positive controls groups ($P < 0.01$), and the status of BCG-C+3.1-69, BCG-C+3.1-72, and BCG-P+3.1-69 groups lasted to the 16th week except the group BCG-P+3.1-72. Finally, the proportions of $CD8^+$ T cells in the BCG-C+3.1-69 group was higher than that in the other 8 groups at the 12th week ($P < 0.05$) (Figure 3).

3.4. Cytokine Production. To determine Th1- and Th2-type immune response, the IFN-γ and IL-4 were detected from restimulated spleen cells by ELISA. According to Figure 4, the results clearly showed that the concentrations of IFN-γ in the group BCG-C+3.1-69 and BCG-C+3.1-72 were higher than those in the other 7 groups at the 12th week ($P < 0.05$), and the IFN-γ concentrations of the BCG-C+3.1-72 were higher than those of the groups BCG-C+3.1-69, BCG-P+3.1-69, PBST, plasmid controls, and positive controls at the 8th week ($P < 0.05$) (Figure 4). IL-4 maintained at a low level, and there were no significantly changes among any groups including PBST group ($P > 0.05$) (data not shown).

4. Discussion

Heterologous prime/boost vaccination strategies employing recombinant bacteria, viruses, proteins, and naked DNA have been shown to elicit stronger and more diverse cellular immune responses than BCG vaccine alone [5–7, 22]. In humans, DNA vaccines alone have not provided satisfactory results, whereas DNA vaccines produced better outcomes when immunized as a prime-boost strategy [29, 30].

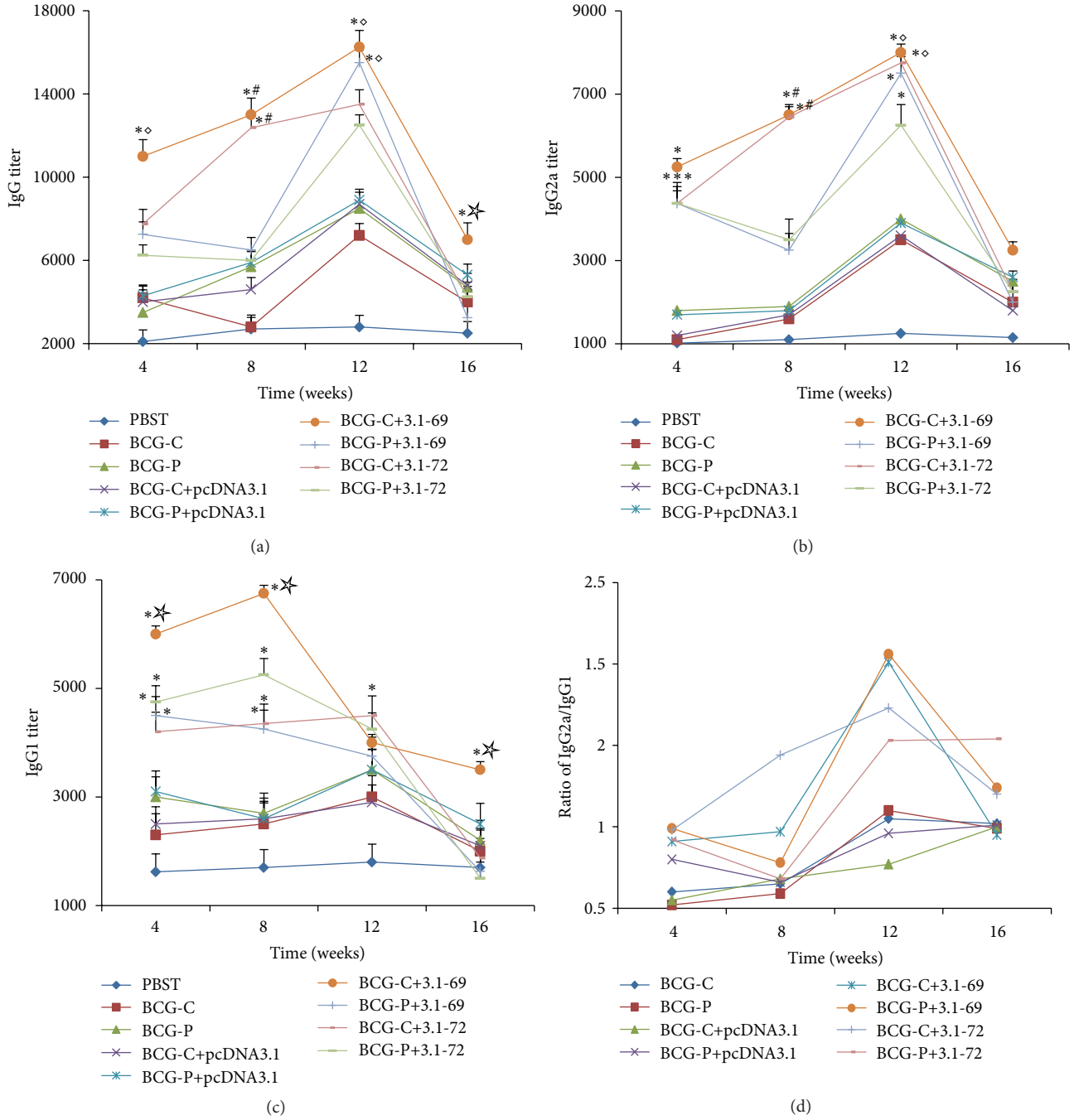

Figure 1: Analysis of the antibody responses via testing the IgG, IgG1, and IgG2a by ELISA. Animals were immunized and harvested at the indicated time points. The sera were obtained and tested for specific antibody levels. Results are expressed as mean ± standard errors. $^{*}P < 0.01$ versus PBST, BCG-C, BCG-P, BCG-C+pcDNA3.1, or BCG-P+pcDNA3.1 groups. $^{\#}P < 0.01$ versus BCG-P+3.1-69 or BCG-P+3.1-72 group. $^{\diamond}P < 0.05$ versus BCG-P+3.1-72 group. $^{\star}P < 0.05$ versus BCG-P+3.1-69, BCG-C+3.1-72 or BCG-P+3.1-72 group.

According to these former observations, we built this work to evaluate the immunogenicity of two genes (Rv1769 and Rv1772) by a heterologous prime/boost strategy. The data of this paper supports the theory that heterologous prime-boost vaccination significantly induces more robust cellular immune responses than BCG vaccine alone.

Previously, numerous prime-boost vaccination protocols have demonstrated varying success when carried out in various infectious disease models. In tuberculosis experiments, prime-boost vaccination protocols include BCG/protein prime-boost [8, 22], DNA/protein prime-boost [31], DNA/adenovirus 5 prime-boost [32], DNA/BCG prime-boost [33],

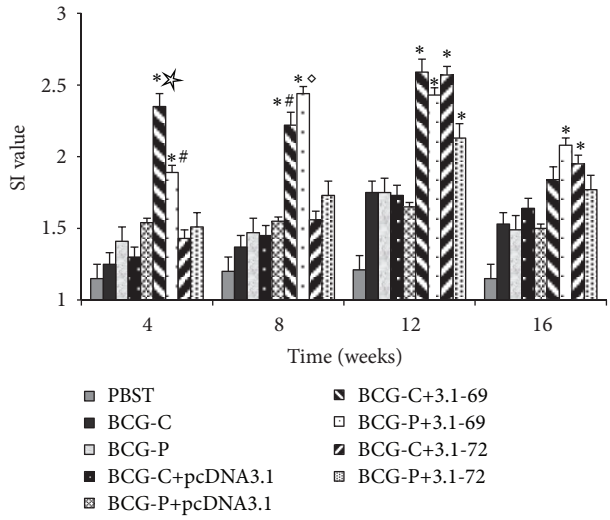

Figure 2: Analysis of the lymphoproliferative response to the prime-boost approach. Splenocytes were prepared from individual mice after the animals were killed, and proliferation was analyzed by MTT method using the TB-PPD stimulating as described in Section 2. The proliferation was measured by SI, and the data are presented as means ± standard errors. $^{*}P < 0.01$ versus PBST, BCG-C, BCG-P, BCG-C+pcDNA3.1, or BCG-P+pcDNA3.1 groups. $^{\#}P < 0.05$ versus BCG-C+3.1-72 group. $^{\Diamond}P < 0.05$ versus BCG-C+3.1-72 or BCG-P+3.1-72 group. $^{\star}P < 0.05$ versus BCG-P+3.1-69, BCG-C+3.1-72, or BCG-P+3.1-72 groups.

and BCG/MVA prime-boost [5] vaccination schedules, and these prime-boost protocols used Ag85A [5, 8], MT_1721 [31], ESAT-6 [33], Rv1769, and Rv1772 [22] as antigens. Considering a BCG immunization is done in early childhood, our study has begun with a BCG prime.

Antigens Rv1769 and Rv1772 are interesting because the coding genes are present in the genome of BCG-China, only deleted from the BCG-Pasteur. We suppose that overexpression of the genes enhances the immune response of the existing BCG. More importantly, we succeeded in improving the vaccine immunogenicity of the BCG by using a prime-boost vaccination.

The pathogenic bacterium of TB is *Mycobacterium tuberculosis*, which is intracellular bacteria and cell immune is very important in clearance of it. In the early infection, the $CD4^+$ T cell can release IFN-γ, IL-2, and TNF-α, which can activate macrophages to fight against *M. tuberculosis* [34]. In this paper, IFN-γ, as the representative, was detected by ELISA, and the results show that groups BCG-C+3.1-69 and BCG-C+3.1-72 were of the highest levels of IFN-γ concentrations. In addition, flow cytometry results show that groups BCG-C+3.1-69 and BCG-C+3.1-72 can induce the greatest ratio of $CD4^+$ T cells. According to the data of flow cytometry, we have observed that $CD4^+$ T cells and IFN-γ levels of BCG-C+3.1-72 rise from 8th week and down after the 12th week; however, great ratio of $CD4^+$ T cells of BCG-C+3.1-69 lasted to even the 16th week. So, we suppose that the group BCG-C+3.1-69 may enhance a stronger and longer-lasting T-cell immune response against *M. tuberculosis* early infection. Recently, numerous studies indicate that $CD8^+$ T cells are critical for the induction of protective TB immunity in humans [35], NHPs [36], rodents [37], and cattle [38]. The $CD8^+$ T cells can secrete perforin, granulysin, and extracellular enzyme to promote bacterial schizolysis [13, 34]. In our research, flow cytometry results show that the proportions of $CD8^+$ T cells in the BCG-C+3.1-69 group was the highest at the 12th week with $P < 0.05$. Considering these, we have thought about the group BCG-C+3.1-69 not only induced polyfunctional $CD4^+$ T cells, but also a robust $CD8^+$ T-cell response in mice.

To measure the TH1-type immune response better, we also determined the antibody responses induced by these vaccine candidates. The results reveal that groups BCG-C+3.1-69 and BCG-C+3.1-72 can elicit high levels of IgG and IgG2a antibodies and also last a long time. Besides, the ratio of IgG2a/IgG1 shows a shift towards a Th1-type immune response.

Lastly, the proliferation rate of splenocytes increased consistently with the other experimental results; the splenocytes proliferation rate in group BCG-C + 3.1-69 rises in the 4th week and reaches the peak value in the 12th week. Due to the arguments above, we believe that the group BCG-C + 3.1-69 can induce stronger and longer-lasting TH1-type immune response than native BCG or other prime-boost groups in mice having $CD4^+$ and $CD8^+$ T cells.

Some research has demonstrated that BCG and recombinant BCG can induce central memory $CD8^+$ T-cell differentiation *in vivo* [6, 39]. Because $CD4^+$ T helper cells are important for driving memory $CD8^+$ T-cell differentiation [40, 41], the ability of BCG to generate memory $CD8^+$ T cells could make it have the propensity to stimulate $CD4^+$ T helper cells growth. It has been suggested that the functional heterogeneity of T-cell responses may be associated with successful containment of microbial infections. The extent of T-cell polyfunctionality has been correlated with the protection against leishmaniasis in mice, HIV-1 in humans [42, 43], and SIV in nonhuman primates [44]. In this study, a prime BCG-boost DNA strategy can induce $CD8^+$ T-cell differentiation as well as $CD4^+$ T cell; we suppose that this vaccination strategy may obtain success against TB in humans and gene Rv1769 may be an excellent vaccine candidate.

The prime BCG-boost plasmid Rv1769 strategy improved the vaccine immunogenicity of BCG, and the subunit vaccination can be used to improve preexisting immunogenicity evoked by BCG and even be used in future clinical trials. More recent protocols show that naked DNA performs better in macaques and humans as part of a prime-boost regime [30]. Therefore, BCG prime and naked DNA boost vaccination should be used for several reasons: firstly BCG needs to be included in future vaccine trials against tuberculosis; secondly naked DNA vaccination has been shown to be effective as a submit vaccine in prime-boost vaccination protocols; lastly this vaccination regime can improve BCG-induced immunogenicity.

In summary, our results provide evidence that a BCG-naked DNA prime-boost vaccination protocol represents

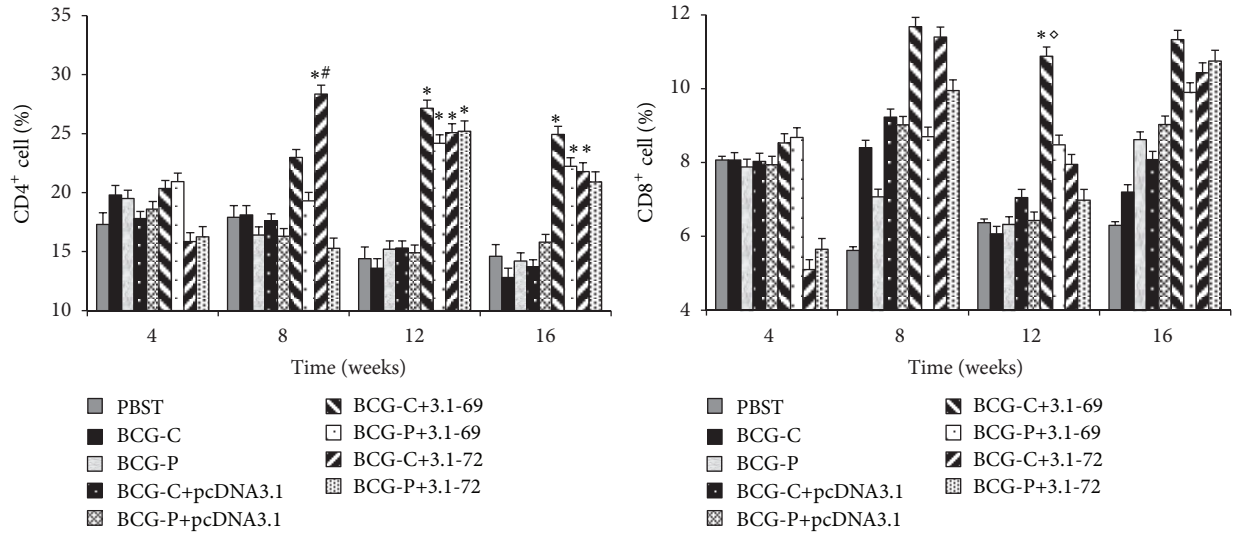

Figure 3: Analysis of the percentages of $CD4^+$ and $CD8^+$ cells (%). Animals were immunized and killed; the splenocytes were collected and handled as described in Section 2. Flow cytometry was used to determine the proportions of splenocyte subsets, and the results are presented as mean ± standard errors. $^*P < 0.01$ versus PBST, BCG-C, BCG-P, BCG-C +pcDNA3.1, or BCG-P+pcDNA3.1 groups. $^\#P < 0.05$ versus BCG-P+3.1-69 or BCG-P+ 3.1-72 group. $^\diamond P < 0.05$ versus BCG-P+3.1-69, BCG-C+3.1-72, or BCG-P+3.1-72 groups.

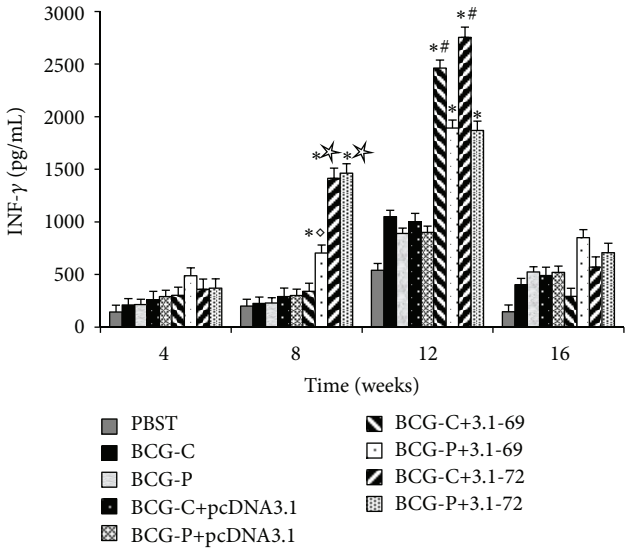

Figure 4: Analysis of IFN-γ released from splenocytes. After animals were harvested; splenocytes were collected and prepared as described in Section 2. IFN-γ concentration in the medium was measured by ELISA kit according to the manufacturer's protocol. Triplicate tests were done for each medium sample. $^*P < 0.01$ versus PBST, BCG-C, BCG-P, BCG-C+pcDNA3.1, or BCG-P+pcDNA3.1 groups. $^\#P < 0.05$ versus BCG-P+3.1-69 or BCG-P+3.1-72 group. $^\diamond P < 0.05$ versus BCG-C+3.1-69 group. $^\star P < 0.05$ versus BCG-C+3.1-69 or BCG-P+3.1-69 group.

a valuable candidate (gene Rv1769) for future vaccine trials targeted at one of the major health problems worldwide.

In the future, we would consider building an *in vivo* challenge model to extend our findings to an infection/disease protection system.

Abbreviations

PBST:	PBS-Tween 80
BCG:	Bacille Calmette-Guérin
BCC-C:	The group immunized with vaccine BCG-China substrain
BCG-P:	The group immunized with vaccine BCG-Pasteur1173 substrain
BCG-C + pcDNA3.1:	The group immunized BCG-China prime plasmid pcDNA3.1 boost
BCG-P+pcDNA3.1:	The group immunized BCG-Pasteur1173 prime plasmid pcDNA3.1 boost
BCG-C+3.1-69:	The group immunized BCG-China prime plasmid pcDNA3.1-Rv1769 boost
BCG-P+3.1-69:	The group immunized BCG-Pasteur1173 prime plasmid pcDNA3.1-Rv1769 boost
BCG-C+3.1-72:	The group immunized BCG-China prime plasmid pcDNA3.1-Rv1772 boost
BCG-P+3.1-72:	The group immunized BCG-Pasteur1173 prime plasmid pcDNA3.1-Rv1772 boost.

Conflict of Interests

The authors declare that there is no conflict of interests regarding the publication of this paper.

Acknowledgments

This work was supported by Grants from the Chinese National Key Project of Infectious Disease (2012ZX10003008-004) and The Fund of Doctoral Scientific Research of MOE (20110181110046).

References

[1] WHO, "BCG, (Tuberculosis)," 2011, http://www.who.int/biologicals/areas/vaccines/bcg/Tuberculosis/en/.

[2] P. E. M. Fine, "Bacille Calmette-Guérin vaccines: a rough guide," *Clinical Infectious Diseases*, vol. 20, no. 1, pp. 11–14, 1995.

[3] S. H. E. Kaufmann, "Is the development of a new tuberculosis vaccine possible?" *Nature Medicine*, vol. 6, no. 9, pp. 955–960, 2000.

[4] I. M. Orme, "Beyond BCG: the potential for a more effective TB vaccine," *Molecular Medicine Today*, vol. 5, no. 11, pp. 487–492, 1999.

[5] E. Z. Tehilian, C. Desel, E. K. Forbes et al., "Immunogenicity and protective efficacy of prime-boost regimens with recombinant ΔureC hly$^+$ *Mycobacterium bovis* BCG and modified vaccinia virus ankara expressing *M. tuberculosis* antigen 85A against *Murine tuberculosis*," *Infection and Immunity*, vol. 77, no. 2, pp. 622–631, 2009.

[6] M. J. Cayabyab, B. Korioth-Schmitz, Y. Sun et al., "Recombinant *Mycobacterium bovis* BCG prime-recombinant adenovirus boost vaccination in rhesus monkeys elicits robust polyfunctional simian immunodeficiency virus-specific T-cell responses," *Journal of Virology*, vol. 83, no. 11, pp. 5505–5513, 2009.

[7] C. Cai, J. Lu, C. Wang et al., "Immunogenicity and protective efficacy against *Murine tuberculosis* of a prime-boost regimen with BCG and a DNA vaccine expressing ESAT-6 and Ag85A fusion protein," *Clinical and Developmental Immunology*, vol. 2011, Article ID 617892, 10 pages, 2011.

[8] J. V. Brooks, A. A. Frank, M. A. Keen, J. T. Bellisle, and I. M. Orme, "Boosting vaccine for tuberculosis," *Infection and Immunity*, vol. 69, no. 4, pp. 2714–2717, 2001.

[9] N. P. Goonetilleke, H. McShane, C. M. Hannan, R. J. Anderson, R. H. Brookes, and A. V. S. Hill, "Enhanced immunogenicity and protective efficacy against *Mycobacterium tuberculosis* of bacille Calmette-Guérin vaccine using mucosal administration and boosting with a recombinant modified vaccinia virus Ankara," *The Journal of Immunology*, vol. 171, no. 3, pp. 1602–1609, 2003.

[10] J. L. Flynn and J. Chan, "Immunology of tuberculosis," *Annual Review of Immunology*, vol. 19, pp. 93–129, 2001.

[11] P. Wong and E. G. Pamer, "CD8 T cell responses to infectious pathogens," *Annual Review of Immunology*, vol. 21, pp. 29–70, 2003.

[12] N. Caccamo, G. Guggino, S. A. Joosten et al., "Multifunctional CD4$^+$ T cells correlate with active *Mycobacterium tuberculosis* infection," *European Journal of Immunology*, vol. 40, no. 8, pp. 2211–2220, 2010.

[13] D. Sud, C. Bigbee, J. L. Flynn, and D. E. Kirschner, "Contribution of CD8$^+$ T cells to control of *Mycobacterium tuberculosis* infection," *The Journal of Immunology*, vol. 176, no. 7, pp. 4296–4314, 2006.

[14] J. S. Woodworth, Y. Wu, and S. M. Behar, "*Mycobacterium tuberculosis*-specific CD8$^+$ T cells require perforin to kill target cells and provide protection in vivo," *The Journal of Immunology*, vol. 181, no. 12, pp. 8595–8603, 2008.

[15] S. H. E. Kaufmann and A. J. McMichael, "Annulling a dangerous liaison: vaccination strategies against AIDS and tuberculosis," *Nature Medicine*, vol. 11, no. 4, pp. S33–S44, 2005.

[16] M. Romano, S. D'Souza, P.-Y. Adnet et al., "Priming but not boosting with plasmid DNA encoding mycolyl-transferase Ag85A from *Mycobacterium tuberculosis* increases the survival time of *Mycobacterium bovis* BCG vaccinated mice against low dose intravenous challenge with *M. tuberculosis* H37Rv," *Vaccine*, vol. 24, no. 16, pp. 3353–3364, 2006.

[17] M. Santosuosso, S. McCormick, X. Zhang, A. Zganiacz, and Z. Xing, "Intranasal boosting with an adenovirus-vectored vaccine markedly enhances protection by parenteral *Mycobacterium bovis* BCG immunization against pulmonary tuberculosis," *Infection and Immunity*, vol. 74, no. 8, pp. 4634–4643, 2006.

[18] J. M. Vuola, S. Keating, D. P. Webster et al., "Differential immunogenicity of various heterologous prime-boost vaccine regimens using DNA and viral vectors in healthy volunteers," *The Journal of Immunology*, vol. 174, no. 1, pp. 449–455, 2005.

[19] J. Liu, V. Tran, A. S. Leung, D. C. Alexander, and B. Zhu, "BCG vaccines: their mechanisms of attenuation and impact on safety and protective efficacy," *Human Vaccines*, vol. 5, no. 2, pp. 70–78, 2009.

[20] A. S. Leung, V. Tran, Z. Wu et al., "Novel genome polymorphisms in BCG vaccine strains and impact on efficacy," *BMC Genomics*, vol. 9, article 413, 2008.

[21] P. J. Cockle, S. V. Gordon, A. Lalvani, B. M. Buddle, R. G. Hewinson, and H. M. Vordermeier, "Identification of novel *Mycobacterium tuberculosis* antigens with potential as diagnostic reagents or subunit vaccine candidates by comparative genomics," *Infection and Immunity*, vol. 70, no. 12, pp. 6996–7003, 2002.

[22] M. Lu, Z. Y. Xia, and L. Bao, "Enhancement of antimycobacterial Th1-cell responses by a *Mycobacterium bovis* BCG prime-protein boost vaccination strategy," *Cellular Immunology*, vol. 285, no. 1-2, pp. 111–117, 2013.

[23] J. Yang, K. Xu, J. Zheng, L. Wei, and J. Fan L, "Limited T cell receptor beta variable repertoire responses to ESAT-6 and CFP-10 in subjects infected with *Mycobacterium tuberculosis*," *Tuberculosis*, vol. 93, pp. 529–537, 2013.

[24] L. Zhang, H. Zhang, Y. Zhao et al., "Effects of *Mycobacterium tuberculosis* ESAT-6/CFP-10 fusion protein on the autophagy function of mouse macrophages," *DNA and Cell Biology*, vol. 31, no. 2, pp. 171–179, 2012.

[25] M. Legesse, G. Ameni, G. Medhin et al., "IgA response to ESAT-6/CFP-10 and Rv2031 antigens varies in patients with culture-confirmed pulmonary tuberculosis, healthy *Mycobacterium tuberculosis*—infected and non-infected individuals in a tuberculosis endemic setting, Ethiopia," *Scandinavian Journal of Immunology*, vol. 78, no. 3, pp. 266–274, 2013.

[26] Y. H. Deng, Z. Sun, X. L. Yang, and L. Bao, "Improved immunogenicity of recombinant *Mycobacterium bovis* bacillus Calmette-Guérin strains expressing fusion protein Ag85A-ESAT-6 of *Mycobacterium tuberculosis*," *Scandinavian Journal of Immunology*, vol. 72, no. 4, pp. 332–338, 2010.

[27] Y. Deng, L. Bao, and X. Yang, "Evaluation of immunogenicity and protective efficacy against *Mycobacterium tuberculosis* infection elicited by recombinant *Mycobacterium bovis* BCG expressing human Interleukin-12p70 and Early Secretory Antigen Target-6 fusion protein," *Microbiology and Immunology*, vol. 55, no. 11, pp. 798–808, 2011.

[28] X. Yang, L. Bao, and Y. Deng, "A novel recombinant *Mycobacterium bovis* bacillus Calmette-Guérin strain expressing human granulocyte macrophage colony-stimulating factor and *Mycobacterium tuberculosis* early secretory antigenic target 6 complex augments Th1 immunity," *Acta Biochimica et Biophysica Sinica*, vol. 43, no. 7, pp. 511–518, 2011.

[29] R. R. MacGregor, R. Ginsberg, K. E. Ugen et al., "T-cell responses induced in normal volunteers immunized with a DNA-based vaccine containing HIV-1 env and rev," *AIDS*, vol. 16, no. 16, pp. 2137–2143, 2002.

[30] S. J. McConkey, W. H. H. Reece, V. S. Moorthy et al., "Enhanced T-cell immunogenicity of plasmid DNA vaccines boosted by recombinant modified vaccinia virus Ankara in humans," *Nature Medicine*, vol. 9, no. 6, pp. 729–735, 2003.

[31] M. J. Cayabyab, S. S. Kashino, and A. Campos-Neto, "Robust immune response elicited by a novel and unique *Mycobacterium tuberculosis* protein using an optimized DNA/protein heterologous prime/boost protocol," *Immunology*, vol. 135, no. 3, pp. 216–225, 2012.

[32] B. C. G. de Alencar, P. M. Persechini, F. A. Haolla et al., "Perforin and gamma interferon expression are required for $CD4^+$ and $CD8^+$ T-cell-dependent protective immunity against a human parasite, *Trypanosoma cruzi*, elicited by heterologous plasmid DNA prime-recombinant adenovirus 5 boost vaccination," *Infection and Immunity*, vol. 77, no. 10, pp. 4383–4395, 2009.

[33] M. A. Skinner, B. M. Buddle, D. N. Wedlock et al., "A DNA prime-*Mycobacterium bovis* BCG boost vaccination strategy for cattle induces protection against bovine tuberculosis?" *Infection and Immunity*, vol. 71, no. 9, pp. 4901–4907, 2003.

[34] M. E. Munk and M. Emoto, "Functions of T-cell subsets and cytokines in mycobacterial infections," *European Respiratory Journal*, vol. 8, no. 20, pp. 668s–675s, 1995.

[35] S. M. Smith, A. S. Malin, P. T. Lukey et al., "Characterization of human *Mycobacterium bovis* Bacille Calmette-Guérin- reactive $CD8^+$ T cells," *Infection and Immunity*, vol. 67, no. 10, pp. 5223–5230, 1999.

[36] C. Y. Chen, D. Huang, R. C. Wang et al., "A critical role for $CD8^+$ T cells in a nonhuman primate model of tuberculosis," *PLoS Pathogens*, vol. 5, no. 4, Article ID e1000392, 2009.

[37] Y. Wu, J. S. Woodworth, D. S. Shin, S. Morris, and S. M. Behar, "Vaccine-elicited 10-kilodalton culture filtrate protein-specific $CD8^+$ T cells are sufficient to mediate protection against *Mycobacterium tuberculosis* infection," *Infection and Immunity*, vol. 76, no. 5, pp. 2249–2255, 2008.

[38] A. E. Hogg, A. Worth, P. Beverley, C. J. Howard, and B. Villarreal-Ramos, "The antigen-specific memory $CD8^+$ T-cell response induced by BCG in cattle resides in the $CD8^+\gamma/\delta$TCR-$CD45RO^+$ T-cell population," *Vaccine*, vol. 27, no. 2, pp. 270–279, 2009.

[39] H. van Faassen, M. Saldanha, D. Gilbertson, R. Dudani, L. Krishnan, and S. Sad, "Reducing the stimulation of $CD8^+$ T cells during infection with intracellular bacteria promotes differentiation primarily into a central (CD62LhighCD44high) Subset," *The Journal of Immunology*, vol. 174, no. 9, pp. 5341–5350, 2005.

[40] D. J. Shedlock and H. Shen, "Requirement for $CD4^+$ T cell help in generating functional $CD8^+$ T cell memory," *Science*, vol. 300, no. 5617, pp. 337–339, 2003.

[41] J. C. Sun and M. J. Bevan, "Defective $CD8^+$ T cell memory following acute infection without $CD4^+$ T cell help," *Science*, vol. 300, no. 5617, pp. 339–342, 2003.

[42] J. R. Almeida, D. A. Price, L. Papagno et al., "Superior control of HIV-1 replication by $CD8^+$ T cells is reflected by their avidity, polyfunctionality, and clonal turnover," *Journal of Experimental Medicine*, vol. 204, no. 10, pp. 2473–2485, 2007.

[43] P. A. Darrah, D. T. Patel, P. M. de Luca et al., "Multifunctional TH1 cells define a correlate of vaccine-mediated protection against Leishmania major," *Nature Medicine*, vol. 13, no. 7, pp. 843–850, 2007.

[44] M. Genescà, T. Rourke, J. Li et al., "Live attenuated lentivirus infection elicits polyfunctional simian immunodeficiency virus Gag-specific $CD8^+$ T cells with reduced apoptotic susceptibility in rhesus macaques that control virus replication after challenge with pathogenic SIVmac239," *The Journal of Immunology*, vol. 179, no. 7, pp. 4732–4740, 2007.